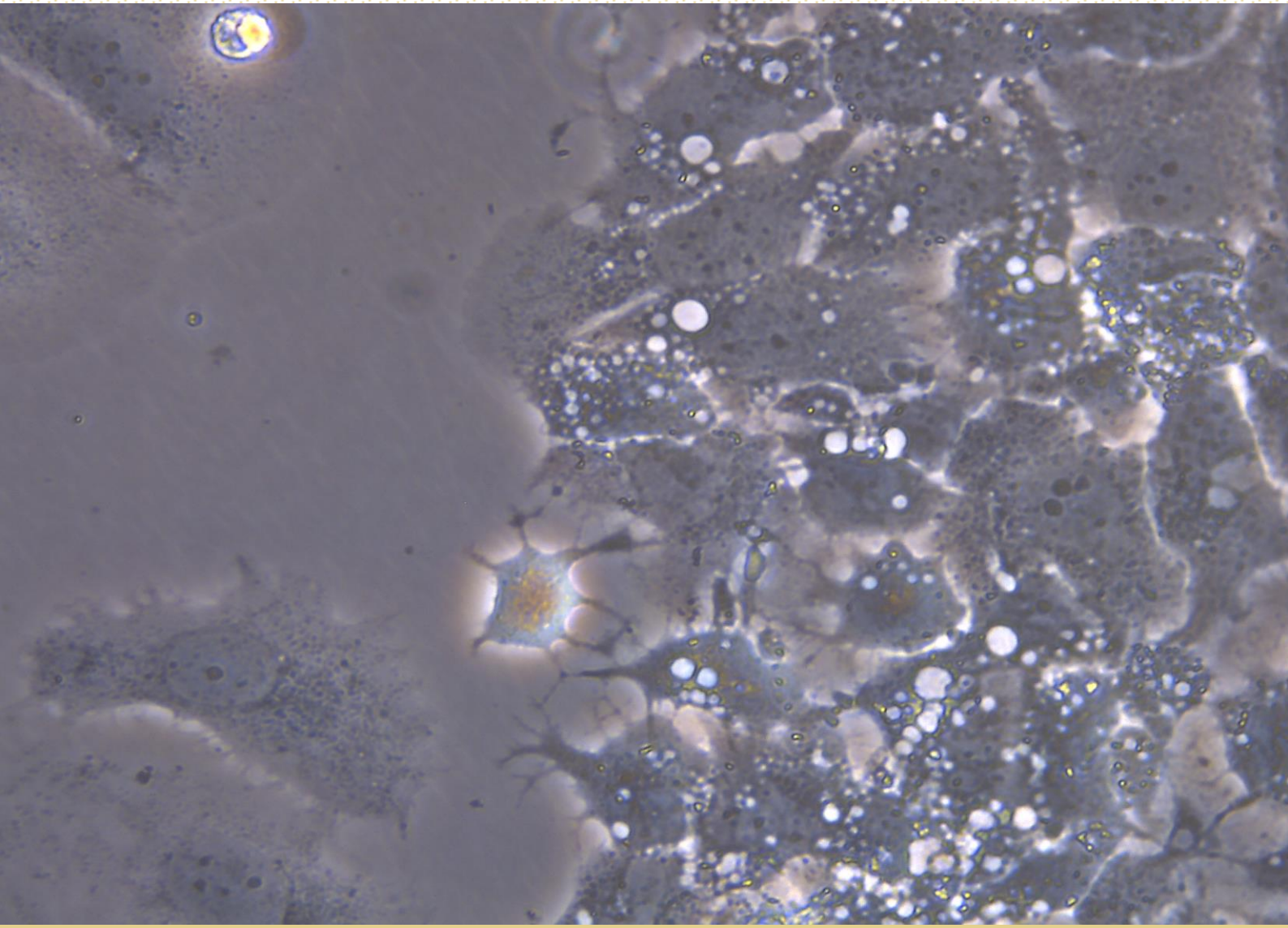

Patricia Santos de Oliveira

SIRT1 and mTOR Interplay as an arising therapeutic target for Bladder Cancer

Dissertation for the attribution of the Master degree in Biomedical Research under the supervision of Doctor Maria Filomena Rabaça Roque Botelho and Doctor Arnaldo José de Castro Figueiredo.

June 2018

· U C ·

Universidade de Coimbra

SIRT1 and mTOR interplay as an arising therapeutic target for Bladder Cancer

Patricia Santos de Oliveira

Dissertation for the attribution of the Master degree in Biomedical Research, submitted to the Faculty of Medicine of the University of Coimbra, Portugal. The research work was performed at the Coimbra Institute for Clinical and Biomedical Research (iCBR), Coimbra, Portugal and at the Biomedical Sciences Institute Abel Salazar (ICBAS), University of Porto, Portugal, under the supervision of Doctor Maria Filomena Rabaça Roque Botelho and Doctor Arnaldo José de Castro Figueiredo.

Dissertação para a obtenção de grau de Mestre em Investigação Biomédica apresentada à Faculdade de Medicina da Universidade de Coimbra. O trabalho de investigação foi realizado no Instituto para a Investigação Clínica e Biomédica de Coimbra (iCBR),da Universidade de Coimbra e no Instituto de Ciências Biomédicas Abel Salazar (ICBAS) da Universidade do Porto, sob orientação científica da Professora Doutora Maria Filomena Rabaça Roque Botelho e do Professor Doutor Arnaldo José de Castro Figueiredo.

Universidade de Coimbra

2018

Front cover:

HT-1376 bladder cancer cells exposed to the combined treatment of EX-527 plus rapamycin (400x magnifcation).

1 AKNOWLEGMENTS/AGRADECIMENTOS

Todo apoio, incentivo e disponibilidade que, de forma direta ou indireta, contribuiu para a concretização desta tese de mestrado não deve passar despercebido. Desta forma, pelo contributo para a minha formação académica, pela força indestrutível para o culminar desta etapa e pela amizade ao longo do ano, o meu enorme e sincero obrigado.

À minha orientadora, Professora Doutora Maria Filomena Botelho, pela transmissão de conhecimento, pelo o apoio e dedicação, pela exigência, pelas críticas, conselhos e correções tão relevantes para a concretização do projeto.

Ao meu co-orientador, Professor Doutor Arnaldo Figueiredo, pelo apoio e motivação, pelo conhecimento clínico transmitido.

Ao Professor Doutor Marco Alves, por me ter dado a oportunidade de realizar esta investigação no seu laboratório e ter depositado a sua confiança em mim ao me encarregar deste projeto tão rico. Pelo apoio, dedicação, exigência e disponibilidade. Pelas críticas, sugestões e correções. Por me impulsionar para mais e melhor. Pela enorme competência científica e orientação tão fundamentais para concluir esta etapa com o maior sucesso.

Ao Professor Pedro Oliveira, por me ter dado a oportunidade de trabalhar com a sua equipa, pela disponibilidade demonstrada, pelo apoio e preocupação, pelo conhecimento científico transmitido, pelas sugestões, críticas e correções.

À Professora Doutora Margarida Abrantes, que mesmo mais distante, a sua orientação foi imprescindível. Pelas oportunidades, apoio, frontalidade e sinceridade, por querer mais e melhor para mim.

À Raquel, pelo perfeito acolhimento recebido, por todos os ensinamentos laboratoriais e transmissão de conhecimentos, por toda a orientação que tão essencial foi. Por exigir sempre o melhor de mim, pela incansável disponibilidade e preocupação. Por nunca se esquecer. Por me chamar à terra. Pela força, dedicação e apoio desmedidos. Pela amizade que quero manter.

À Ana Maria, por ter sido uma das melhores pessoas que se atravessou no meu caminho. Por toda a sabedoria, porque de cada conversa, recebo tão gratificamente uma avalanche de conhecimento. Pela enorme ajuda no laboratório. Pelo apoio incondicional, pela preocupação, disponibilidade e dedicação sem limites. Por mostrar que há sempre um lado positivo. Por tornar tudo mais fácil. Pelas palavras de força e bondade.

À Ivana Jarak pela disponibilidade e apoio na obtenção de resultados de ressonância magnética nuclear.

Aos meus colegas de laboratório que tanto me aturaram e acompanharam: Susana, Catarina, David, Bruno, Tito, Luís e Juliana, pelos bons conselhos, pela ajuda e disponibilidade no laboratório. E fora dele.

Aos meus colegas do mestrado pela união, pelo espírito, pelo apoio, pelas festas e pelos estudos conjuntos. Em especial à Salomé e à Kátia pela presença constante, pelas conversas e desabafos, pela partilha e pela amizade desmedida que mesmo distante se criou e fortaleceu.

Aos meus pais e ao Eduardo, por terem estado sempre presentes, por terem sido o meu ‘porto de abrigo’, pela força incondicional e pelo amor sem fronteiras. Pelo apoio nas minhas decisões e coragem para alcançar o mundo.

Obrigada,

2 SUMMARY

Bladder cancer (BC) has a high incidence and recurrence rate. In addition, the patients show a poor survival expectancy illustrating a high demand for a more accurate stage-specific classification of the tumour that will aid much for prognosis and better tailoring of the treatment based on characteristics such as recurrence and progression. Thus, the molecular classification and characterization of bladder cancer are pivotal as tools to predict clinical outcomes, responses to chemotherapy and develop novel treatments. Herein, we hypothesize that sirtuin1 (SIRT1) has a role in bladder cancer progression and interacts with mammalian target of rapamycin (mTOR) pathway to control the metabolic and bioenergetics profiles of bladder cancer cells. To test our hypothesis, we used HT-1376 cells, which represent a stage III and TCCSUP that signify a highly invasive stage IV of the disease, and subjected them to sirtuin1 activation/inhibition with YK-3-237 (1 μM) and EX-527 (1 μM) respectively, to mTOR inhibition with rapamycin (0.1 μM) and a joint treatment with mTOR and sirtiuin1 inhibition, during 24 hours.

Cell viability, proliferation, membrane toxicity and mitochondrial toxicity were evaluated by 3-(4,5-dimethylthiazol-2-yl)-2,5-diphenyltetrazolium bromide (MTT), sulforhodamine B (SRB), lactate dehydrogenase (LDH) and mitochondrial potential (JC-1) assays, respectively. qPCR was used for evaluating *GLUT3, MCT1, MCT4, LDH, BAX* and *BCL-2* expression in cells from each experimental group. Nuclear magnetic resonance was also performed in the cell medium from each experimental group to analyse the production and consumption of metabolites and establish a metabolic profile. Mitochondrial DNA (mtDNA) copy number was determined for HT-1376 and TCCSUP cells exposed to the experimental treatments and mitochondrial respirometry was performed to treated TCCSUP cells to analyse mitochondrial performance.

Our results show that sirtuin1 pathway promotes a differential response concerning the bladder cancer cells stage suggesting that progression of bladder cancer from stage III to stage IV may be associated with a role for sirtuin1 pathway. This differential effect of sirtuin1 according to the bladder cancer stage was particularly noted in its activation in a higher stage, since it was useful to avoid the excessive lactate production by these cells. Our results also suggest that *GLUT3* may mediate the differential response of cells from different stages of bladder cancer to mTOR inhibition. In addition, our results showed that the combined treatment of TCCSUP cells with inhibition of both pathways resulted in a clear reduction of cell viability that was followed by decreased cell density, thus illustrating the great potential of the inhibition of both pathways for bladder cancer treatment and progression. Mitochondrial potential was severely depressed in HT-1376 and TCCSUP cells after inhibition of both pathways. Taken

together, these results suggest that although there is still a differential response of HT-1376 and TCCSUP cells to the combined treatment with sirtuin1 and mTOR inhibitors, the cells from the highly proliferative and invasive stage are sensitive to this treatment. Thus, the joined treatment of higher bladder cancer stages with mTOR and sirtuin1 inhibitors may have positive effects on the treatment of this pathology.

Keywords: Bladder cancer, sirtuin1 (SIRT1), mammalian target of rapamycin (mTOR), cancer metabolism, cancer bioenergetics.

3 RESUMO

O cancro da bexiga tem uma alta taxa de incidência e recorrência. Além disso, os doentes mostram uma baixa taxa de sobrevivência, o que demonstra uma necessidade por uma classificação específica e precisa do estádio do tumor, o que poderá ajudar muito no prognóstico e na melhor adaptação do tratamento com base em características da recorrência e progressão. Assim, a classificação e a caracterização molecular do cancro da bexiga são fundamentais como um meio para prever desfechos clínicos, respostas à quimioterapia e desenvolver novos tratamentos. Neste trabalho, colocou-se como hipótese que a sirtuina 1 tem um papel na progressão do cancro da bexiga e interage com a via do mTOR para controlar os perfis metabólico e bioenergético das células deste cancro. Para testar a nossa hipótese, usamos células HT-1376, que representam um estádio III e TCCSUP que representam um estádio IV altamente invasivo da doença, e submetemo-las à ativação/inibição da sirtuina 1 com YK-3-237 (1 µM) e EX-527 (1 µM), respetivamente, à inibição do mTOR com rapamicina (0.1 µM) e ao tratamento conjunto com inibição do mTOR e sirtuina1, durante 24 horas.

A viabilidade celular, a proliferação, a toxicidade da membrana e a toxicidade mitocondrial foram avaliadas pelos ensaios do brometo de 3-(4,5-dimetiltiazol-2-il)-2,5-difeniltetrazólio (MTT), sulforrodamina B (SRB), lactato desidrogenase (LDH) e potencial mitocondrial (JC-1), respetivamente. O qPCR foi utilizado para avaliar a expressão de *GLUT3, MCT1, MCT4, LDH, BAX* e *BCL-2* nas células de cada grupo experimental. A ressonância magnética nuclear também foi também realizada no meio celular de cada grupo experimental para analisar a produção e consumo de metabolitos e estabelecer um perfil metabólico. O número de cópias do DNA mitocondrial (mtDNA) foi determinado para as células HT-1376 e TCCSUP expostas aos tratamentos experimentais e a respirometria mitocondrial foi realizada após as células TCCSUP serem tratadas, com o objetivo de analisar o desempenho mitocondrial.

Os nossos resultados mostram que a via da sirtuina 1 promove uma resposta diferencial em relação ao estádio das células de cancro da bexiga, sugerindo que a progressão do cancro da bexiga do estádio III para o estádio IV pode estar associada a um papel dessa mesma via. Este efeito diferencial da sirtuina 1 de acordo com o estádio do cancro da bexiga foi particularmente observado na sua ativação num estádio mais elevado, uma vez que foi relevante para evitar a produção excessiva de lactato por essas células. Os nossos resultados também sugerem que o *GLUT3* pode mediar a resposta diferencial de células de diferentes estádios do cancro da bexiga perante a inibição da via do mTOR. Além disso, os nossos resultados mostram que o tratamento combinado de células TCCSUP com inibição de ambas as vias resultou numa clara redução da viabilidade celular que foi seguida pela

diminuição da densidade celular, ilustrando assim o grande potencial de inibição das duas vias para o tratamento e progressão do cancro da bexiga. O potencial mitocondrial foi severamente deprimido nas células HT-1376 e TCCSUP após a inibição de ambas as vias. Em conjunto, os nossos resultados sugerem que, embora ainda haja uma resposta diferencial das células HT-1376 e TCCSUP ao tratamento combinado com os inibidores da sirtuina 1 e mTOR, as células do estádio altamente proliferativo e invasivo são sensíveis a este tratamento. Assim, o tratamento conjunto de estádios mais elevados do cancro da bexiga com inibidores do mTOR e da sirtuina 1 pode ter efeitos positivos no tratamento desta patologia.

Palavras-chave: cancro da bexiga, sirtuina 1 (SIRT1), mTOR, metabolismo, bioenergética.

4 TABLE OF CONTENTS

4.1 List of figures

4.2 List of tables

5 ABBREVIATIONS

µL	Microliter
µg	Microgram
µM	Micromolar
4E-BP1	Eukaryotic Translation Initiation Factor-Binding Protein 1
Akt	Protein kinase B
ALL	Acute Lymphoblastic Leukemia
ATCC	American Type Culture Collection
BAX	Bcl-2 associated X protein
BC	Bladder Cancer
BCL	B-cell lymphoma
BRCA	Breast Cancer
BSA	Bovine Serum Albumin
ºC	Celsius degree
cDNA	Complementary DNA
CIS	Carcinoma *In Situ*
CML	Chronic Myeloid Leukemia
CNS	Central Nervous System
CO_2	Carbon Dioxide
COPD	Chronic Obstructive Pulmonary Disease
COX	Cyclooxygenase
DMEM	Dulbecco's Modified Eagle Medium
DMSO	Dimethyl sulfoxide
DNA	Deoxyribonucleic acid
EDTA	Ethylenediaminetetraacetic acid
et al.	*et alteri*
FBS	Fetal Bovine Serum
FCCP	Carbonyl cyanide-p-trifluoromethoxyphenylhydrazone
FDA	Food and Drug Admnistration
FKBP12	Protein FK506-binding-protein
FOXO	Forkhead Box
GLUT	Glucose Transporter
H_2O	Water
HCC	Hepatocellular Carcinoma

HCL	Hydrochloric acid
HDAC	Histone Deacetylases
KDAC	Lysine Deacetylases
ITS	Insulin-Transferrin-Selenite
LDH	Lactate Dehydrogenase
LSC	Leukemia Stem Cells
mA	Miliampere
MCT	Monocarboxylate Transporter
mg	Miligram
MIBC	Muscle Invasive Bladder Cancer
mL	Mililiter
mm	Milimeter
M-per	Mammalian Protein Extraction Reaction
mtDNA	Mitochondrial DNA
mTOR	Mammalian Target Of Rapamycin
MTT	3-(4,5-Dimethylthiazol-2-yl)-2,5-Diphenyltetrazolium Bromide
Na_2CO_3	Sodium Carbonate
NF-κB	Nuclear Factor Kappa B
ng	Nanogram
nM	Nanomolar
NMIBC	Non-Muscle Invasive Bladder Cancer
NMR	Nuclear Magnetic Resonance
qPCR	Quantitative Polymerase Chain Reaction
p70S6K	Phosphorylation of p70 ribosomal S6 Kinase
PBS	Phosphate-buffered saline
PCR	Polymerase Chain Reaction
PDK1	Phosphoinositide-dependent Kinase 1
PER2	Period Circadian Regulator 2
PI-4,5-P2	Phosphatidylinositol-4,5 bisphosphate
PI3K	Phosphoinositide 3-kinase
PIP3	Phosphatidylinositol-3,4,5-trisphosphate
PLND	Pelvic Lymphadenectomy
PTEN	Phosphatase and tensin homolog
RNA	Ribonucleic acid

SCC	Squamous Cell Carcinoma
SDS	Sodium dodecyl sulphate
SIRT	Sirtuin
SRB	Sulforhodamine B
TCC	Transitional Cell Carcinoma
TSC	Tuberous Sclerosis
TNBC	Triple Negative Breast Cancer
TNM	Tumour-Node-Metastasis
TopBP1	Topoisomerase 2-binding protein 1
TURBT	Transurethral Resection of Bladder Cancer Tumour
USA	United States of America
WT	Wild-Type

6 INTRODUCTION

6.1 General Topics

6.1.1 Carcinogenesis and energy metabolism in brief

Carcinogenesis, the development of cancer, involves not only the acquisition of several DNA alterations but also cell transformation and cancer initiation. In addition, there is a marked reprogramming of energy metabolism, which is essential to maintain the high proliferation and biomass production needed for division by cancer cells. Indeed, the metabolic profile of cancer cells, specific even for each stage during cancer progression, offers a viable target for treatment that is not subject to high genetic variability (2, 3). Therefore, it is crucial to understand the alterations in cancer metabolism so that it can provide new possible therapies.

6.1.2 Basic aspects of bladder functioning

The bladder is an extraperitoneal muscular organ localized behind pubis symphysis of the pelvis. It acts as a reservoir of urine, which can accommodate 300 – 600 mL in adult age. Its ability to storage and release the bladder contents is due to a complex coordination of neurological, physiological and musculoskeletal functions. The central nervous system sends signals of bladder fullness sensation and necessity to urinate when the urine volume reaches 400 mL. However, the micturition can be delayed voluntarily by contraction of the external urethral sphincter or involuntarily, mostly, when the neural circuit that controls this process suffers injuries, leading to incontinence (4, 5).

The bladder wall is constituted by four layers, which are made of different cellular types. The outermost layer is a fibrous connective tissue, the adventitia which is coated by a fatty tissue that separates the bladder from neighbouring organs. The external layer is followed by the muscular layer that have a complex structure with three directions of smooth muscle bundles. Inside this one there is a thin layer of loose connective tissue with nerves and blood vessels, the submucosa. The innermost one is called mucosa and consists of a transitional epithelium or urothelium, constituted by 3- to 7-cell mucosal layer. The former is where the majority of bladder cancer (BC) cases begin and as the tumour develops through outer layers, is becomes more advanced and more difficult to treat (6, 7).

6.2 Bladder Cancer

6.2.1 Epidemiology and Etiology

Bladder Cancer is the second most common and deadly malignancy of the genitourinary tract. It is the fifth most prevalent cancer in European Union among men and women. Bladder cancer, in male sex, is the third most prevalent in Portugal and the sixth most incident around the world (8, 9). It mostly affects males comparing with females, by a rate ratio of 3:1 (10). In 2017, there were estimated about 79 000 new bladder cancer cases in USA and almost 17 000 people were estimated to die of this disease (11).

This cancer mostly affects people over 55 years and a strong correlation between tobacco smoking and a high risk of tumour development is observed (10-13). However, increased bladder carcinoma risk has also been reported in individuals which occupations are associated with organic chemicals, petroleum products, and dyes (6). Furthermore, the smoking status and the occupational exposure is also related with higher risk of bladder cancer recurrence (14). In developing countries, the schistosomiasis, infection caused by parasitic worms, is responsible for the majority of bladder squamous cell carcinoma (SCC), the rarest cancer in the lower urinary tract. Indeed, in normal epithelia, the total antigen of *S. haematobium* is able to increase proliferation, invasion and to inhibiting apoptosis (6, 8).

6.2.2 Pathophysiology

The bladder cancer type and stage are the most important characteristics to define the cancer treatment and to have a better knowledge of the prognosis.

The urothelial carcinoma or transitional cell carcinoma (TCC) is the most common type of bladder cancer and it develops from the inner layer cells, named transitional cells. It can be described depending on how far it invaded the bladder wall as a non-muscle invasive bladder cancer (NMIBC) or muscle invasive bladder cancer (MIBC). In the first type, the cancer still remains in the inner cell layer and have not grown into deeper barriers. However, if untreated, it might penetrates the basement membrane, invade the connective tissue and adjacent layers, where it can metastasize and progress to the second type, which leads to a more intensive treatment (6, 7, 15, 16). Regarding the Tumour-Node-Metastasis (TNM) classification system to describe how far the tumour has spread, the NMIBC can be classified as Ta, Tis and T1 and the MIBC as T2, T3 and T4 (7, 17). The tumour development and classification are represented in Figure 1. Approximately 15% of the patients with BC are diagnosed with MIBC while 75% present NMIBC form, which has a high potential to develop and invade (18, 19).

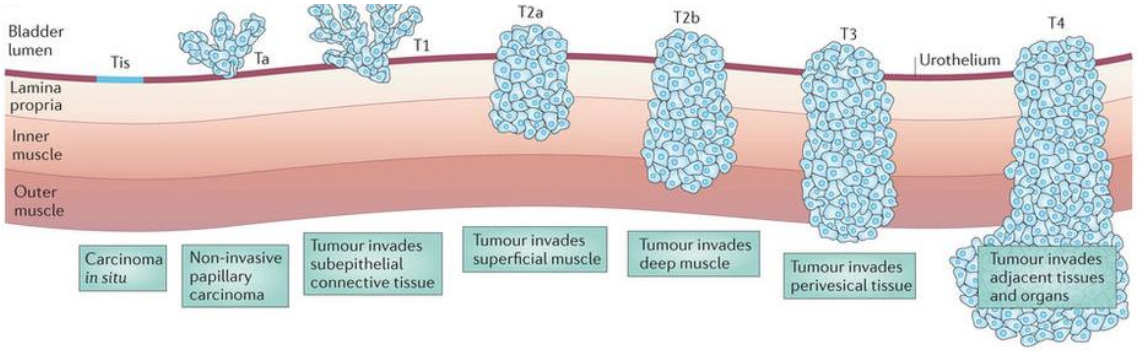

Figure 1: **Bladder Cancer classification according to the TNM system.** Tis: the tumour is flat and growing only in the inner lining layer. Ta: the tumour has grown towards the hollow center but not into the connective tissue. T1: the tumour reached the connective tissue layer but not the muscle layer. T2a: the tumour has invaded the inner muscle layer. T2b: the tumour has grown into the outer muscle layer. T3: the tumour has passed the layer of muscle and invaded the fatty tissue layer that surrounds the bladder. T4: the tumour spread into adjacent organs such as prostate or uterus. (Adapted from Knowles et al. 2015).

The general pathway of TCCs (Figure 2) begins with the development of a papillary tumour. It is characterized by finger-like projections growth, from the inner layer toward the hollow center and mostly without invade into deeper layers. This type of tumour is known as non-invasive papillary cancer. However, a different pathway from TCCs (Figure 2) is the flat carcinoma that spreads along the surface of the bladder and do not grow into its hollow. The popular name for this type of tumour it carcinoma *in situ* (CIS) (6, 16).

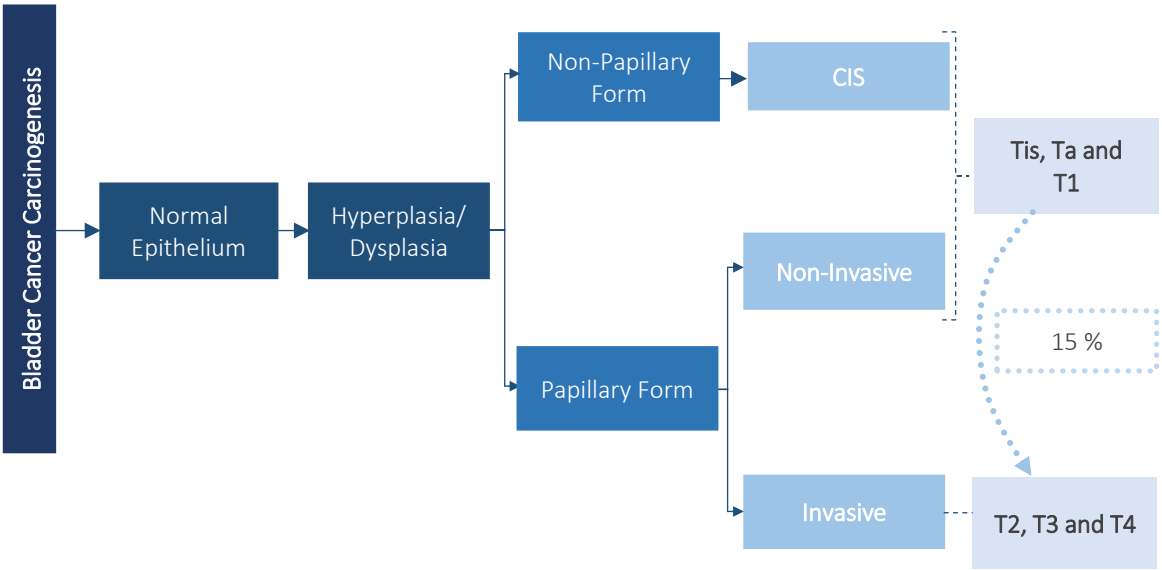

Figure 2: Schematic diagram of TCC carcinogenesis. The urothelium suffers hyperplasia or dysplasia and might develop into a non-papillary or a papillary form. The first one originates the carcinoma in situ. On the other hand, the papillary form can be non-invasive, which might be classified as Ta or T1, or can be invasive, classified as T2, T3 or T4.

Another type of bladder cancer is the squamous cell carcinoma (SCC), derived from the bladder urothelium and with a squamous phenotype. The cells have a flat form, appearing as the cells that are found on the skin surface. SCC is usually invasive and more common in developing countries caused by worm infection (6, 7, 15, 16).

A very rare type of bladder cancer is the adenocarcinoma, estimated as 1% of BC cases. It develops from gland cells that produce and release mucus and other fluids and it is commonly invasive. Less than 1% of BC cases are small cell carcinomas, which are malignant neoplasms that arises from urothelial stem cells and have a diverse neuroendocrine markers expression. Sarcoma, a type of cancer that begins in the bladder muscle, is also very rare (6, 7, 15, 16).

The poor survival of bladder cancer the patients is due to the heterogeneity of intrinsic biological characteristics of the tumour providing it a specific radio- and chemo-resistance (3, 19). It urges to unveil the molecular mechanisms responsible for tumour establishment and progression. That will allow the identification of biomarkers that can either serve as targets for diagnosis or even for treatment.

6.2.3 Diagnostic and Treatment

The bladder cancer diagnostic includes, first of all, urine studies, following by urinary cytology, cystoscopy and upper urinary tract imaging. No blood tests are usually requested specifically for bladder cancer, however, prior to therapy initiation, a general evaluation is needed (6).

Bladder cancer therapeutic differs according to tumour stage. For NMIBC, the treatment begins with transurethral resection of bladder cancer tumour (TURBT) (Fig 3). Subsequent treatment, for lower grade BC, a single postoperative dose of intravesical chemotherapy is performed. Towards high risk BC, an intravesical bacillus of Calmette-Guérin vaccine is mandatory (6).

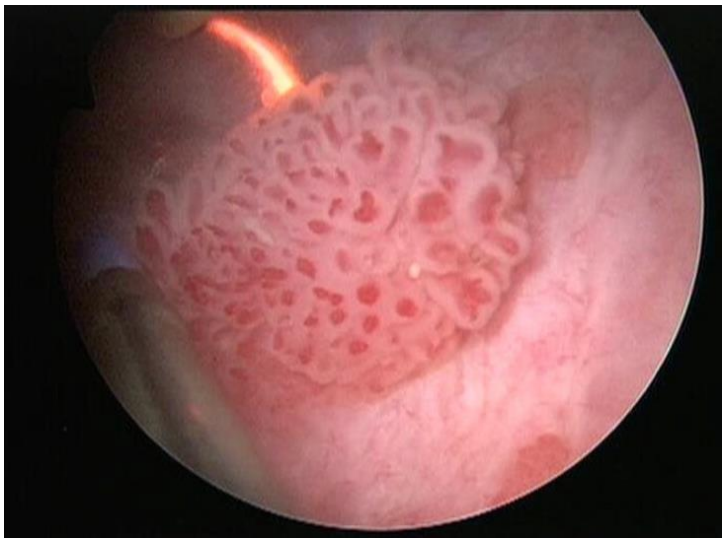

Figure 3: Bipolar transurethral resection of a lateral papillary bladder tumour, allowing a more precise ablation. (From Geavlete et al, 2013 (1))

For MIBC, the treatment is more radical. It follows cystoprostatectomy in men and an anterior pelvic exenteration in women, a bilateral pelvic lymphadenectomy (PLND), generation of a urinary diversion and neoadjuvant chemotherapy. This chemotherapy for bladder cancer may include a set of methotrexate, vinblastine, doxorubicin and cisplatin or the conjugation gemcitabine and cisplatin. The first set has a considerable toxicity and therefore it must be weighed against the expected advantages. Currently, the last is considered the first line treatment for BC. Some bladder cancer treatment drugs have been in use for more than 30 years and demonstrate low effectiveness and high recurrence rate (6). However, FDA has now approved the immunotherapy with PDL1 inhibitors for advanced BC, such as atezolizumab, nivolumab, durvalumab (20). The therapy evolution of the past 30 years for advanced BC is shown in Figure 4.

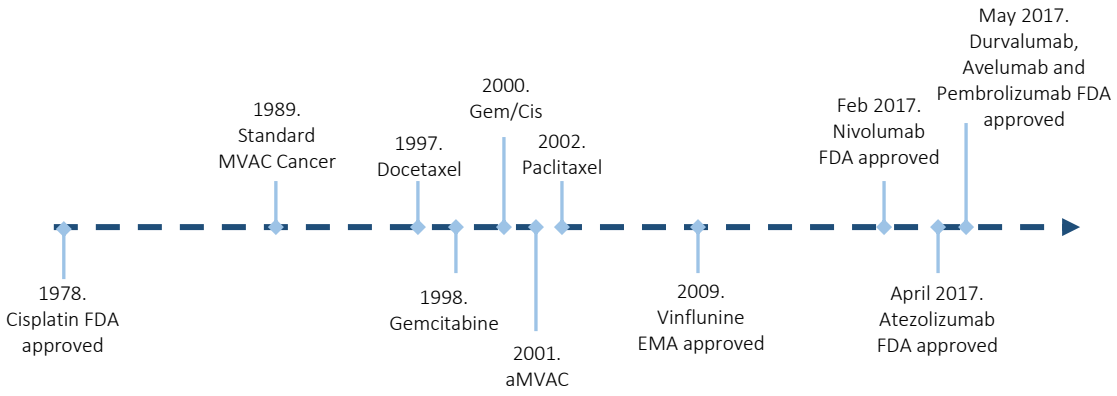

Figure 4: Advanced bladder cancer treatment evolution over the past 30 years. In 1978, cisplatin had FDA approval; 20 years later, it current combined drug, gemcitabine, has been approved and after two years the combined therapy has begun. The course of treatment did not develop much until 2017, when FDA approved immunotherapy agents. (Adapted from George D, 2016)

6.3 Bladder Cancer Metabolism and mTOR signalling: an overview

The metabolic profile of the tumour reflects the activity inherent of each cancer, which can provide information about unique pathways that are activated through its development. There is a hallmark of tumour cells characterized by a peculiar shift to metabolize glucose, even in aerobic conditions, skipping mitochondrial oxidative phosphorylation, a phenomenon named as the Warburg effect (21, 22). This effect has been described in bladder cancer cells and has also been associated with tumour aggressiveness (3, 23). One of the main alterations in bladder cancer cells metabolism is associated with the mammalian target of rapamycin (mTOR) pathway, which is an essential regulator of signalling and protein synthesis and therefore of cell growth and survival (19). It is well documented that aberrant activation of the phosphoinositide-3-kinase (PI3K)/serine-threonine kinase (Akt)/mTOR signalling pathway plays an important role in oncogenesis. Among those, strong growth advantage, metastatic ability and chemoresistance are also correlated with tumour development as well as with poor survival in patients with urothelial carcinoma (3, 24-26). Inhibition of this significant pathway was shown to be favourable in controlling cell growth and invasion of bladder cancer (27-29). This signalling pathway is extremely conserved and it is regulated by a diversity of extracellular signals such as stress conditions, nutrients, hormones and energy levels (30). These signals stimulate tyrosine kinase receptor in recruiting PI3K, which catalyses, through phosphorylation, the conversion of phosphatidylinositol-4,5 bisphosphate (PI-4,5-P2) to phosphatidylinositol-3,4,5-trisphosphate (PIP3). The tumour suppressor phosphatase and tensin homolog (PTEN) has the ability to reverse this reaction, by dephosphorylating PIP3, hence inhibiting signalling progression (30, 31). PIP3 also recruits molecules to the cell membrane, such as the oncogene Akt and phosphoinositide-dependent kinase 1 (PDK1), which are activated through their binding to PIP3 (32). Akt full activation requires the phosphorylation at two different sites by PDK-1 and mTORC2, hereafter, Akt activates mTOR through phosphorylation or inactivating TSC1/TSC2 complex, which negatively regulates mTOR (30, 32, 33). Protein synthesis, cell growth and proliferation is trigged by mTOR through various downstream effectors, by phosphorylation of p70 ribosomal S6 kinase (p70S6K) and the eukaryotic translation initiation factor-binding protein 1 (4E-BP1), enhancing expression levels of glycolytic proteins (3, 30, 33). The last phosphorylation prevents its binding to eukaryotic initiation factor 4E (eIF4E), facilitating eIF4E to promote cap-dependent translation (33).

According to the literature, the mTOR pathway is altered in 72% of bladder cancer cases (34). These alterations involve activating mutations in Pi3K α-subunit (PiK3CA), which are present among 21-25% of MIBC, mutations in Akt, observed in 2-3% of bladder cancer and alterations in TCS1 and TCS2 are detected in 40-50% and 15% of bladder cancer, respectively (32, 34-36). Another event that has been shown to occur in BC is the inactivation

of the tumour suppressor PTEN function, through loss of heterozygosity (LOH) on chromosome 10q, homozygous deletion of PTEN *locus* and inactivating mutations in the PTEN coding region (36-38). All alterations culminate in increased mTOR signalling and resistance of bladder cancer cells to apoptosis. Besides, inactivation of both P53 and PTEN increase the potential of bladder cancer cells to migrate and invade via up-regulation of mTOR signalling and therefore, this is associate with the aggressiveness of the tumour and may be correlate with the patient's poor survival (39). Hence, there are evidence that a better knowledge of the mTOR pathway and the proteins associated may be potential therapeutic targets to counteract cancer progression and aggressiveness. Despite this, until now there is no perfect therapy directed to mTOR and its related proteins suggesting that the multiple sites of mTOR pathway regulation and the diversity of genetic alterations that may regulate this pathway will be very useful to develop novel biomarkers and strategies to avoid cancer establishment, progression or towards personalized medicine to have better prognostics.

6.3.1 mTOR inhibition in bladder cancer

Due to the significant role of mTOR pathway in cancer and particularly in bladder cancer, the mTOR inhibitors have been raising a lot of expectations as potent anticancer drugs. Numerous studies have been focusing in this pathway and trying to find the perfect drug or treatment conjugation for cancer treatment (synthesized in Table 1).

The discovery of rapamycin remotes to 1975 and was firstly described as an antifungal, isolated from the strain *Streptomyces hygroscopicus* from an Easter Island soil sample. It demonstrated to be able to inhibit *Candida albicans*, *Trichophyton granulosum* and *Microsporum gypseum* (40, 41).

The first mTOR inhibitor described was sirolimus, a macrolide antibiotic that demonstrated to have potent immunosupressive and antifungal activity (42, 43). The interest on this drug was kindled even more with subsequent studies proving its antiproliferative effects in human tumour cells (43-45).

The mechanism of action consists in the formation of a complex with the protein FK506-binding-protein (FKBP12), which in turn binds to the FRB domain of mTOR. The relation between mTOR and raptor is prevented and the signal is not transmitted. Consequently, the downstream targets 4EBP1 and p70S6K phosphorylation is inhibited, which results in cell cycle blockage at G1 phase and decreased cell proliferation and metabolism and angiogenesis. The FKBP2-sirolimus complex is mostly associated with mTORC1, however, a higher exposure to this drug demonstrated to be able to disrupt mTORC2 and AKT signalling (42, 46).

The sirolimus therapeutic potential encouraged the pharmaceutic studies to focus in sirolimus analogues and subsequently several mTOR inhibitors (rapalogs) were developed such as temsirolimus and everolimus. These drugs have been tested as anticancer agents and are already approved for the treatment of some cancers. Everolimus is recommended for the treatment of metastatic renal cell carcinoma after failure of sunitinib or sorafenib treatment, breast cancer and pancreatic neuroendocrine tumours (47, 48). Temsirolimus is only indicated for advanced renal cell carcinoma treatment (49).

Chiong et al. investigated the effect of everolimus on human bladder cancer cell lines and in an *in vivo* nude mouse model. They demonstrated that everolimus is able to inhibit the growth of bladder cancer cell lines through mTOR inhibition and to effectively treat the *in vivo* tumours (50). Offering less encouragement, everolimus did not demonstrated any significantly effect in an *in vivo* study from *Vasconcelos-Nóbrega* (51) and colleagues. Moreover, were only observed effects on proliferation and apoptosis in superficial derived bladder cancer lines while in the invasive cell lines, no effect was detected. In a phase II study of everolimus, *Seront et al.* (52) showed not only that the PTEN loss might be related with the drug resistance but also that this agent has clinical activity in advanced TCC. In addition, everolimus showed to have antiangiogenic properties. In a prospective study, everolimus was associated with low rate of severe adverse effects and also with prolonged progression-free survival in progressive advanced pancreatic neuroendocrine tumours (53).

Korfel et al. (54) tested temsirolimus in patients with relapsed or refractory primary central nervous system lymphoma as a phase II trial. They found that temsirolimus had clinical activity as a single-agent at a weekly dose, nevertheless, the results were short lived. With the aim to know the safety of temsirolimus in metastatic renal cell carcinoma, *Levakov et al.* (55) monitored the renal function during this therapy and concluded that temsirolimus had no important influence on the remaining renal function.

Despite the studies that have been performed, there is still no perfect therapy for bladder cancer. The results are not promising and have demonstrated that the use of rapalogs as single agents is not that effective as expected in most tumours. The currently therapeutic used in bladder cancer treatment is more than 30 years old. The idea of a combined treatment appeared to improve therapy efficacy. Several investigations have been performed, trying to target not only the mTOR protein itself but also other related biological pathways. Because of the heterogeneity founded in mTOR inhibition therapy in bladder cancer cells, the combination has been tested.

Dong et al. (56) aimed to investigate the anticancer effects of the therapy combination of everolimus and paclitaxel in human cervical cancer cells. Indeed, they demonstrated that

the combinatorial therapy had better results than the single treatment of everolimus or paclitaxel alone, suggesting a novel therapeutic method for cervical cancer. In addition, *Baselga et al.* (57) showed that the combination of everolimus with endocrine therapy improved progression free-survival in patients with hormone-receptor-positive advanced breast cancer.

Although Ku0063794 inhibits both mTORC1 and mTORC2 and everolimus only inhibits mTORC1, *Lee* and colleagues (58) aimed to understand the anticancer effects of both drugs combination in *in vitro* and *in vivo* models of hepatocellular carcinoma. Indeed, they demonstrated that these anticancer efficacy was enhanced by the combination therapy. Besides, they found that these results were obtained through a decrease in autophagy, which was prompted by sirtuin 1. Furthermore, still highlighting the autophagy process as a cellular survival mechanism, *Singla* and *Bhattacharyya* (59) explored the therapy combination of chloroquine as an autophagy inhibitor with temsirolimus. Towards renal cell carcinoma, they observed an improved antitumor activity in epithelial-mesenchymal transition cells, using this therapy regimen. In another study, from *Lin* and colleagues (60), the mTOR inhibition by everolimus was combined with the autophagy inhibition by bafilomycin A1. This strategy significantly increased apoptosis in bladder cancer cells and therefore, was suggested as a potential treatment for bladder cancer. A greater antiproliferative effect was observed in bladder cancer cell lines combining gemcitabine with everolimus. In addition, *Pinto-Leite et al.* (61) found increased apoptotic cells and frequency of DNA damage in bladder cancer cell lines when treated with both agents simultaneously.

Juengel et al. (62) tested the combinatorial therapy of temsirolimus with valproic acid an HDAC inhibitor and suggested it as an innovative strategy for this cancer.

Although temsirolimus did some difference in cell proliferation, apoptosis and autophagy in bladder cancer cell lines, *Pinto-Leite et al.* (63) also showed that the anticancer effects were improved by the combination of chemotherapy based in cisplatin or gemcitabine with temsirolimus.

Taking this into account, it can be concluded that mTOR is not the only responsible for tumour aggressiveness. In fact, even with mTOR pathway inhibition, cancer cells have still escaping pathways that promote their development. Therefore, it is particularly important to found novel therapeutic targets in bladder cancer.

Table 1: Summary of *in vitro*, *in vivo* or clinical trials studies for the treatment of different cancers by mTOR inhibitors alone or in combination with other agents.

Name [1]	**Disease**	**Study type**			**Combination** [2]	**Dose**	**Reference**
		*In vitro**	*In vivo***	Clinical Trial			
Sirolimus	Pancreatic Cancer	X	-	-	-	10 nM-50 nM	*Dai et al.* (44)
		X	-	-	FTY720	[1] 2 µM-20 µM [2] 1 µM-15 µM	*Shen et al.* (45)
Everolimus	Bladder cancer	X	X	-	-	*0.1 nM-100 nM ** 5 mg/kg	*Chiong et al. (50)*
		X	X	-	-	*0.05 µM-2 µM ** 5 mg/kg	*Vasconcelos-Nóbrega et al. (51)*
		-	-	X	-	10 mg/daily	*Seront et al. (52)*
		X	-	-	Gemcitabine	[1] 0.05-2 µM [2] 100 nM	*Pinto-Leite et al. (61)*
		X	-	-	Bafilomycin A1	[1] 1 or 5 µM [2] 200 nM	*Lin et al. (60)*
	Human cervical cancer	X	-	-	Paclitaxel	[1] 100 nM [2] 100 nM	*Dong et al. (56)*
	Advanced breast cancer	-	-	X	Exemestame	[1] 10 mg/daily [2] 25 mg/daily	*Baselga et al. (57)*
	Hepatocellular Carcinoma	X	X	-	Ku0063794	*[1]100 nM *[2]1 µM ** [1] 0.5 mg/kg ** [2] 1 mg/kg	*Lee et al. (58)*
Temsirolimus	Primary or refractory CNS lymphoma	-	-	X	-	25 mg/weekly 75 mg/weekly	*Korfel et al. (54)*
	Metastatic Renal Cell Carcinoma	-	-	X	-	25 mg/weekly	*Levakov et al. (55)*
	Renal Cell Carcinoma	X	-	-	Chloroquine	[1] 10 µM [2] 50 µM	*Singla et al. (59)*
	Bladder cancer	X	-	-	Valproic Acid	[1] 1 µM [2] 1 M	*Juengel et al*. (62)
		X	-	-	[2] Cisplatin [3] Gemcitabine	[1] 500-4000 nM [2] 2.5 µg/mL [3] 100 nM	*Pinto-Leite et al. (63)*

6.4 Emerging role for sirtuin 1 in cancer cell metabolism

Sirtuins were firstly described as part of Sir2-like proteins family and discovered by *Klar et al*. in 1979 (64). They are a highly conserved family of enzymes present in different organisms, from archaebacteria to eukaryotes (65, 66). Sirtuins are a special class of lysine deacetylases (KDACs) enzyme family, a class III of histone deacetylases (HDACs), which use the NAD^+ as a cofactor to cleave off not only acetyl groups but also acyl groups from the ε-amino group (66, 67). Besides of histones, a diverse group of non-histone proteins was found to serve as sirtuins substrates in the last years, including P53 (68), NF*k*B (69) and α-tubulin (70).

Per phylogenetic analyses, sirtuins were classified in five different classes, denominated I, II, III, IV and U, the last contains predominantly sirtuins from Gram-positive bacteria (65). There are seven mammalian sirtuins, named from 1 to 7, which belong to classes classified from I to IV (Table 2). This family is characterized by a highly conserved 275 amino acid catalytic core and the subcellular localization differs in specific localization sequences, regulated by C- and N-terminal, that together are responsible for their different binding partners and metabolic functions (65, 71). In line with literature, SIRT1 and SIRT2 were reported to have the ability of intercalating between nucleus and cytoplasm, nevertheless SIRT1 is the most important nuclear sirtuin and SIRT2 the most significant cytosolic sirtuin (71, 72). SIRT1 has been implicated in diverse cellular processes and diseases, however, its role in cancer, particularly in bladder cancer, is not well described. SIRT3 is a mitochondrial sirtuin, as well as SIRT4 and SIRT5, however it was already described the presence of an isoform of SIRT3 in the nucleus (73-75). SIRT6 is, exclusively, a nuclear sirtuin and SIRT7 is confined to the nucleolus and it was also found, by Kiran S. et al., its presence in the cytoplasm (75-77). The class I sirtuins, SIRT1-3, have a very strong activity of deacetylation and cleave off others acyl groups as well. On the other hand, the sirtuins of classes II – IV have a limited deacylase activity (66).

Table 2: Class and cell localization of sirtuins isotypes.

Class	Isotype	Localization
I	SIRT1	Nucleus + Cytoplasm
	SIRT2	Nucleus + Cytoplasm
	SIRT3	Nucleus + Mitochondria
II	SIRT4	Mitochondria
III	SIRT5	Mitochondria
IV	SIRT6	Nucleus
	SIRT7	Nucleolus + Cytoplasm

Sirtuins are known to be involved in a wide range cellular processes such as aging (78, 79), metabolism (80-82), cellular redox balance (78), apoptosis (82, 83), tumorigenesis (81, 84, 85), transcription (86, 87) and inflammation (88). Recently, sirtuins have been also implicated in the pathogenesis of several diseases such as cancer (89, 90), type 2 diabetes (91) and neurodegenerative diseases (92). Among the several characteristics associated with the pathogenesis of these diseases, the dysregulation of cellular metabolism represents a relevant common feature highlighting a possible intervention for sirtuins.

In addition to the role of sirtuins as metabolic regulators, these proteins are essential in the regulation of de genomic stability, therefore, they are potential candidates to regulate tumorigenesis (93, 94). However, among the diverse sirtuin isotypes and their different functions, their role in cancer development is controversial. Some isotypes can act as tumour suppressors, such as SIRT2, 4 and 6; act as an oncogene, such as SIRT5 and 7 or have both functions such as SIRT1 and 3 (95).

6.5 Sirtuin 1

SIRT1 is the isotype best characterized among the mammalian sirtuins. Due to the double cellular localization, this sirtuin is able to interact with diverse nuclear and cytoplasmic substrates, to date more than 50 have been discovered (66). It is intimately linked to transcription regulation via deacetylation of histones H1(96), H3(96) and H4 (96), directly, or via deacetylation of transcription factors such as NF-κB (97), FOXO1 (98) and FOXO4 (99), indirectly. These phenomena on transcriptional regulation have an important impact on diverse cellular processes (Figure 5).

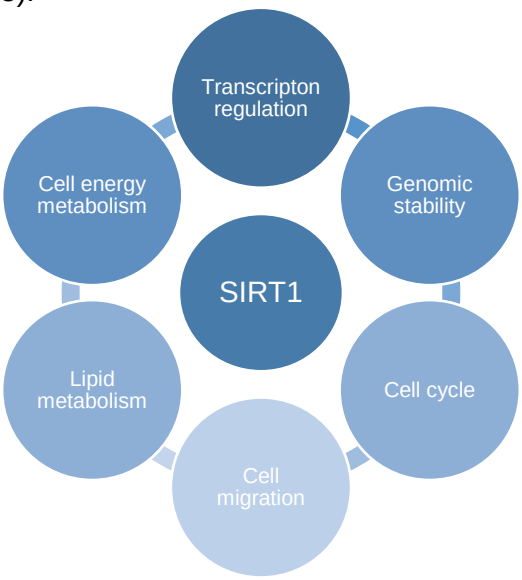

Figure 5: SIRT1 evolvement in diverse cellular processes. Since SIRT1 is able to interact with different substrates, it has an important role in transcription regulation, cell energy, lipid metabolism, genomic stability, cell cycle and cell migration.

Particularly, SIRT1 coordinates the formation of heterochromatin by deacetylating H1K23Ac, H3K9Ac and H4K16Ac and by promoting the methylation of H3K9me3, through Suv39h1, the histone methyltransferase of the chromatin organization. These events are crucial to the chromatin regulation, structure and epigenetics (96, 100). Also, SIRT1 has been reported to have an important impact in DNA repair and genome stability maintenance, which are essential for preserving the fidelity of the genomic information. *Wang et al.* (101) showed that SIRT1$^{-/-}$ embryos had more chromosomal abnormalities and reduced DNA repair than wild-type (WT) embryos. *Yuan et al.* (102) showed that SIRT1 is associated with the function of nijmegen breakage syndrome protein, which is a checkpoint factor involved in the detection of DNA damage and the activation of DNA repair. In addition, a relation between SIRT1 and KU70 was found, since the acetylation condition of this protein inhibits mitochondrial apoptosis and induces DNA repair (103).

However, SIRT1 not only is involved in chromatin regulation and DNA repair, but also in multiple metabolic processes. Since the catalytical activity of SIRT1, as for others sirtuins, is dependent on NAD^+ presence, the SIRT1's activity is intimately linked with the energetic state of the cell. SIRT1 is capable of positively regulate the liver X receptor, through deacetylation, and consecutively modulate the biosynthesis of cholesterol and other factors related with lipid metabolism (104). In addition, deacetylation and activation of acetyl-CoA synthetase 1 is associated with an increase of endogenous fatty acid synthesis (105). Also, deacetylation of FOXO1 is linked to an increase in adiponectin transcription, which has the ability to modulate glucose regulation and fatty acid oxidation (106).

Furthermore, SIRT1 interferes with cell cycle and migration through deacetylation of DNA Topoisomerase 2-binding protein 1 and cortactin, respectively (107, 108). Interestingly, it regulates the circadian clock by deacetylate the period circadian regulator 2 (PER2), which plays an important role in circadian rhythms (109).

SIRT1 is associated with diverse biological functions and thus, as expected, it is also associated with numerous diseases. Its presence can be related either with pathogenesis or inhibition of disease's establishment and development.

In the recent years, researchers have been studying a possible link between SIRT1 and diabetes. For instance, *Lou et al.* (110) found decreased SIRT1 activity in early type-2 diabetic hearts and *Mortuza et al.* (111) attributed a protective function to SIRT1, since they showed that its reduction is associated with renal and retinal injury.

Another interesting association is between SIRT1 and psoriasis, since its expression and activity is decreased in fibroblasts from psoriatic patients (112, 113). It has already been

studied the use of SIRT1 activator as psoriasis treatment in patients with favourable results (114), therefore further studies are still warranted.

Sepsis is a life-threatening condition that affects thousands of people and it has been associated with SIRT1 due to its ability to interfere with cell energy metabolism. Khader et al. (115) proposed SRT1720, a SIRT1 activator, as a treatment strategy for sepsis, since this drug mitigates organ injury in septic mice and decreases proinflammatory cytokines. However, years before, another group found that SIRT1 inhibition might be a potential sepsis treatment option for the hypoinflammatory phase, since it enhanced immunity (116).

Recently, some studies focused in the relation between SIRT1 and chronic obstructive pulmonary disease (COPD). They found that SIRT1 levels were decreased in serum COPD patients comparing with control patients, without COPD, proposing the hypothesis of SIRT1 as a biomarker for this pathology (117). Months later, *Wang et al.* (118), proposed resveratrol, a SIRT1 activator, as a treatment option for COPD, since they found therapeutic effects which could be correlated with the reduction of oxidative stress and inflammatory response.

Although many advances have been made in trying to understand the development of neurodegenerative diseases and to find a perfect therapy, there is still no treatment for brain disorders, such as Huntington's disease, Alzheimer's disease and Parkinson's disease. However, SIRT1 has been shown to be involved in diverse neuronal processes and consequently, several studies have been developed in this field (119). Indeed, *Jiang et al.* (120) described a neuroprotective effect of SIRT1 overexpression in mammalian Huntington's disease models, since it improved motor function, decreased brain atrophy and reduces the metabolic abnormalities mediated by mutant-HTT. Furthermore, they found that mutant-HTT interacts with SIRT1, inhibiting its deacetylase activity and resulting in hyperacetylation of SIRT1 substrates, which inhibits the survival functions. Conversely, the SIRT1 overexpression contradicted this effect. In another study, performed by *Jeong et al.* (121), the overexpression of SIRT1 also improve survival, whereas its knockout intensified the brain pathology in Huntington's disease mouse model, through BDNF transcription repression. Despite the neuroprotective effect induced by SIRT1 overexpression, the opposite outcome was also found. *Smith et al.* (122) showed that selisistat, a SIRT1 inhibitor supressed the Huntington's disease in cell and animal models, suggesting that SIRT1 inhibition can serve as therapeutic treatment. In a matter of fact, the inhibition of SIRT1 has already completed phase I and II in clinical trials for Huntington's disease treatment, suggesting this drug as a candidate for further disease's clinical trials (123, 124).

SIRT1 has been linked to cancer through the regulation of many essential factors that play an important role in carcinogenesis. Among these, P53 (68), KU70 (125) and FOXO (126) proteins emerged as essential. The deacetylation of these tumour suppressors promotes their inactivation, which leads to an antiapoptotic effect and therefore to an oncogenic role. Another link of SIRT1 to cancer is associated with the β-catenin/WNT signalling, since β-catenin is the main effector involved in this pathway and it is responsible to regulate diverse cellular processes. Alterations in this way have been found in many cancers, such as colorectal, breast and ovary cancers and melanoma.

SIRT1 was found to be overexpressed in different types of cancer. *Huffman et al.* showed that this sirtuin isotype was increased in mice with adenocarcinoma and in human prostate cancer cells, suggesting SIRT1 as a tumour promoter (127). In another study, about Chronic Myeloid Leukaemia (CML), *Yuan et al.* (125) showed that SIRT1 activation by BCR-ABL is pivotal for CML development, promoting cell survival and proliferation through deacetylation of different substrates, including P53, FOXO1 and KU70. An interesting experiment, performed by *Wang et al.*(128), demonstrated that although SIRT1 might be involved in DNA repair, it can promote the acquisition of genetic mutations that improves drug resistance in CML cells.

Furthermore, SIRT1 expression was found to be correlated with tumour invasiveness and shorter disease-free survival in triple negative breast cancer (TNBC), suggesting that SIRT1 can be a prognostic indicator and/or a therapeutic target (129). The SIRT1 overexpression and its association with short survival was also observed in patients with endometrial carcinoma, where *Asaka et al.* (130) found that this up-regulated SIRT1 increased the proliferation of endometrial carcinoma cell lines and the resistance to cisplatin and paclitaxel. Therefore, it was suggested that SIRT1 can be linked with the acquisition of an aggressive behaviour.

Relatively to retinoblastoma, SIRT1 functions are associated to the tumour suppressor retinoblastoma (Rb), whose activity is regulated by phosphorylation and acetylation at different residues. SIRT1 interacts with Rb through its deacetylation, inhibiting Rb-dependent apoptosis (85).

In a different function, SIRT1 was associated with breast cancer, since it is involved in the suppression of the apoptosis inhibitor, survivin, which is overexpressed in cancers. In normal cells, BRCA1, a tumour suppressor particularly vital in breast and ovarian cancer, is located at SIRT1 promoter and is able to increase the expression of this sirtuin, which in turn, through deacetylation, inhibits survivin expression (131), suggesting a suppression activity. This hypothesis is corroborated by the role of SIRT1 in the regulation of chromatin and genome

stability while being also involved in DNA repair and multiple metabolic processes. In an interesting study, *Herranz et al.* found that old SIRT1-tg mice, overexpressing SIRT1, exhibit lower levels of DNA damage, decreased expression of *P16* (which is a gene associated with aging) and fewer spontaneous sarcomas and carcinomas. In general, old SIRT1-tg mice expressed a better health than WT mice. Furthermore, the group that overexpressed SIRT1 developed a metabolic syndrome-associated liver cancer, in which those mice showed a reduced susceptibility to liver cancer and a greater hepatic protection when compared with WT mice (132). Another interesting interaction is between SIRT1 and the oncogene c-Myc. This binds to the SIRT1 promoter, inducing sirtuin overexpression, however, *Yuan et al*. found that SIRT1 deacetylates c-Myc and therefore reduces c-Myc target gene expression and its cellular transformational ability. Hence, it was suggested that SIRT1 can have a tumour suppression function through a c-Myc-SIRT1 feedback loop (133).

SIRT1 deacetylates β-catenin and consequently its localization to the nucleus is supressed, reducing the ability of this protein to activate transcription, hence, SIRT1 has also been proposed as a tumour suppressor due to that function (84).

P53 protein is a tumour suppressor crucial for cell cycle checkpoint regulation and apoptosis. It was reported that SIRT1 has the ability to inactivate P53 through deacetylation and consecutively it promotes the inhibition of P53-dependent apoptosis (68, 89). These observations led us to suggest that SIRT1 expression may increase cancer risk by inhibiting P53-induced apoptosis. Additionally to P53 deacetylation, *Bereshchenko et al*. (134) demonstrated that SIRT1 deacetylates the proto-oncogene BCL6, which is involved in B-cell lymphoma and therefore is also able to decrease the effects of P53 tumour suppression.

With regard to FOXO proteins, a family of transcription factors that plays an important role in cell cycle arrest, DNA repair and apoptosis, are also involved in tumour suppression. *Brunet et al.* (126) demonstrated that SIRT1 deacetylates FOXO3, inhibiting its ability to induce apoptosis after stress conditions and in turn, it increases its ability to induce cell cycle arrest. Nevertheless, in $SIRT1^{-/-}$ cells, FOXO3 is not so capable to promote cell cycle arrest.

Overall, these studies point towards a possible role for SIRT1 in cancer establishment and progression. This is an hypothesis that is still under debate and remains unknown.

6.6 The controversial use of SIRT1 in cancer therapeutics

Since the discovery of SIRT1 as a potential therapeutic target, due to its overexpression in many tumours and its ability to inactivate some tumour suppressor proteins, SIRT1 drug inhibitors have been widely studied as a possible anti-cancer agent. However, during the last years, a controversial role of SIRT1 in tumorigenesis has been demonstrated, since it has been reported to act as a tumour promoter and as a tumour suppressor (Figure 6). This apparent contradictory function suggests that SIRT1 activity may diverge in type and grade of the tumour and depend on the factors that regulate its function (95, 135). SIRT1 has the ability to promote genomic stability and to block cancer metabolism and therefore it might prevent tumour development. However, SIRT1 is also able to inhibit P53 or FOXO proteins and this activity might be beneficial to cancer cells survival instead of induce cancer cells death. Currently, SIRT1 inhibitors (Table 3) and activators (Table 4) are both available and can be used either alone or in combination with other drugs.

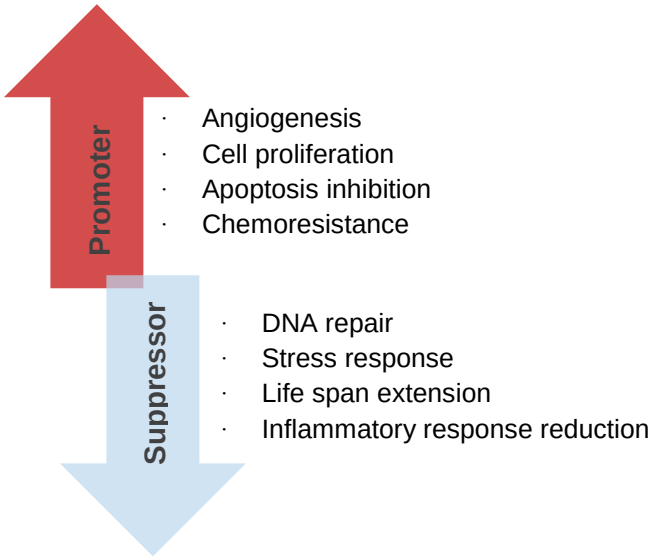

Figure 6: SIRT1 evolvement in tumorigenesis, acting as a tumour promoter or suppressor. There are indicated some different SIRT1 functions associated with both roles.

6.6.1 SIRT1 Inhibitors

The characterization of SIRT1 inhibitors in cancer cells or animal models has been providing some hope for cancer treatment. The first SIRT1 inhibitor capable of promoting anticancer effects in xenografts models was discovered one decade ago by *Heltweg et al.* (136) and it showed the ability of inhibiting both SIRT1 and SIRT2. The group studied the drug in Burkitt lymphoma cells and xenografts models, where they found that this treatment induced apoptosis and inhibited cell growth, through hyperacetylation of BCL6 and P53. After this discovery, there were made studies to analyse cambinol antitumor properties in cell lines and orthotopic xenograft HCC models (137). This discovery also promoted new investigations to compare this compound to tenovin-6 (138) and benzimidazoles (139) in several cancer cell lines.

Additionally to the discovery of the role between SIRT1 and BCR-ABL in CML, *Yuan et al.* (125) proposed a combined treatment with imatinib and SIRT1 inhibition. This proposal was further confirmed by *Li et al.* (140), who showed the overexpression of SIRT1 in leukemia stem cells (LSC) and demonstrated that the inhibition of this sirtuin isotype not only promoted apoptosis in LSC chronic phase and reduced their growth but also increased the activation of P53 in its acetylation and transcriptional activity. In acute lymphoblastic leukemia (ALL), *Jin et al.* (141) discovered an increased level of SIRT1 in primary ALL cells compared with control cells and they found that tenovin-6, a SIRT1 inhibitor, induces apoptosis in ALL cells also through the expression of tumour suppressor genes. Tenovin-6 was also tested by *Dai et al.* (142) in uveal melanoma (UM), since this drug showed to be able to induce apoptosis, to inhibit cell growth and to kill cancer stem cells in uveal melanoma cell lines. Discovered by *Lain et al.* (143), tenovin-6 is able to inhibit SIRT1 but also the SIRT2, a characteristic that is also intrinsic to cambinol and benzimidazole and therefore, the double inhibition of these medicines can induce additional effects to those intended.

Considering another agent to chemotherapy, isoalantolactone, a SIRT1 inhibitor, was tested in two breast cancer cell lines by *Li et al.* (144) in which induced cell apoptosis via downregulation of SIRT1. In addition, this agent proved to be a potential anti-cancer treatment for head and neck squamous cell carcinoma, since it induced apoptosis and cell cycle arrest in G1 phase (145). In human lung squamous carcinoma, isoalantolactone also demonstrated promising results. In a study led by Jin and colleagues, this drug promoted intrinsic apoptosis in this cancer cell lines via P53 signalling pathway.

Years ago, *Zhang et al.* (146) reported a new small molecule that effectively inhibits SIRT1, denominated inauhzin. They found that this drug, through inhibition of SIRT1, could reactivate P53 and promote P53-induced apoptosis in cell lines and that was able to inhibit cell proliferation and repress the growth of xenograft tumours without induce toxicity to normal

tissues. Another group, tested this same drug combined with nutlin3 in human colon and lung cancer cell lines, where they also observed the cell growth inhibition and the promotion of apoptosis (147).

In 2005, *Napper et al.* (148), from Elixir Pharmaceuticals, discovered a potent and selective SIRT1 inhibitor, denominated as EX-527. This compound is able to inhibit SIRT1 with an IC_{50} value of 98 nM, thus representing a great advantage over other drugs mentioned above. Moreover, this compound has been widely tested in cellular and animal models with the aim of understanding its effects. Indeed, Smith et al. (122) showed that EX-527 can effectively supress the Huntington's disease in different animal and cell models, suggesting it as a potential therapeutic treatment. In pancreatic cancer, *Oon et al.* (149) found distinct effects of EX-527 between *in vitro* and *in vivo* studies, the first ones having better results with reduction of proliferation and increased sensitivity to gemcitabine treatment. Another experiment with EX-527 was tested in endometrial carcinoma, which resulted in suppression of cell proliferation, of tumour growth and cisplatin resistance. Additionally, they did not observed any adverse effects in the mice they tested, suggesting this SIRT inhibitor, a possible treatment agent (130).

Table 3: Summary of *in vitro* or *in vivo* studies for the treatment of different cancers by SIRT1 inhibitors alone or in combination with other agents.

Name [1]	**Disease**	**Study Type**		**Combination** [2]	**Dose**	**Reference**
		In vitro*	In vivo**			
Cambinol	Hepatocellular Carcinoma	X	X	-	*25 µM-100 µM **100mg/kg	*Portmann et al.* (137)
Tenovin-6	Acute Lymphoblastic Leukemia	X		-	*1 µM-10 µM	*Jin et al.* (141)
	Uveal Melanoma	X			*2.5 µM-15 µM	*Dai et al.* (142)
	Chronic Myelogenous Leukemia	X	X	Imatinib	*[1]0.5 µM-2 µM [2]2.5 µM **[1]50 mg/kg [2]200 mg/kg	*Li et al.* (140)
	Colon Cancer	X	X	Oxaliplatin	*[1]2 µM-10 µM [2] 2 µM ** [1]30 mg/kg [2]5 mg/kg	*Ueno et al*. (150)

Isoalantolactone	Breast Cancer	X		-	5 µM-15 µM	*Li et al.* (144)
	Head and Neck Squamous Cell Carcinoma	X		-	25 µM-50 µM	*Wu et al.* (145)
	Lung Squamous Carcinoma	X		-	20 µM-40 µM	*Jin et al.* (151)
Inauhzin	Non-smal-cell Lung Carcinoma/ Colon Cancer	X	X	Nutlin3	*[1]1 µM [2]4 µM-10 µM **[1]15 mg/kg [2]150 mg/kg	*Zhang et al.* (147)
EX-527	Endometrial Carcinoma	X	X	Cisplatin	*[1] 1 µM [2] 20 µM **[1] 10 mg/kg [2] 5 mg/kg	*Asaka et al.* (130)
	Pancreatic Cancer	X	X	Gemcitabine	*[1] 1 µM [2] 4 nM **[1] 10 mg/kg [2] 25 or 50 mg/kg	*Oon et al.* (149)

6.6.2 SIRT1 Activators

Due to the controversial role of sirtuin 1, diverse activators were tested after discovered. The first tests were made by *Howitz et al.* (152), who showed the activation of SIRT1 mediated by resveratrol and which extended the lifespan of *Saccharomyces cerevisiae*. However, years before, *Jang et al.* (153) had already investigated the role of resveratrol in cancer, which concluded that this compound had cancer chemopreventive activity *in vitro* and *in vivo*. Since then, several studies have been made to try to use resveratrol as a therapeutic agent to different types of tumour (154-157). Nevertheless, this compound is also able to inhibit the COX1 activity and reduce the COX2 (153, 157) and therefore, it can promote different effects to those anticipated.

Sirtris Pharmaceuticals intensively studied SIRT1 activators, which resulted in the discovery of several compounds, including the SRT1720 (158). This highly potent drug was investigated in both cellular and animal models and demonstrated to have potential benefits suppressing inflammation, improving insulin sensitivity and extending lifespan (159, 160). However, this drug was identified also as a potent SIRT3 inhibitor, which may result in altered outcomes (161). Furthermore, SRT1720 was described to be able of promoting tumour cell migration and lung metastasis of breast cancer in mice models (162).

A potent SIRT1 activator, YK-3-237, was described by *Kong* and colleagues (163) as an anti-proliferative agent, capable of inhibit human cancer cell growth and angiogenesis, with minimum values, within a range of 10 to 200 nM. Indeed, *Yi et al.* (164) demonstrated that the

proliferation of triple negative breast cancer cells was inhibited by this SIRT1 activator. However, there does not exist a lot of studies based on this activator and therefore, more investigations are needed.

Table 4: Summary of *in vitro* or *in vivo* studies for the treatment of different cancers by SIRT1 activators alone.

Name [1]	**Disease**	**Study type**		**Dose**	**Reference**
		In vitro*	In vivo**		
Resveratrol	Colon Cancer		X	200 µg/kg	*Tessitore et al.* (155)
	Neuroblastoma	X	X	*25 µM **40 mg/kg	*Chen et al.* (156)
YK-3-237	Triple Negative Breast Cancer	X		1 µM	*Yi et al.* (164)

Bladder cancer has particular alterations, which play an important role in the progression of the disease. Naturally, there is much more to understand about the role between SIRT1 and carcinogenesis, however the studies that have been made with SIRT1 modulators demonstrate that they might have an important role in cancer therapies.

7 AIM OF THE PROJECT

The bladder cancer high incidence, its high recurrence rate and the patient's poor survival expectancy led us to develop this project. Bladder cancer heterogeneity is mediated by several signalling pathways. The mTOR pathway is altered in the majority of bladder cancer cases, however there is still no suitable therapy directed to this pathway. Interestingly, the role of SIRT1 in carcinogenesis is a matter of controversy since it acts as a tumour promoter or suppressor suggesting that SIRT1 has different functions according with the type and grade of the tumour. Herein, we hypothesize that SIRT1 has a role in bladder cancer progression and interacts with mTOR pathway and mitochondrial biogenesis. We intended to use HT-1376 cells, which represent a stage III and TCCSUP which represent a highly invasive stage IV of the disease, and expose them to SIRT1 modulators and to mTOR inhibiton, combined or alone.

The main goals of this project are: (I) understand the role of SIRT1 in bladder cancer cells from different stages, (II) understand the mTOR and SIRT1 interplay in bladder cancer development, (III) determine the involvement of SIRT1 in these bladder cancer cells metabolism, (IV) test if the interaction between SIRT1 and mTOR pathways is correlated with mitochondrial dynamics and biogenesis. As secondary goals, we aim to understand if mTOR and SIRT1 interplay might be implicated in apoptosis in these bladder cancer cells.

8 METHODS

8.1 Reagents

Dulbecco's Modified Eagle Medium (DMEM), Bovine Serum Albumin (BSA) and trypsin-EDTA were obtained from Sigma Aldrich (MO, USA). Fetal Bovine Serum (FBS) were puchased from Biochrom (Germany). EX-527 and rapamycin were purchased from Alfa Aesar (USA) and YK-3-237 from Biogen (USA).

5,5′,6,6′-tetrachloro-1,1′,3,3′-tetraethylbenzimidazolylcarbocyanine iodide (JC-1) was obtained from Invitrogen (UK). Mammalian Protein Extraction Reagent (M-PER), BCA Protein and Lactate Desidrogenase (LDH) were obtained from Thermo Scientific (Denmark). Sulforhodamine B (SRB) was purchased from Biotium (CA, USA) and 3-(4,5-Dimethylthiazol-2-yl)-2,5-Diphenyltetrazolium Bromide (MTT) from Amresco (OH, USA). Dried milk was obtained from Regilait (Saint-Martin-Belle-Roche, France). Dimethyl sulfoxide (DMSO) was obtained from Bimake (Germany). Other reagents were purchased from Sigma-Aldrich (MO, USA), unless stated otherwise.

8.2 Bladder cancer cell lines

The human bladder cancer cell lines TCCSUP and RT4 were purchased from Leibniz Institute DSMZ-German Collection of Microorganisms and Cell Cultures (Braunschweig, Germany). The HT-1376 cell line was obtained from American Type Culture Collection (ATCC), USA.

RT4 cell line was established from a human transitional cell papilloma, classified as grade II, of a 63 year-old man. TCCSUP cell line was obtained from a transitional cell carcinoma, highly invasive of grade IV, of a 67 year-old woman. HT-1376 cell line was obtained from a grade III carcinoma of a 58 year-old woman. All cell lines have epithelial origin.

Cells were cultured in 75 cm^2 flasks (#156499, Thermo Scientific, Denmark) in DMEM supplemented with 5% FBS, 4.5 g/L glucose (Sigma-Aldrich, Germany), 7.14 g/L HEPES, 2.4g $NaCO_3$, 1% antibiotic containing penicillin-streptomycin and 500 µL of gentamicine (50 mg/mL, Sigma-Aldrich, Germany). The cultures were maintained in sterile conditions at 37ºC with 5% CO_2.

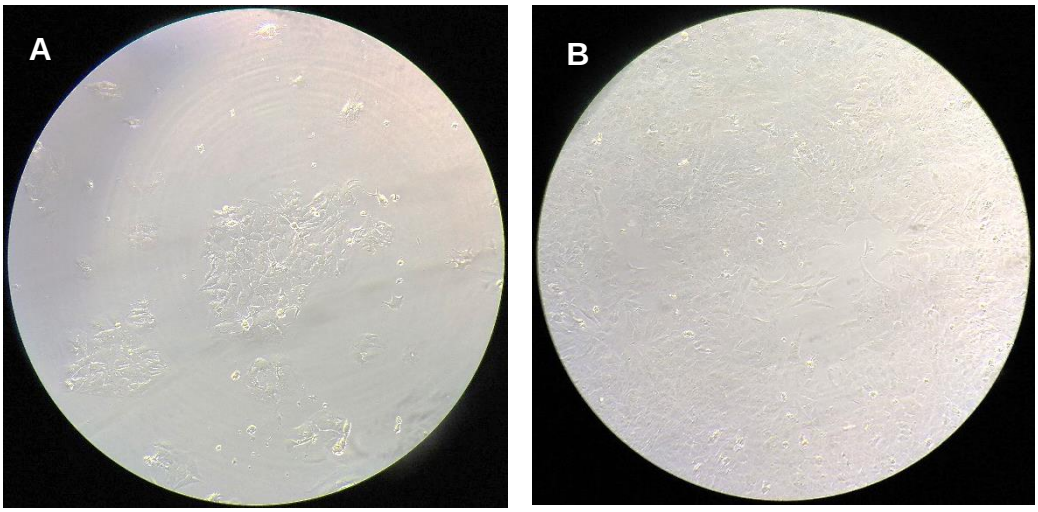

Figure 7: Bladder cancer cell lines culture. A) HT-1376 cell line. B) TCCSUP cell line.

8.3 Experimental Design

To evaluate the effect of SIRT1 inhibition/activation and mTOR inhibition on bladder cancer cells, there were defined five conditions: i) a control group, supplemented with DMEM as described above containing 0.02% DMSO; ii) a group supplemented with Rapamycin at 0.1 µM (inhibition of mTOR); iii and iv) the SIRT1 inhibition and activation groups supplemented with EX-527 at 1 µM and YK-3-237 at 1 µM, respectively and v) the combination group, corresponding to mTOR and SIRT1 inhibition simultaneously with 0.1 µM of rapamycin and 1 µM of EX-527, respectively.

The five conditions were selected based on proliferation and cytotoxicity assays. Therefore, cells were treated individually with increased concentrations of EX-527 (0.1 µM, 1 µM and 10 µM), YK-3-237 (0.1 µM, 1 µM and 10 µM) and rapamycin (0.01 µM, 0.1 µM and 1 µM).

The studies that have been made with SIRT1 modulators demonstrate that they might play an essential role in cancer treatments. To test the SIRT1 modulation, the selected conditions were those with the lowest concentration capable of promoting some difference comparing to control group. mTOR, a well-known component in carcinogenesis was also studied individually with rapamycin. Additionally, since mTOR is not the only responsible for tumour aggressiveness, a combined treatment was also selected, in which it was intended to inhibit SIRT1 and mTOR by 1 µM of EX-527 and 0.1 µM of rapamycin.

After groups' definition, cells were cultured in 100mm x 2mm dishes (Corning Incorporated, USA) and were treated when a 70% confluence was reached. After a 24-hour treatment in an incubator (MCO-19AIC, Sanyo) with 5% CO_2 at 37ºC, cells were detached with trypsin-EDTA solution and collected for total number counting of living cells using a Neubauer chamber (Marienfeld). The cells were collected for protein, ribonucleic acid (RNA) and deoxyribonucleic acid (DNA).

8.4 Living cells

Living cells were counted through trypan blue (Gibco, Life Techonologies) exclusion test. This dye confers a distinct blue colour to non-viable cells, while the viable ones remain unstained. For viable cell number determination, 10 µL of trypan blue solution added to 10 µL of the cell suspension. Afterwards, 10 µL were transferred into a Neubauer chamber. Stained cells of the four big squares were counted and the cell number per 1 mL of the cell suspension was assessed using the following formula, in which the chamber factor corresponds to 10 000 and, in this case, dilution factor corresponds to 2.

$$[\text{cells}]/\text{mL} = \frac{\text{total number of stained cells}}{4} \times \text{Chamber factor} \times \text{Dilution factor}$$

8.5 Cell proliferation assay

The growth curve of each cell line was evaluated by colorimetric SRB assay. This assay relies on the SRB ability to bind cellular proteins towards mild acidic conditions and then can be detached under basic conditions. Hence, the quantity of bound SRB is associated with cellular mass and can be then extrapolated to determine cell proliferation (165, 166).

Cells were cultured in a 24-well culture plate, with different concentrations per line. At each day, the medium of a column was discarded and allowed to dry in the incubator, the remained cells still with medium, were allowed to grow, until day 8. At this time, the SRB assay was performed. Cells were washed with phosphate buffered saline (PBS) and fixed with 1% acid acetic in methanol for at least 1 hour at -20ºC. After fixation, cells were stained with 0.05% SRB for 1 hour at 37ºC. The unbounded SRB was discarded and washed with 1% acid acetic. Afterwards, the SRB attached was extracted with Tris 10mM in a shaker for 10 minutes. A blank was made with Tris 10mM. The absorbance was determined at 490 nm.

The effect of YK-3-237, EX-527 and rapamycin in HT-1376 and TCCSUP cells proliferation was evaluated through SRB assay. Cells were cultured in a 24-well culture plate,

left to grow for 48 hours and treated individually with increased concentrations of YK-3-237 (0.1 µM, 1 µM and 10 µM), EX-527 (0.1 µM, 1 µM and 10 µM) and rapamycin (0.01 µM, 0.1 µM and 1 µM). Two combined treatments were also tested, corresponding to 1 µM EX-527 with 0.1 µM rapamycin. After 24-hour treatment, the SRB assay was performed.

8.6 Cell viability assay

The effect of YK-3-237, EX-527 and rapamycin in HT-1376 and TCCSUP cells viability was evaluated through MTT colorimetric assay. The conversion of MTT into formazan, a purple coloured product, is performed by viable cells with active metabolism. On the other hand, non-viable cells do not have the ability to convert the MTT. Formazan quantity is determined spectrophotometrically, being directly proportional to the quantity of viable cells (167, 168). Cells were cultured in a 24-well culture plate, left to grow for 48 hours and treated with the same concentrations mentioned above to SRB assay. After 24-hour treatment, cells were washed in PBS and incubated with 50 µL MTT (5 mg/mL, dissolved in PBS) for 2 hours at 37ºC, protected from light. Then, cells were washed with DMSO and 100 µL of each well was transferred to a 96-well culture plate. DMSO was the blank used and the optical densities were determined at 570 nm.

8.7 Mitochondrial membrane potential assay

To evaluate the mitochondrial membrane potential in HT-1376 and TCCSUP cells it was performed the JC-1 assay. Cells were cultured in a 96-well culture plate, left to grow for 48 hours and treated. After 24-hour treatment, cells were washed in PBS and incubated for 30 minutes at 37ºC with 2 µM JC-1. Then, the solution was discarded and culture medium without FBS was added. The JC1 accumulation in mitochondria is relative to mitochondrial membrane potential. JC-1 forms aggregates that emit an intense red fluorescence that is detected at 550/590 nm (excitation/emission), associated with high membrane potential, from healthy cells. However, when JC-1 remains as a monomer exhibiting green fluorescence that is detected at 485/535 nm (excitation/emission), it is associated with poor membrane potential and therefore, from unhealthy cells. The fluorescence was determined at the wavelengths mentioned. The ratio of aggregates/monomers was calculated as a parameter of mitochondrial viability.

8.8 Lactate dehydrogenase assay

LDH is a cytoplasmic enzyme that is released into extracellular space when the membrane is damaged and therefore is considered as a cellular toxicity indicator (169). To analyse the effect of the drugs in plasma membrane, the LDH assay was performed according manufacturer's instructions. The kit measures extracellular LDH through an enzymatic reaction that produces red formazan, which is directly proportional to LDH quantity released in the medium (170). Briefly, 50 µL of cell medium was transferred to a 96-well plate and added 50 µL of LDH reagent mix. The plate was incubated for 30 minutes at room temperature and the LDH activity analysed through spectrophotometric absorbance at 490 nm.

8.9 Total protein extraction

After indicated treatment to HT-1376 and TCCSUP cell lines and corresponding pellet collection, total protein was extracted. Briefly, protein extraction was performed using M-PER buffer, supplemented with 100 mM sodium orthovanadate (AppliChem, Nürnberg, Germany) and 1% of protease inhibitor cocktail (Bimake, Germany). The cells were mixed at room temperature for 10 minutes and then, centrifuged at 14000xG for 20 minutes. The protein was in the supernatant and concentration was determined using BSA method, in which different BSA concentrations were used as standards for calibration. The absorbance was determined at 595 nm.

8.10 Western Blot

Western blot was performed to analyse individual protein expression from OXPHOS complex. Hence, 50µg of protein of each sample were mixed with sample buffer (60mM Tris HCl, 10% glycerol, 5% β-mercaptoethanol, 2% SDS, 0.01% bromophenol blue at pH 6.8) and denatured for 15 minutes at 37ºC. To electrophoresis, were used 15% polyacrylamide gels and protein were fractioned for 90 minutes at 30mA per gel. Proteins were transferred from gels to previously activated polyvinylidene difluoride membranes (Merck Milipore, Germany) in a mini trans-blot cell (Bio-Rad, UK) for 75 minutes at 100V. Ponceau solution was used to detect if proteins were well transferred. Membranes were blocked for 3 hours in 5% non-fat milk solution, washed with washing buffer solution and incubated overnight at 4ºC with the primary antibody total OXPHOS. Afterwards, membranes were incubated for 90 minutes at room temperature with secondary antibody. Antibody characteristics are listed in Table 5. Membranes were revealed with WesternBright ECL and read with Bio-Rad ChemiDoc XR

equipment (Bio-Rad, UK). Band densities were obtained with Image Lab Software (Bio-Rad, UK) and normalized with control group value.

Table 5: Antibodies used for western blot assay and respective molecular weight, host specie, dilution and vendor.

Antibody	Molecular Weight	Host Specie	Dilution	Vendor
OXPHOS	20, 30, 40, 48 and 53	Mouse	1:1000 1:500	Abcam, UK
Mouse	-	Goat	1:5000	Sigma-Aldrich, Germany

8.11 RNA extraction

After treatment with selected concentrations and corresponding pellet collection, the RNA was extracted. RNA extraction from HT-1376 and TCCSUP cells was performed using Total RNA isolation kit (NZYTECH, Portugal) and according to the manufacturer's instructions. Nanodrop 1000 Spectrophotometer (Thermo Scientific, Wilmington, DE, USA) was used to determined RNA concentration to each sample and to measure sample purity at A260/A280 and A260/230.

8.12 DNA extraction

The DNA was extracted from the pellet of HT-1376 and TCCSUP treated cells. The extraction was performed with Tissue DNA Kit (D3396-02, OMEGA, USA) and according to manufacturer's instructions. To determine DNA concentration of each sample and to measure the sample purity, it was used Nanodrop 1000 Spectrophotometer (Thermo Scientific, Wilmington, DE, USA).

8.13 Complementary DNA (cDNA) synthesis

RNA extracted from each sample was reversely transcribed. Therefore, it was firstly used a mixture of 2.5 µL random hexamer primers at 50 ng/µL, 1 µL of dNTPs at 10 Mm, 1 µL of RNA and sterile H_2O to reach a 17 µL of total volume. The mixture was incubated at 65ºC for 5 minutes to denature the RNA and random hexamer primers. After that, a mix of 1 µL of M-MuLV reverse transcriptase and 2 µL of reaction buffer was added to each sample and incubated at 25ºC for 10 minutes, 37ºC for 50 minutes and 70ºC for 15 minutes. To evaluate

sample integrity, the obtained cDNA was tested with the housekeeping gene 18S ribosomal RNA, in a polymerase chain reaction (PCR).

8.14 PCR

PCR was used to confirm sample integrity and to adjust the temperature and cycle's number of each primer to both cell lines. After cDNA synthesis of both cell lines, each PCR contained 1 µL of cDNA, 6.5 µL of NZYTaq Green Master Mix, 0.1 µL of each primer at 50 µM, forward and reverse, and sterile H_2O for a final volume of 12.5 µL. At the end of each PCR, samples were run in agarose gel (1%) electrophoresis with 2 µL of GreenSafe for 200 mL, for 40 minutes at 120 V, to evaluate the conditions to use. The used marker to compare the products' size was DNA ladder VI. The agarose gel was observed in Bio-Rad ChemiDoc (Bio-Rad, UK) by the software ImageLab (Bio-Rad, USA).

8.15 Quantitative PCR (qPCR)

mRNA expression levels of glucose transporter 1 (*GLUT1*), glucose transporter 3 (*GLUT3*), monocarboxylate transporter 1 (*MCT1*), monocarboxylate transporter 4 (*MCT4*), lactate dehydrogenase (*LDH*), B cell lymphoma 2 (*BCL-2*) and BCL-2-associated X (*BAX*) were analysed in all five conditions that both HT-1376 and TCCSUP cell lines were submitted through qPCR. The reactions were carried out in a CFX 96 qPCR (Bio-Rad, CA, USA) equipment. Serial dilutions of cDNA (1:3, 1:15, 1:75) were used to test primers' conditions for each reaction. qPCR contained 1 µL of cDNA (1:15), 10 µL NZY qPCR Green Master Mix, 0.8 µL of forward and reverse primers (10 µM) and sterile H_2O until 20 µL of final volume. qPCR conditions for each pair of primers were firstly optimized and determined by melting curves. Amplification started with denaturation for 5 minutes at 95ºC followed by 40 cycles for each gene of a 3 steps cycle: first of all, a denaturation step for 30 seconds at 95ºC, an annealing step for 30 seconds at a specific temperature for each pair of primers (Table 6) and finally, an extension step for 1 minute at 72ºC. β_2-microglobulin (*B2M*) was used to normalized mRNA expression levels of all target genes. Characteristics of analysed genes, sequences and annealing temperature are described at table 6. The relative expression ratio was calculated following the model proposed by Pfaffl (171) using the formula: $2^{-\Delta\Delta Ct}$.

8.16 Mitochondrial DNA copy number quantification

mtDNA copy number in treated HT-1376 and TCCSUP cell lines was assessed by qPCR, as described before. Briefly, qPCR reactions containing 10µL of NZY qPCR Green Master Mix, 0.8µL of forward and reverse primers, 20ng of mtDNA and sterile H2O. Annealing temperatures and number of cycles are specific to each pair of primers (Table 6). qPCR was carried out in an CFX 96 qPCR equipment (Bio-Rad, CA, USA). The quantification of the mitochondrial copy number was performed using the mitochondrially encoded NADH dehydrogenase 1 (*ND1*) and its normalization was assessed through the nuclear encoded β2-microglobulin (*β2Mnc*) gene transcript levels, following the mathematical model proposed by Pfaffl (Pfaffl 2001).

Table 6: Gene, respective primers' sequence and conditions for PCR of *GLUT1*, *GLUT3*, *MCT1*, *MCT4*, *LDH*, *BAX*, *Bcl-2*, *β2M*, *ND1* and *β2Mnc* .

Gene	Sequence (5' – 3')	Amplicon (bp)	Annealing Temperature	Cycles
GLUT1	Forward: AGCAGCAAGAAGCTGACGGGTC	269	60	35
	Reverse: CGCCGGCCAAAGCGGTTAAC			
GLUT3	Forward: TCAGGCTCCACCCTTTGCGGA	228	50	30
	Reverse: TGGGGTGACCTTCTGTGTCCCC			
MCT1	Forward: CCGGGGTTGGGAGACTTTGTC	174	58	35
	Reverse: CTGGGACCGGCATCTTAGCA			
MCT4	Forward: TTCGTTTTTGTGCAGGTCCC	174	57	35
	Reverse: GTCAGTCCCATCCCAGAACG			
LDH	Forward: ATTCAGCCCGATTCCGTTAC	131	52	35
	Reverse: GACACCAGCAACATTCATTCC			
BAX	Forward: CCCGAGAGGTCTTTTTCCGAG	260	56	35
	Reverse: TGGAGACAGGGACATCAGTCG			
Bcl-2	Forward: TTCTTTGAGTTCGGTGGGGT	189	58	35
	Reverse: GAAATCAAACAGAGGCCGCAT			
B_2-Microglobulin	Forward: ATGAGTATGCCTGCCGTGTG	92	58	30
	Reverse: CAAACCTCCATGATGCTGCTTAC			
ND1	Forward: CGATTCCGCTACGACCAACT	121	58	25
	Reverse: AGGTTTGAGGGGGAATGCTG			
B_2-Microglobulin$_{nc}$	Forward: GAGGCTATCCAGCGTGAGTC	306	58	30
	Reverse: GACGCTTTCGACGCCCTAA			

8.17 Nuclear magnetic resonance spectroscopy to follow bladder cancer cells metabolic turnover

TCCSUP and HT-1376 cells were cultured in 100 mm diameter cell culture plates and after reaching a confluence of 70-80%, cells were washed thoroughly with PBS and treated for 24 hours with 7.5 mL culture medium supplemented with 0.02% DMSO (maximal compounds solvent concentration, working as control), 1 µM YK-3.237, 1 µM EX-527, 0.1 µM rapamycin or 1 µM EX-527 with 0.1 µM rapamycin (combined treatment). At time zero of incubation were collected 1.5 mL of medium (corresponding to basal composition, with no metabolization) and flash freezed in -80ºC, for later ^{1}H-NMR analysis. After 24 hours treatment, 1.5 mL of medium from each plate were collected and also flash freezed. To 180 µL of each sample were added 45 µl of a 10 mM sodium fumarate solution (final concentration of 2 mM, reference solution for peak quantification) in 99.9% $^{2}H_2O$.

^{1}H-NMR spectra of the collected samples were acquired at 14.1 Tesla, at 25ºC, using a Varian (Varian Inc, Palo Alto, CA) 600MHz spectrometer equipped with a 3mm indirect detection probe to determine metabolite variation in the different experimental groups during the time-course of the experiment using previously described methods (adapted from *Rato et al.* (172)).

Briefly, each ^{1}H-NMR spectra consisted of 21.5k points defining a 7.2kHz spectral width. A minimum of 64 scans were averaged using an interpulse delay of 10 seconds and a 30° radiofrequency pulse to ensure full relaxation of magnetization, towards quantitative analysis. Sodium fumarate was used as an internal reference (singlet, 6.50 ppm) to quantify metabolites in solution: lactate (doublet, 1.33 ppm), alanine (doublet, 1.45 ppm), pyruvate (singlet, 2.36 ppm), and H1-α glucose (doublet, 5.22 ppm). The relative areas of ^{1}H-NMR resonances were quantified using the curve-fitting routine supplied with the NUTSpro NMR spectral analysis program (Acorn, NMR Inc, Fremont, CA). Before Fourier transform each FID was zero filled and multiplied by a 0.2 Hz Lorentzian.

Metabolite consumption or production per cell was calculated by measuring the accumulated variation of the metabolite (versus time zero) after 24 hours and dividing it by the total number of cells in each plate.

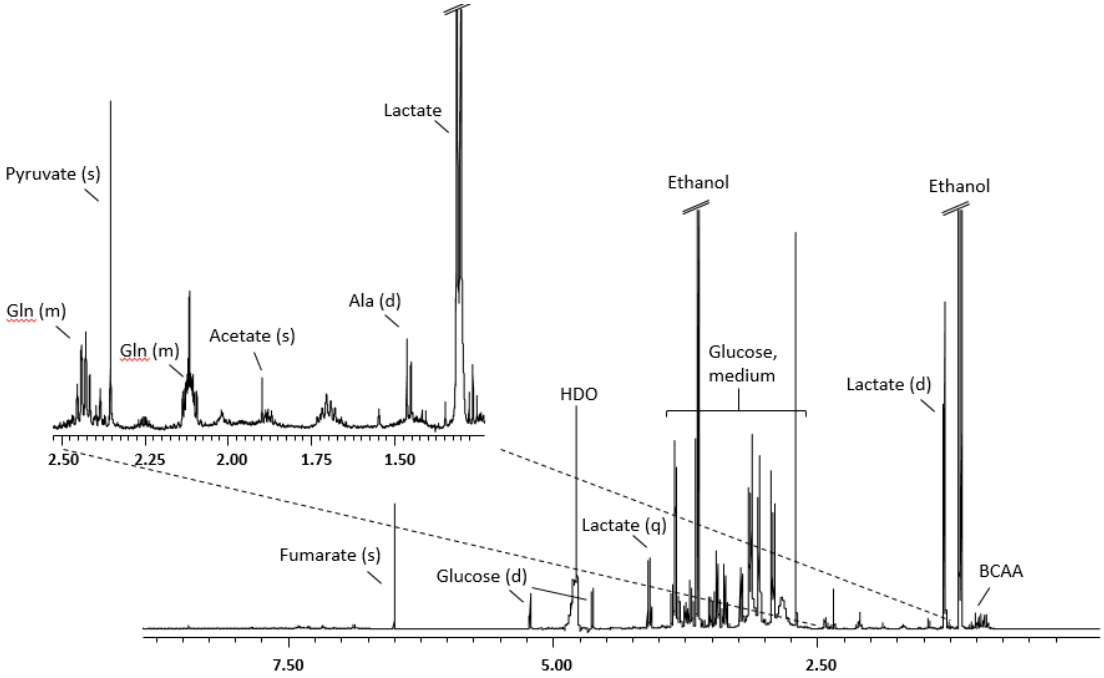

Figure 8: Typical ^{1}H-NMR spectrum of cell medium. The position and multiplicity of some metabolites are indicated: s (singlet), d (doublet), q (quadruplet), m (multiplet). The region between 1.10 and 2.5 ppm (the region of the majority of analysed metabolites) was zoomed in. Fumarate: internal standard used for metabolite quantification. HDO: deuterated solvent.

8.18 Respirometry to assess mitochondrial fitness in TCCSUP bladder cancer cells

TCCSUP were cultured in 100 mm diameter cell culture plates during a week, reaching around 70-80% confluence and prior to the 24 hours treatment with different compounds, cells were washed thoroughly with PBS and refilled with 7.5 mL culture medium supplemented with 0.02% DMSO (maximal compounds solvent concentration, working as control), 1 µM YK-3.237, 1 µM EX-527, 0.1 µM Rapamycin or 1 µM EX-527 with 0.1 µM rapamycin (combined treatment). Prior to assay, cells were trypsinized, resuspended in 1 mL respiration medium and counted in a Neubauer chamber.

Respiration medium composition was based on cell culture medium, DMEM D5523 with a total of 15 mM Glucose and 4 mM L-Glutamine, without FBS, and supplemented with 1% ITS (0.01 mg/mL recombinant human insulin, 0.0055 mg/mL human transferrin -substantially iron-free-, and 0.005 µg/mL sodium selenite) from BD Biosciences (USA).

To assess the oxygen consumption rates, we did open-chamber oxygen measurements in a thermostatized (by a water jacket, at 37 ºC) 1 mL volume chamber, using

a Clark-type electrode from Hansatech Oxytherm System, connected to a personal computer with Oxytrace Plus data acquisition software.

Each assay starts with a 30 minutes' initial respiration until reaches a steady-state. Then, a sequential addition of mitochondrial modulators, oligomycin 2 µg/mL, FCCP (Carbonyl cyanide-p-trifluoromethoxyphenylhydrazone) 2 µM and a mixture of rotenone 0.5 µM with antimycin A 2.5 µM was performed (each modulation period lasting, in average, 15 minutes) to assess the rates needed to calculate the parameters *Basal Respiration* (initial respiration minus Rotenone with Antimycin A state), *Maximal respiration* (FCCP state minus Rotenone with Antimycin A state) , *ATP turnover* (Initial respiration minus Oligomycin state), *Proton leak* (Oligomycin state minus Rotenone with Antimycin A state), *Spare Respiratory capacity* (FCCP state minus initial respiration) and *Non-Mitochondrial Respiration* (Rotenone with Antimycin A state). The procedure was adapted from *Mamchaoui et al*. (173), *Djafarzadeh et al.* (174) and *Silva et al.* (175).

8.19 HT-1376 cells migration

HT-1376 cells were cultured on Transwell-Clear Inserts, Polyester (PET) membrane (with 8 µm pore diameter) (#3464, Corning) in 24 wells cell culture plates for a week, reaching the maximal confluence possible. Prior to the treatment with different compounds, cells were washed thoroughly with PBS and refilled with 300 µL culture medium (with 0% FBS) supplemented with 0.02% DMSO (maximal compounds solvent concentration, working as control), 1 µM YK-3.237, 1 µM EX-527, 0.1 µM rapamycin or 1 µM EX-527 with 0.1 µM rapamycin (combined treatment). In counterpart, lower chambers were filled with medium with 10% serum, supplemented with the same compounds. 24 hours later, non-migrated cells on the top of the insert were removed by cotton swab scrubbing. Cells on the lower side of the insert were fixed in 70% ethanol overnight. After drying, cells were stained with 0.2% crystal violet, during a half of hour. Excess of dye was cleared with water and inserts were dried again. To perform a qualitative evaluation, we observed five quadrants/insert, under a 100x magnification (microscope Leica DMi1).

To quantify migrated cells, violet crystal was recovered by destaining with 33% glacial acetic acid solution (incubated during 10 minutes, at 37 ºC) and optical density was measured in a UV/Vis plate reader (Multiskan™ FC Microplate Photometer, Thermo Fisher) at 570 nm. Values were presented in relation to the control. Adapted from *Gong et al.* (176), *Hong et al.* (177).

8.20 Morphological analysis

HT-1376 and TCCSUP cells were cultured in 100 mm diameter cell culture plates for a week, reaching around 70-80% confluence. Prior to the 24 hours treatment with different compounds, cells were washed thoroughly with PBS and refilled with 7.5 mL of culture medium supplemented with the specific treatment conditions, 0.02% DMSO (maximal compounds solvent concentration, working as control), 1 µM YK-3.237, 1 µM EX-527, 0.1 µM rapamycin or 1 µM EX-527 with 0.1 µM rapamycin (combined treatment). Using a bright field microscope (Leica DMi1), cells were observed and microphotographed 4-5 fields under 100x, 200x and 400x magnification, comparing the different cell lines, as well as the different pharmacological treatments. We evaluated and compared shape, size and particular organelles/structures.

8.21 Statistical analysis

The statistical analysis of the samples variation among the five experimental groups was performed using two-way ANOVA. In some samples, t-test student was also performed. The control sample is mostly represented by 100, and results are presented by relative variation in comparison with control group. All results are shown as mean ± SEM, with n=6 for each condition. Statistical analysis was assessed using GraphPad Prism 5 (GraphPad Software, San Diego, CA, USA). Outliers were removed through ROUT method with a q value of 1%. Significant results were considered when $p < 0.05$.

9 RESULTS

9.1 Growth profile of bladder cancer cells from different stages of the disease

An evaluation of cell growth was made for both cell lines, HT-1376, grade III and TCCSUP, grade IV, with the aim to determine the best concentration by which the cells should be seeded as well as the best time point to perform the studies of drug exposition. This first study was essential to avoid a cell confluence too high or a too low cell concentration for treatment response. Moreover, it was important to ensure that the cells did not inhibit each other during drug exposure and that the selected concentration was enough to have cells at the time of the treatment.

Concerning to the cells representing the lower grade of bladder cancer, HT-1376, they only reached the exponential growth within 6 days, however, this behaviour was important for further planned studies in mitochondrial respirometry (Figure 9, panel A). On the other hand, the two best seeding concentrations for the cells representing the highest grade of bladder cancer, TCCSUP were $15x10^3$ cell/mL and $20x10^3$ cell/mL, since for both concentrations, cells were still in exponential growth, even at the 8^{th} day (Figure 9, panel B). The attained results allowed to settle the selected cell seeding concentration for cytotoxic assays as $15x10^3$ cell/mL and for the experimental protocol as $20x10^3$ cell/mL. In addition, we also settled that the treatment should start at day two after seeding. Although it could not be concluded an exact seeding concentration and time for drug administration for HT-1376 cell line, the selected parameters were equal for both cell lines for comparative purposes.

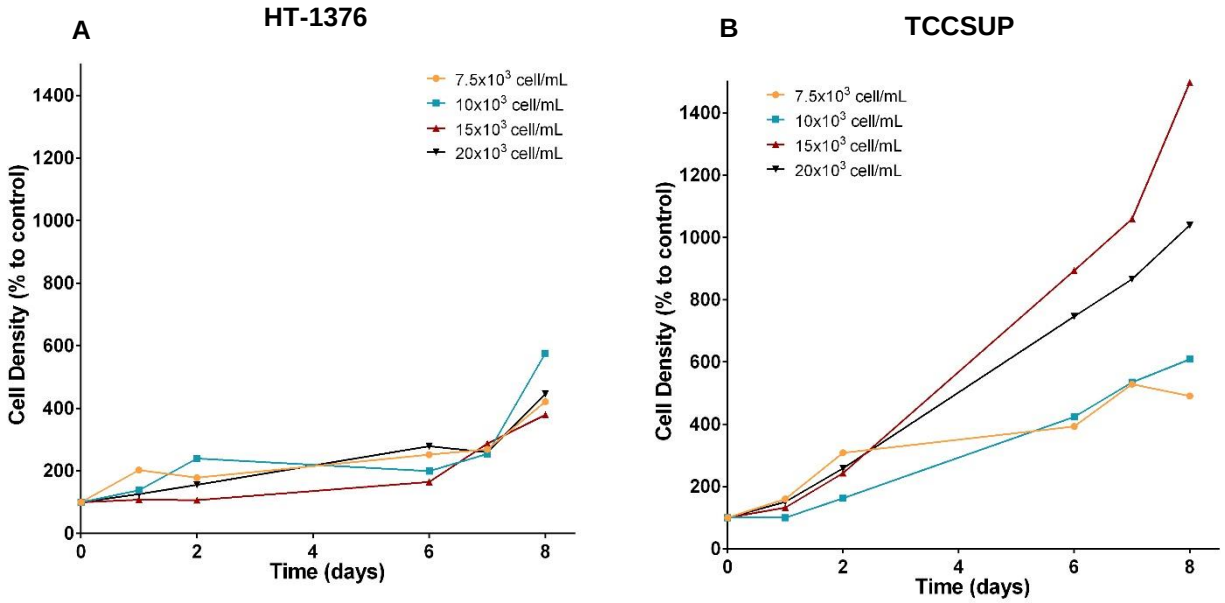

Figure 9: Representative growth profile of HT-1376 (A) and TCCSUP (B) bladder cancer cell lines. Growth profile was assessed through cell density by SRB assay. Cells were seeded in a 24 well plate with different concentrations ($7.5x10^3$ cell/mL, $10x10^3$ cell/mL, $15x10^3$ cell/mL and $20x10^3$ cell/mL) for 8 days, the medium was removed at day 0, 1, 2, 6, 7 and 8. The results are presented as mean, demonstrating a representative growth profile of both cell lines and are normalized to control (n=3).

9.2 Selective action of SIRT1 inhibition and activation in bladder cancer cells of different stages

To study the possible involvement of SIRT1 in bladder cancer progression, we studied its signalling in two human bladder cancer cell lines, the HT-1376 cell line, which represents a grade III bladder cancer carcinoma and the TCCSUP cell line, which represents a transitional bladder cancer cell carcinoma, highly invasive of grade IV. Indeed, recently SIRT1 has been in the spotlight demonstrating a controversial role depending on the pathology studied, suggesting that it can act as a tumour suppressor or as a promoter. However its role in bladder cancer remains unclear (135). Therefore, to better understand if SIRT1 is a suppressor or a promoter in the establishment and progression of bladder cancer, it is important to study the modulation of this protein by inhibition or activation. Thus, we studied how SIRT1 expression was changed in both, HT-1376 and TCCSUP cell lines, after activation and inhibition during 24 hours. In addition, cell viability was analysed after 24 hours of treatment by MTT assay.

Considering cells of an early stage of the tumour, represented by the HT-1376 cell line, SIRT1 inhibition by EX-527, through stabilization of the closed enzyme conformation, inhibits cell viability to 61.21±8.69%, 58.55±9.86% and 63.96±7.31% after exposure to concentrations of 0.1 µM, 1 µM and 10 µM of EX-527, respectively (Figure 10, panel A). Also, SIRT1 activation by YK-3-237, which mechanism of action remains unknown inhibits cell viability to

89.93±3.80%, 80.97±6.91% and 74.14±2.75% after exposure to concentrations of 0.1 µM, 1 µM and 10 µM, respectively. On the other hand, at a more advanced stage of the tumour, represented by TCCSUP cell line, SIRT1 activation by YK-3-237 increases cell viability to 172.2±14.91%, 169.1±13.18% and 145.5±16.97% after exposure to concentrations of 0.1 µM, 1 µM and 10 µM, respectively (Figure 10, panel B). The inhibition of SIRT1, by EX-527, also interferes with cell viability, which was increased after exposure to concentrations of 1 µM (140.0±14.55%) and 10 µM (134.3±11.47%). Therefore, SIRT1 seems to be an important player for bladder cancer cell viability at different stages.

In addition to SIRT1, mTOR signalling has also been reported as essential for cancer establishment and progression (19, 34). However, our results did not show any significant differences in cell viability ($p>0.05$), for both cells lines after exposure to rapamycin at any of the tested concentrations (Figure 10). Additionally, for HT-1376 cells, no significant differences were detected after exposure to any of the combined treatments (rapamycin with EX-527 and rapamycin with YK-3-237, $p>0.05$) (Figure 10, panel A). Interestingly, towards an advanced stage, in TCCSUP cells, no significant differences ($p>0.05$) were observed concerning cell viability after having been exposed to the lower concentration of EX-527 (0.1 µM), nor to the combined treatment of rapamycin with EX-527 (Figure 10, panel B). Nevertheless, the treatment of SIRT1 activation by YK-3-237, combined with mTOR inhibition by rapamycin, significantly decreased cell viability of TCCSUP by almost 40% illustrating that the interplay between mTOR and SIRT1 interferes with bladder cancer cells (Figure 10, panel B).

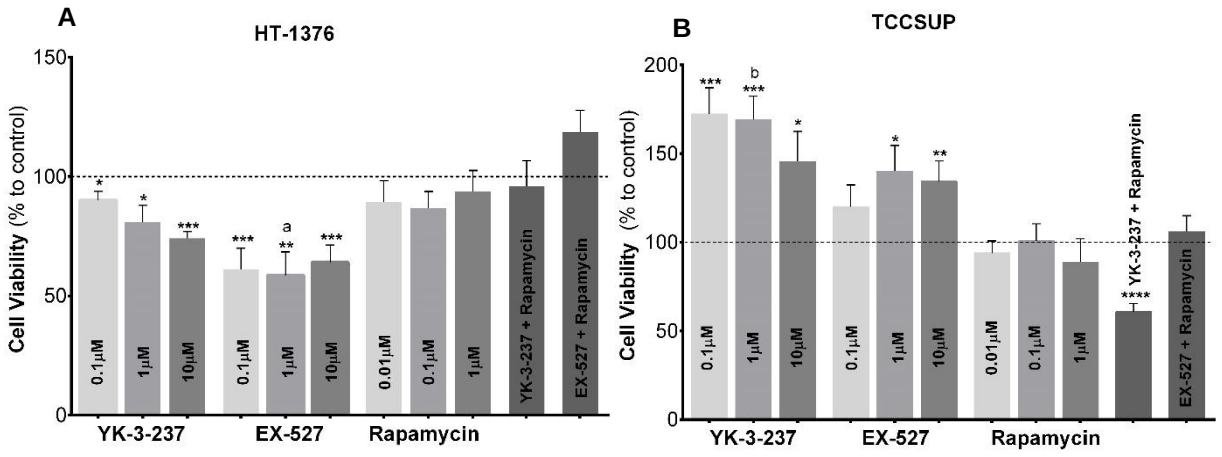

Figure 10: Effects of the inhibition of SIRT1 with EX-527 or activation with YK-3-237 as well as inhibition of mTOR pathway with rapamycin in cell viability of bladder cancer cells of different stages, HT-1376 (A) which represents a grade III and TCCSUP (B) which represents a grade IV. The effects of combined inhibition of mTOR and SIRT1 pathways on cell viability of HT-1376 and TCCSUP cell lines were also determined. The figure shows pooled data of independent experiments indicating fold variation of cell viability of HT-1376 and TCCSUP cell lines treated during 24 hours with different concentrations of YK-3-237 (in µM: 0.1, 1, and 10), EX-527 (in µM: 0.1, 1 and 10) and rapamycin (in µM: 0.01, 0.1 and 1) individually and with the combination YK-3-237 (1 µM) with rapamycin (0.1 µM) and EX-527 (1 µM) with rapamycin (0.1 µM), when compared to control group (dashed line). Results were obtained by MTT assay and are presented as mean±SEM (n=6). *Indicates significantly different relatively to control group ($p<0.05$). **Indicates significantly different relatively to control group ($p<0.01$). ***Indicates significantly different relatively to control group ($p<0.001$). ****Indicates significantly different relatively to control group ($p<0.0001$). a – indicates significant result relative to EX-527+rapamycin group. b - indicates significant result relative to YK-3-237+rapamycin group

Cell proliferation, assessed by SRB assay, was performed with the same purpose described above for cell viability: to understand the effects of SIRT1 modulation as well as the inhibition of mTOR in bladder tumour development.

Although SIRT1 inhibition by EX-527 did not change cell density, its activation by YK-3-237 decreased cell proliferation in both bladder cancer cells from different stages by ~30% for HT-1376 ($p<0.01$) (Figure 11, panel A) and by ~25% for TCCSUP ($p<0.001$) (Figure 11, panel B), exposed to 10 µM of YK-3-237. In addition, mTOR inhibition by rapamycin also decreased the proliferation of bladder cancer cells from stage III, HT-1376 after exposure to concentrations of 0.01 µM, 0.1 µM and 1 µM of rapamycin (52.46±5.00%, 64.52±14.22 and 46.53±8.15 respectively, $p<0.05$) (Figure 11, panel A). The same was detected after exposure of bladder cancer cells from stage IV, TCCSUP, to rapamycin at 0.1 µM (83.46±5.22%, $p<0.01$) and 1 µM concentration (78.10±5.09%, $p<0.05$) (Figure 11, panel B). The combined treatment of bladder cancer cells from both stages to YK-3-237 combined with rapamycin, decreased cell density to 76.76±8.83% for HT-1376, $p<0.05$ (Figure 11, panel A) and to 80.78±2.81% for TCCSUP, $p<0.0001$ (Figure 11, panel B).

EX-527, the SIRT1 inhibitor, at concentrations of 0.1 µM, 1 µM and 10 µM and YK-3-237, the SIRT1 activator, at concentrations of 1 µM and 10 µM did not change cell density ($p>0.05$) of any of the tested bladder cancer cell lines comparing with the control group (Figure 11).

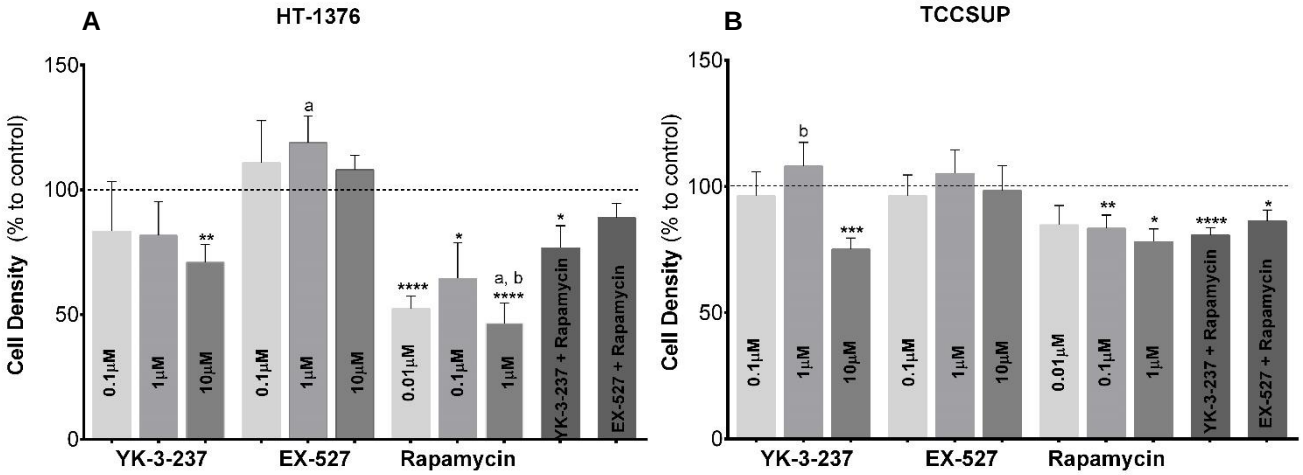

Figure 11: Effects of the inhibition of SIRT1 with EX-527 or activation with YK-3-237 as well as inhibition of mTOR pathway with rapamycin in cell proliferation of bladder cancer cells of different stages, HT-1376 (A), which represents a grade III and TCCSUP (B), which represents a grade IV. The effects of combined inhibition of mTOR and SIRT1 pathways on cell proliferation of HT-1376 and TCCSUP cell lines were also determined. The figure shows pooled data of independent experiments indicating fold variation of cell density of HT-1376 and TCCSUP cell lines treated 24 hours with different concentrations of YK-3-237 (in µM: 0.1, 1, and 10), EX-527 (in µM: 0.1, 1 and 10) and rapamycin (in µM: 0.01, 0.1 and 1) individually and with the combination of YK-3-237 (1 µM) plus rapamycin (0.1 µM) and EX-527 (1 µM) plus rapamycin (0.1 µM), when compared to control group (dashed line). Results were obtained by SRB assay and are presented as mean±SEM (n=6). *Indicates significantly different relatively to control group ($p<0.05$). **Indicates significantly different relatively to control group ($p<0.01$). ***Indicates significantly different relatively to control group ($p<0.001$). ****Indicates significantly different relatively to control group ($p<0.0001$). a – indicates significant result relative to EX-527 + rapamycin group. b – indicates significant result relative to YK-3-237+rapamycin group.

9.4 Mitochondrial potential of bladder cancer cells of different stages is repressed after exposure to the combined treatment of mTOR inhibition with SIRT1 activation/inhibition

Activation and inhibition of SIRT1 have demonstrated some relevant properties to cancer prevention/treatment, although their role remain a matter of intense debate (135). In addition, mTOR signalling has also been related to cancer establishment and progression (19, 34) and has been proposed as a therapeutic target for cancer although the molecular mechanisms by which it acts remain a matter of intense debate. Thus, we hypothesized that a combined treatment of SIRT1 (inhibition or activation) with mTOR inhibition could result in differences in mitochondrial membrane potential of bladder cancer cells from different stages. We assessed mitochondrial membrane potential by the JC-1 assay in HT-1376 and TCCSUP cells after 24 hours exposure to a combined treatment of SIRT1 activator/inhibitor with mTOR inhibition.

The treatment of bladder cancer cells from different stages with the SIRT1 inhibitor EX-527 only significantly decreased mitochondrial membrane potential after exposure to 1 μM for HT-1376 cells (90.63±2.38%, $p<0.01$) (Figure 12, panel A) and 10 μM for TCCSUP cells (84.63±3.48%, $p<0.01$) (Figure 12, panel B). The exposure to the remaining concentrations of YK-3-237, EX-527 and rapamycin alone did not affect mitochondrial membrane potential in bladder cancer cells from the stages tested ($p>0.05$) (Figure 12). Nevertheless, when combining mTOR inhibition with exposure to drugs that interfere with SIRT1 (EX-527 for inhibition or YK-3-237 for activation), the mitochondrial membrane potential was significantly ($p<0.0001$) affected in both bladder cancer cell lines tested when compared to the control group, being the decrease almost 100% for HT-1376 cells (Figure 12, panel A) and ~90% for TCCSUP cells (Figure 12, panel B).

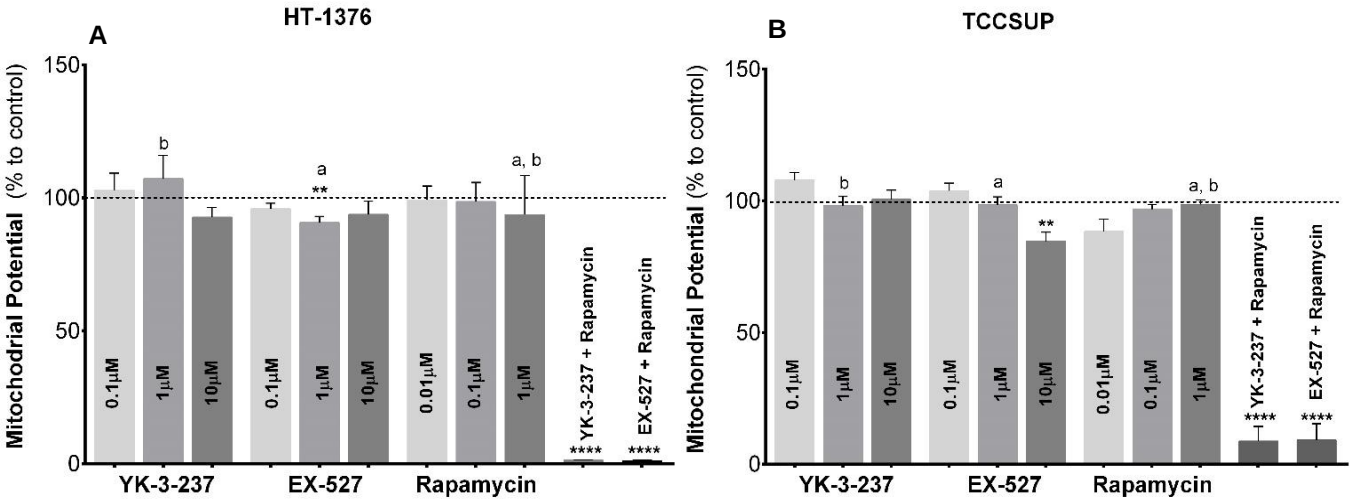

Figure 12: **Effects of the inhibition of SIRT1 with EX-527 or activation with YK-3-237 as well as inhibition of mTOR pathway with rapamycin in mitochondrial potential of bladder cancer cells of different stages, HT-1376, which represents a grade III and TCCSUP, which a grade IV. The effects of combined inhibition of mTOR and SIRT1 pathways on mitochondrial potential of HT-1376 (A) and TCCSUP (B) cell lines were also determined.** The figure shows pooled data of independent experiments indicating fold variation of mitochondrial potential of HT-1376 and TCCSUP cell lines treated 24 hours with different concentrations of YK-3-237 (in μM: 0.1, 1, and 10), EX-527 (in μM: 0.1, 1 and 10) and rapamycin (in μM: 0.01, 0.1 and 1) individually and with combination of YK-3-237 (1 μM) with rapamycin (0.1 μM) and EX-527 (1 μM) with rapamycin (0.1 μM), when compared to control group (dashed line). Results were obtained by JC-1 assay and are presented as mean±SEM (n=6). **Indicates significantly different relatively to control group ($p<0.01$). ****Indicates significantly different relatively to control group ($p<0.0001$). a – indicates significant result relative to EX-527+rapamycin group. b – indicates significant result relative to YK-3-237+rapamycin group.

9.5 Lactate dehydrogenase release is further decreased in bladder cancer cells of different stages after exposure to the combined treatment of mTOR inhibition with SIRT1 activation/inhibition

To further analyse the effect of SIRT1 activation and inhibition, as well as mTOR inhibition or a combined treatment in the membrane of bladder cancer cells from different stages, we performed the LDH assay. LDH release is considered a biomarker for cellular toxicity since its release into extracellular space only occurs when the membrane is damaged (170).

Both individual inhibition of mTOR by rapamycin and SIRT1 by EX-527 were able to significantly ($p<0.0001$) reduce LDH release with all drug concentrations for both cell lines, HT-1376 (Figure 13, panel A) and TCCSUP (Figure 13, panel B), relative to control group. At the lower stage represented by HT-1376 cell line (Figure 13, panel A) LDH release decreased to 78.63±3.77% ($p<0.001$), 82.20±1.99% ($p<0.0001$) and 87.76±4.32% ($p<0.05$) for 0.1 μM, 1 μM and 10 μM of EX-527, respectively and 82.54±3.88% ($p<0.01$), 81.85±4.28% ($p<0.01$) and 78.80±4.1% ($p<0.001$) for 0.01 μM, 0.1 μM and 1 μM of rapamycin, respectively. At the higher

bladder cancer stage represented by TCCSUP cells (Figure 13, panel B), LDH release was reduced to 79.06±3.56% ($p<0.001$), 74.96±3.17% ($p<0.0001$) and 76.71±1.82% ($p<0.0001$) for 0.1 µM, 1 µM and 10 µM of EX-527, respectively and for 0.01 µM, 0.1 µM and 1 µM of rapamycin, it was reduced to 87.56±3.16% ($p<0.01$), 89.63±1.54% ($p<0.0001$) and 88.80±3.01% ($p<0.01$), respectively.

SIRT1 activation by YK-3-237 also affected LDH release however only towards one concentration for each cell line. For HT-1376 (Figure 13, panel A), with 0.1µM of YK-3-237, LDH release significantly ($p<0.01$) decreased until 90.30±2.64% and for TCCSUP (Figure 13, panel B) with 10 µM of YK-3-237 it significantly ($p<0.05$) decreased until 83.33±7.10% relative to the control group. However, the exposure to YK-3-237 at 1 µM and 10 µM did not affect LDH release of HT-1376 cells ($p>0.05$). Equally, for TCCSUP cells, YK-3-237 did not affect LDH release at 0.1 µM and 1 µM ($p>0.05$).

Analysing the effects of drug combination, both treatment, mTOR inhibition by rapamycin with SIRT1 inhibition with EX-527 or SIRT1 activation by YK-3-237, strongly affected LDH release by ~50% in HT-1376 cells (Figure 13, panel A) and almost by ~50% in TCCSUP cells (Figure 13, panel B) treated with EX-527 and rapamycin. YK-3-237 and rapamycin decreased LDH release in more than 60% in TCCSUP cells ($p<0.0001$).

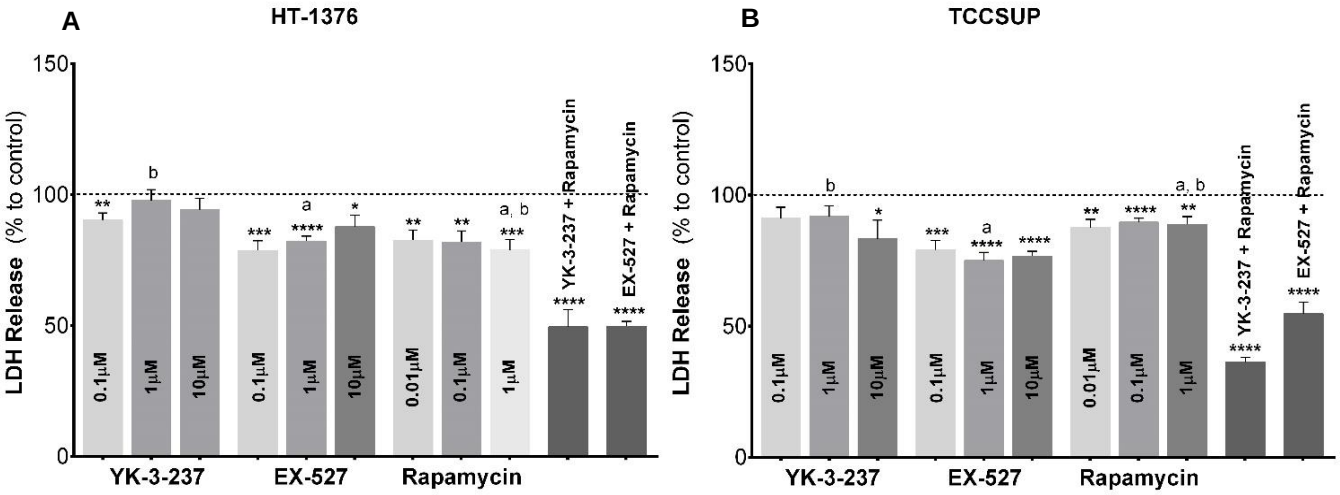

Figure 13: **Effects of the inhibition of SIRT1 with EX-527 or activation with YK-3-237 as well as inhibition of mTOR pathway with rapamycin in LDH release of bladder cancer cells of different stages, HT-1376 (A), which represents a grade III and TCCSUP (B), which represents a grade IV. The effects of combined inhibition of mTOR and SIRT1 pathways on LDH release of HT-1376 and TCCSUP cell lines were also determined.** The figure shows pooled data of independent experiments indicating fold variation of LDH release of HT-1376 and TCCSUP cell lines treated 24 hours with different concentrations of YK-3-237 (in µM: 0.1, 1, and 10), EX-527 (in µM: 0.1, 1 and 10) and rapamycin (in µM: 0.01, 0.1 and 1) individually and with the combination of YK-3-237 (1 µM) plus rapamycin (0.1 µM) and EX-527 (1 µM) with rapamycin (0.1 µM), when compared to control group (dashed line). Results were obtained by LDH release assay and are presented as mean±SEM (n=6). *Indicates significantly different relatively to control group ($p<0.05$). **Indicates significantly different relatively to control group ($p<0.01$). ***Indicates significantly different relatively to control group ($p<0.001$). ****Indicates significantly different relatively to control group ($p<0.0001$). a – indicates significant result relative to EX-527+rapamycin group. b – indicates significant result relative to YK-3-237+rapamycin group.

9.6 *GLUT3* mRNA expression is highly increased in bladder cancer cells from grade III after mTOR inhibition and SIRT1 activation

To study if inhibition or activation of SIRT1 by EX-527 or YK-3-237, respectively, modulates the metabolic profile of HT-1376 cells we determined the expression of *GLUT3*, since it is a glucose transporter and some metabolites present in the extracellular media, including glucose, pyruvate and glutamine, which are involved in cellular metabolism (23). In addition, we further studied the inhibition of mTOR in those processes and the combined treatment of SIRT1 activation/inhibition with mTOR inhibition.

mRNA expression of *GLUT3* was highly increased not only after exposure to rapamycin (2.16±0.59, $p<0.05$) but also to YK-3-237 (1.45±0.25, $p<0.05$) when compared with the control group (0.63±0.16) (Figure 14, panel A). All the other treatments, including the combined treatment of rapamycin with EX-527 or EX-527, did not affect the expression of this gene. Since GLUT3 is a main mechanism for glucose transport in bladder cancer cells (23) and its expression was affected in some conditions, we determined glucose levels in the extracellular media of cultured cells. Our results show that none of the treatments induce changes in glucose levels, $p>0.05$ (Figure 14, panel B). Indeed, HT-1376 in control condition consumed 53.99±14.78 µmol/10^6cells of glucose while glucose consumption after exposure to YK-3-237 was 52.61±14.62 µmol/10^6cells, after exposure to EX-527 was 72.09±17.64 µmol/10^6cells, after exposure to rapamycin was 86.02±21.31 µmol/10^6cells and after exposure to combination of EX-527 and rapamycin was 72.85±4.20 µmol/10^6cells (Figure 14, panel B).

Additionally to glucose, cultured cells mostly consume glutamine and pyruvate. Concerning glutamine and pyruvate levels, there were no significant alterations ($p>0.05$) when cells were exposed to YK-3-237, EX-527, rapamycin, nor after the combined treatment of EX-527 with rapamycin, when compared to control group. Control cells consumed 7.23±3.18 µmol/10^6cells of glutamine while after exposure to YK-3-237, EX-527, rapamycin or the combined exposure to EX-527 plus rapamycin the cells consumed 8.45±2.62 µmol/10^6cells, 9.67±2.54 µmol/10^6cells, 14.57±3.96 µmol/10^6cells, 9.13±0.89 µmol/10^6cells of glutamine, respectively (Figure 14, panel C). Relatively to pyruvate levels, control cells consumed 1.65±0.72 µmol/10^6cells of pyruvate while exposure to YK-3-23, EX-527, rapamycin or combined exposure to EX-527 plus rapamycin the cells consumed 2.10±0.55 µmol/10^6cells, 2.28±0.66 µmol/10^6cells, 3.50±1.09 µmol/10^6cells, 2.78±0.14 µmol/10^6cells of pyruvate, respectively (Figure 14, panel D).

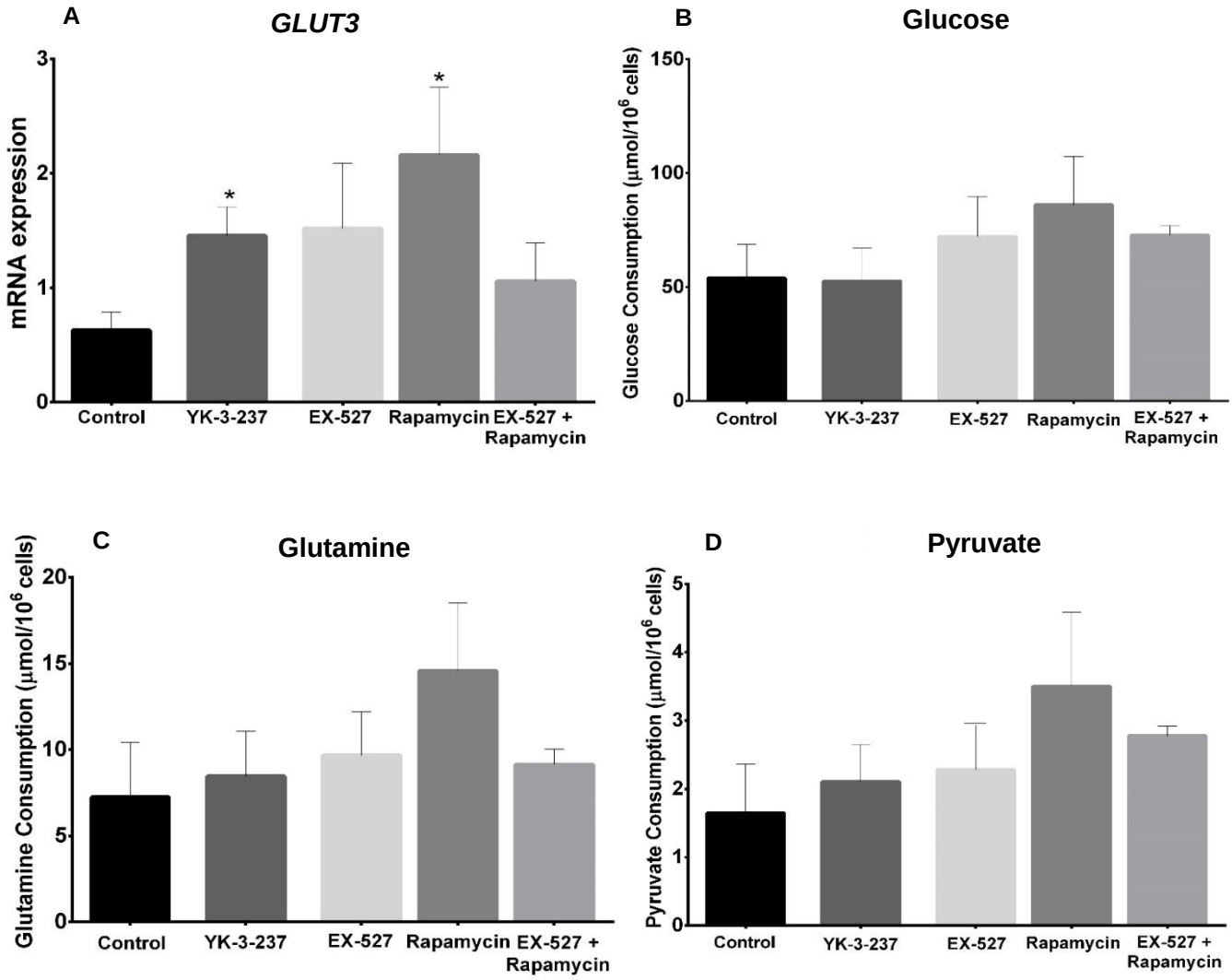

Figure 14: Effect of the inhibition of SIRT1 with EX-527 or activation with YK-3-237 as well as inhibition of mTOR pathway with rapamycin in mRNA expression of *GLUT3* gene and extracellular concentrations of glucose, glutamine and pyruvate of bladder cancer cells HT-1376, which represents a grade III. The effect of combined inhibition of mTOR and SIRT1 in HT-1376 cells on the same parameters was also determined. The figure shows pooled data of independent experiments, indicating mRNA expression of *GLUT3* gene (A) and consumption concentrations of glucose (B), glutamine (C) and pyruvate (D) of HT-1376 cells exposed 24 hours to the single compounds of rapamycin, EX-527 and YK-3-237 (0.1 µM, 1 µM and 1 µM respectively) and to the combined treatment of rapamycin (0.1 µM) with EX-527 (1 µM). mRNA expression results are presented in arbitrary units. Results are presented as mean±SEM (n=6). *Indicates significantly different relatively to control group ($p<0.05$).

To further characterise if bladder cancer progression is associated with a distinct metabolic profile of bladder cells we also determined the expression of *GLUT3* and the extracellular concentration of glucose, pyruvate and glutamine in TCCSUP cells, which represent a grade IV of bladder cancer.

Although our results showed significant differences concerning *GLUT3* mRNA expression after HT-1376 cells were exposed to YK-3-237 and to rapamycin, in TCCSUP cells, our results showed no significant difference ($p>0.05$) in any of the experimental groups tested (Figure 15, panel A), however we can observe a tendency to increase in cells exposed to rapamycin.

Regarding the three metabolites determined, glucose, glutamine and pyruvate, no significant differences ($p>0.05$) were found in their consumption levels in TCCSUP cells exposed to YK-3-237, EX-527, rapamycin or after the combined treatment with EX-527 plus rapamycin. Indeed, TCCSUP cells in control condition consumed 26.37±9.80 µmol/10^6cells of glucose while after exposure to YK-3-237, EX-527, rapamycin or the combined exposure to EX-527 plus rapamycin the cells consumed 16.25±3.07 µmol/10^6cells, 17.95±2.66 µmol/10^6cells, 20.32±5.22 µmol/10^6cells, 42.77±16.03 µmol/10^6cells of glucose, respectively (Figure 15, panel B). Concerning to glutamine levels, control cells consumed 4.59±1.41 µmol/10^6cells of glutamine while after exposure to YK-3-23, EX-527, rapamycin or combined exposure to EX-527 plus rapamycin the cells consumed 2.53±0.63 µmol/10^6cells, 2.13±0.29 µmol/10^6cells, 2.97±0.55 µmol/10^6cells, 4.11±1.91 µmol/10^6cells of glutamine, respectively (Figure 15, panel C). Relatively to pyruvate consumption, TCCSUP cells consumed 2.02±0.38 µmol/10^6cells of pyruvate while after exposure to YK-3-23, EX-527, rapamycin or combined exposure to EX-527 plus rapamycin the cells consumed 3.13±1.08 µmol/10^6cells, 1.82±0.28 µmol/10^6cells, 1.40±0.18 µmol/10^6cells, 2.18±0.49 µmol/10^6cells of pyruvate, respectively (Figure 15, panel D).

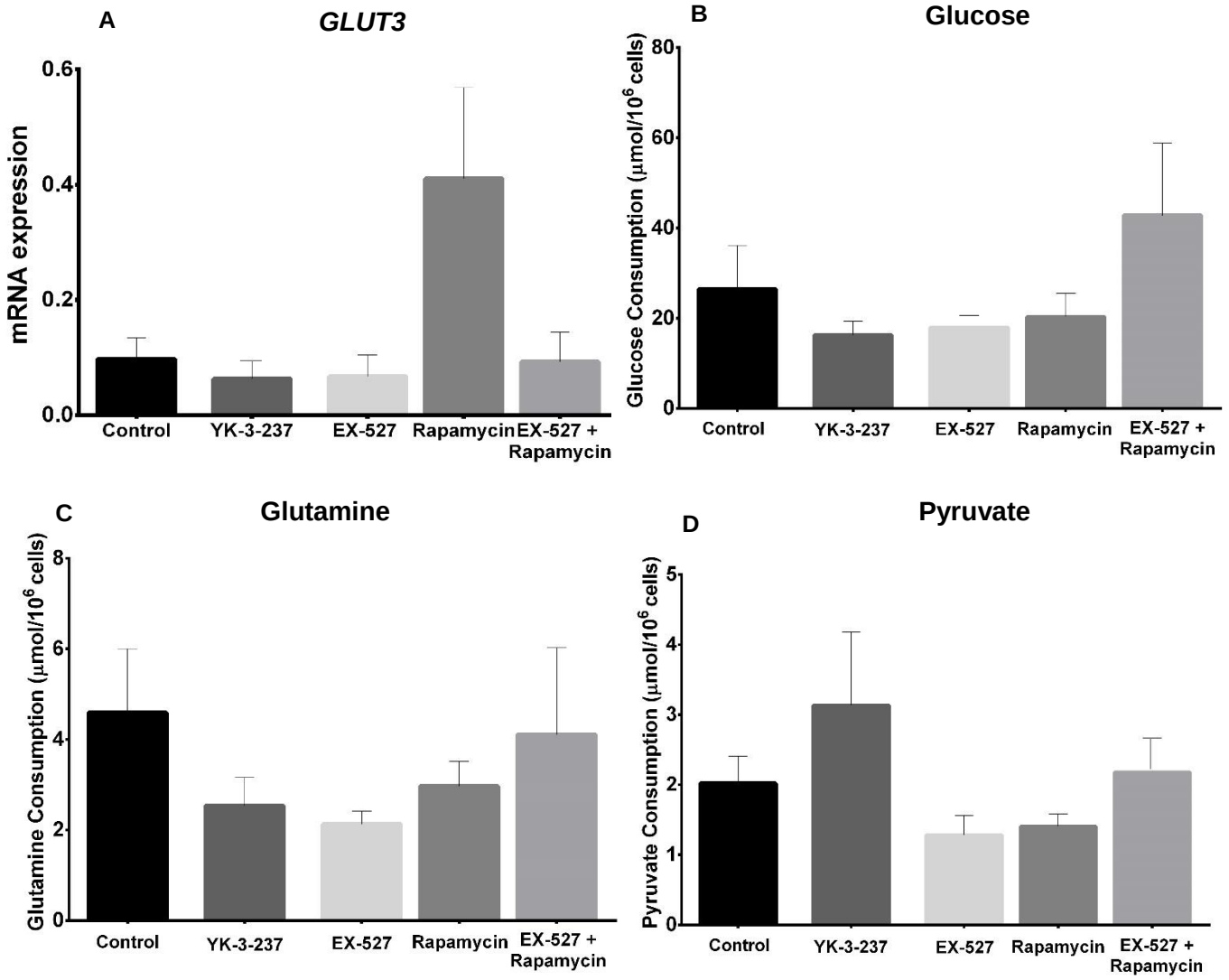

Figure 15: Effect of the inhibition of SIRT1 with EX-527 or activation with YK-3-237 as well as inhibition of mTOR pathway with rapamycin in mRNA expression of *GLUT3* gene and extracellular concentrations of glucose, glutamine and pyruvate of bladder cancer cells TCCSUP, which represents a grade IV. The effect of combined inhibition of mTOR and SIRT1 in TCCSUP on the same parameters was also determined. The figure shows pooled data of independent experiments, indicating mRNA expression of GLUT3 gene (A) and consumption concentrations of glucose (B), glutamine (C) and pyruvate (D) of TCCSUP cells exposed 24 hours to the single compounds of rapamycin, EX-527 and YK-3-237 (0.1 µM, 1 µM and 1 µM respectively) and to the combined treatment of rapamycin (0.1 µM) with EX-527 (1 µM). mRNA expression results are presented in arbitrary units. Results are presented as mean±SEM (n=6).

9.7 mTOR inhibition highly increase *MCT1* and *MCT4* expression on bladder cancer cells from different stages of the disease

To understand if the inhibition of SIRT1 by EX-527 or its activation by YK-3-237, as well as the inhibition of mTOR by rapamycin interferes with lactate pathway on HT-1376 cells, the expression of *MCT1, MCT4 and LDH* and lactate concentration present in the extracellular media were determined.

mRNA expression of *MCT1* in HT-1376 cells was significantly increased ($p<0.05$), comparing to control group (0.03±0.01), when treated with the individual compounds of YK-3-237 (0.21±0.062), EX-527 (0.21±0.061) or with rapamycin (0.21±0.063) (Figure 16, panel A). The combined treatment of EX-527plus rapamycin did not significantly change ($p>0.05$) the mRNA expression of *MCT1* (0.21±0.08).

On the other hand, for *MCT4* , its mRNA expression only increased significantly in HT-1376 cells treated with rapamycin to 0.59±0.14 comparing to control group, $p<0.01$ (0.089±0.016) (Figure 16, panel B). The treatments with YK-3-237 (0.17±0.03), EX-527 (0.088±0.016) and the combined treatment with EX-527 plus rapamycin (0.32±0.09) did not significantly changed *MCT4* mRNA expression, $p>0.05$ (Figure 16, panel B).

However, concerning *LDH* mRNA expression (Figure 16, panel C) and extracellular lactate concentration in the extracellular medium (Figure 16, panel D), none of the experimental groups induced significant differences, when compared to control group ($p>0.05$). mRNA expression of *LDH* when HT-1376 cells were exposed to YK-3-237, EX-527, rapamycin alone or to the combined treatment with EX-527 plus rapamycin was 1.14±0.20, 0.94±0.24, 1.24±0.31, 0.81±0.20 respectively, whereas for the control group was 0.87±0.33 (Figure 16, panel C). HT-1376 cells in control condition produced 59.04±13.85 µmol/10^6cells of lactate while after exposure to YK-3-23, EX-527, rapamycin or combined treatment of EX-527 plus rapamycin the cells produced 99.87±20.56 µmol/10^6cells, 55.17±10.59 µmol/10^6cells, 100.7±21.62 µmol/10^6cells, 83.40±9.11 µmol/10^6cells of lactate, respectively (Figure 16, panel D).

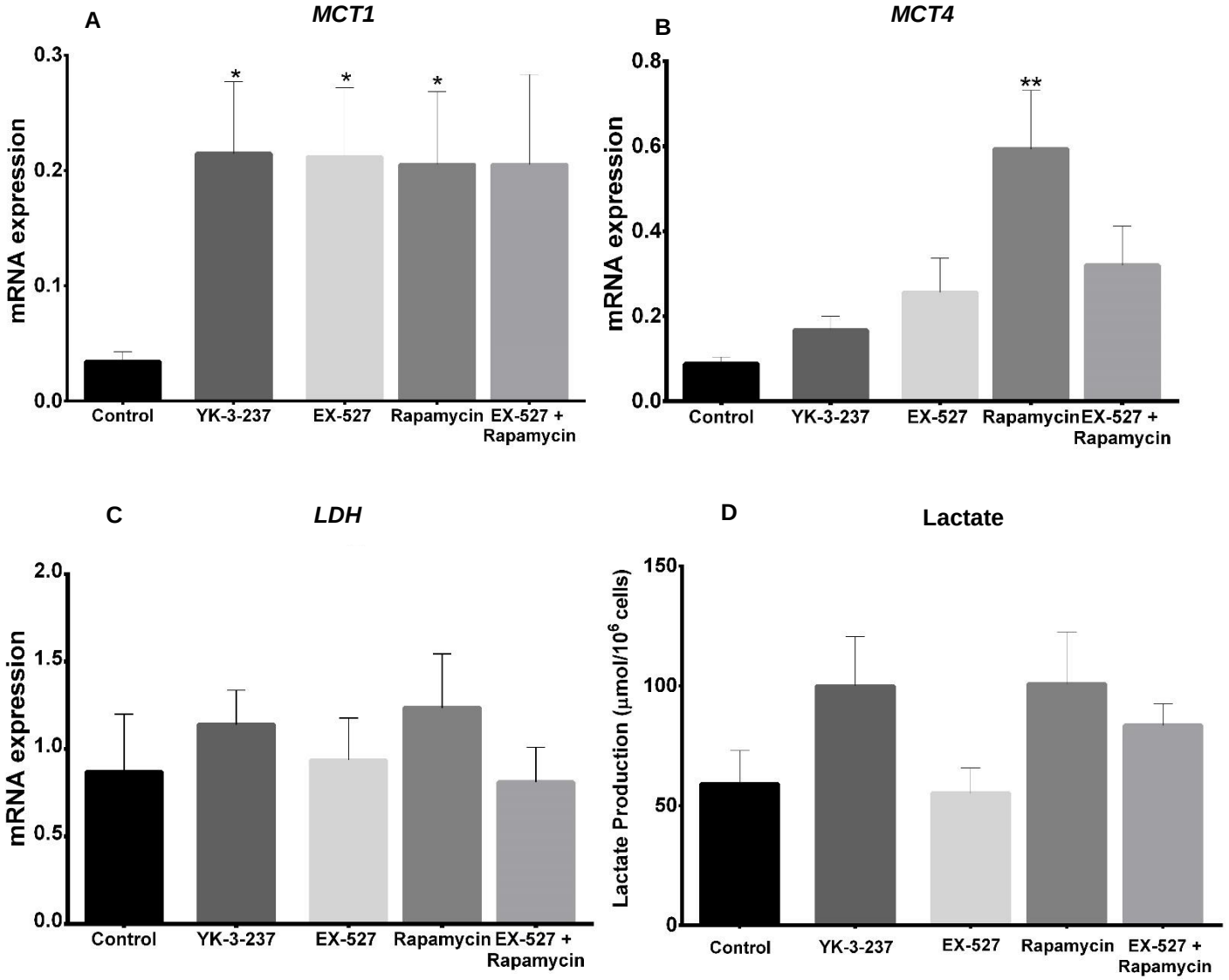

Figure 16: Effect of the inhibition of SIRT1 with EX-527 or activation with YK-3-237 as well as inhibition of mTOR pathway with rapamycin in mRNA expression of *MCT1, MCT4* and *LDH* genes and extracellular concentration of lactate of bladder cancer cells HT-1376, which represents a grade III. The effect of combined inhibition of mTOR and SIRT1 in HT-1376 cell line on the same parameters was also determined. The figure shows pooled data of independent experiments, indicating mRNA expression of *MCT1* (A), *MCT4* (B) and *LDH* (C) genes and production concentration of lactate (D) of HT-1376 cells exposed 24 hours to the single compounds of rapamycin, EX-527 and YK-3-237 (0.1 μM, 1 μM and 1 μM respectively) and to the combined treatment of rapamycin (0.1 μM) with EX-527 (1 μM). mRNA expression results are presented in arbitrary units. Results are presented as mean±SEM (n=6). *Indicates significantly different relatively to control group ($p<0.05$). **Indicates significantly different relatively to control group ($p<0.01$).

The expression of the same genes referred above, *MCT1, MCT4 and LDH* and the extracellular concentration of lactate were also determined for TCCSUP cells (grade IV of bladder cancer) cultured in the same conditions as HT-1376.

mRNA expression of *MCT1* (Figure 17, panel A) and *LDH* (Figure 17, panel C) in TCCSUP cells did not change ($p>0.05$), comparing to control group after exposure to any of the experimental groups. mRNA expression of *MCT1* when TCCSUP cells were exposed to YK-3-237, EX-527, rapamycin alone, as well as after the combined treatment with EX-527 plus rapamycin was 0.003±0.002, 0.017±0.01, 0.015±0.01, 0.02±0.01 respectively, whereas for the control group it was 0.016±0.01 (Figure 17, panel A). Concerning *LDH* mRNA expression when TCCSUP cells exposed to YK-3-237, EX-527, rapamycin alone, as well as after exposure to the combined treatment with EX-527 plus rapamycin was 0.096±0.02, 0.18±0.10, 0.31±0.10, 0.14±0.04 respectively, whereas for the control group it was 0.15±0.024 (Figure 17, panel C).

On the other hand, *MCT4* (Figure 17, panel B) mRNA expression was strongly increased after treatment with rapamycin alone to 0.16±0.019 ($p<0.001$), comparing to control group (0.02±0.08). The same was not detected when TCCSUP cells were exposed to YK-3-237 (0.04±0.02), EX-527 (0.05±0.03) and to the combined exposure to EX-527 plus rapamycin (0.08±0.03), since no significant differences were observed ($p>0.05$). Regarding extracellular lactate levels, our results show a significant decrease ($p<0.01$) after exposure to the combined treatment of TCCSUP cells with EX-527 and rapamycin (12.42±3.15 µmol/10^6cells), comparing not only to the control group (29.73±4.34 µmol/10^6cells), but also after exposure to rapamycin (26.19±4.87 µmol/10^6cells) and EX-527 (23.47±0.73 µmol/10^6cells) alone (Figure 17, panel D). However, when TCCSUP cells were exposed to YK-3-237 (45.34±10.35 µmol/10^6cells) lactate production was not significantly altered when comparing with the control group.

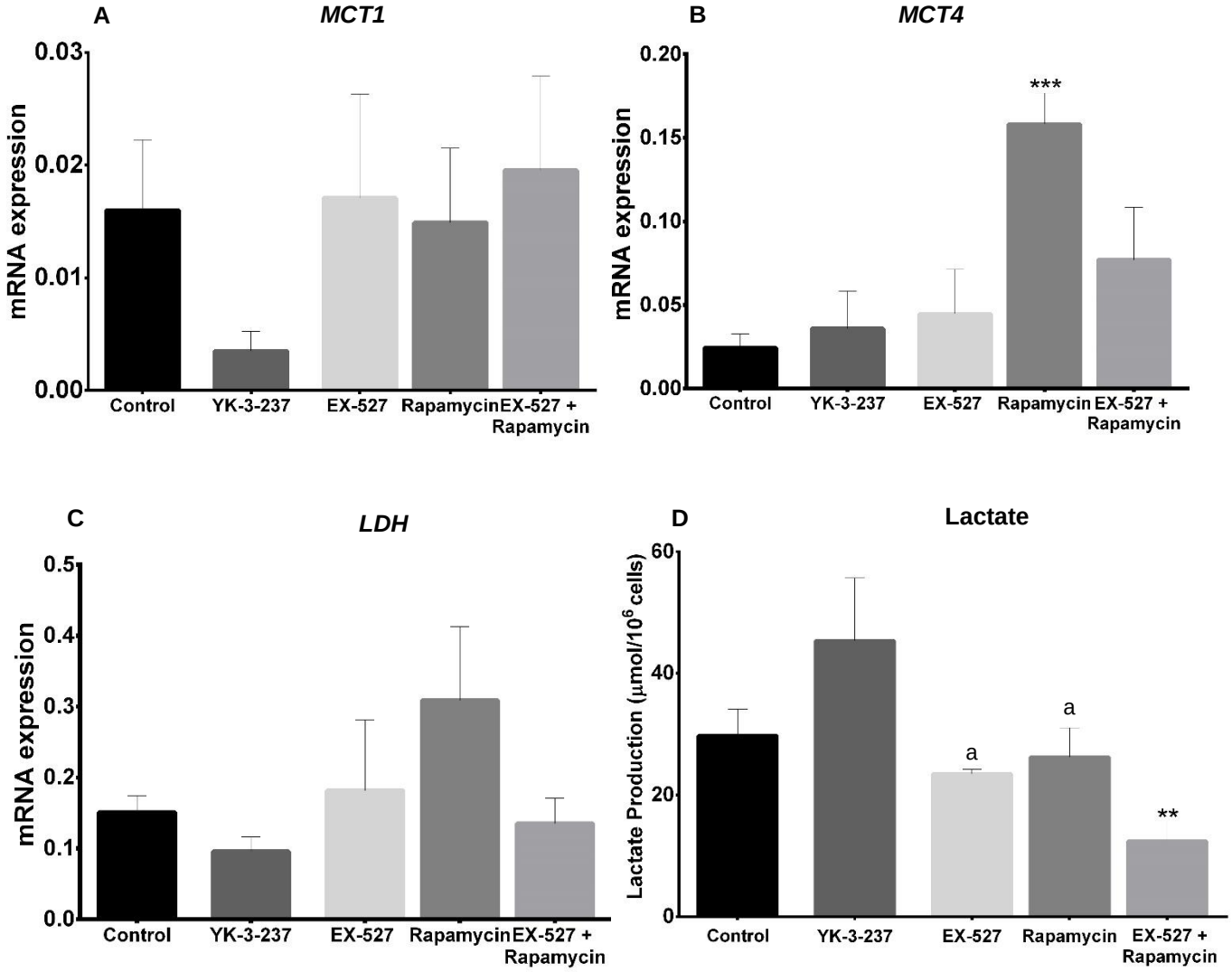

Figure 17: Effect of the inhibition of SIRT1 with EX-527 or activation with YK-3-237 as well as inhibition of mTOR pathway with Rapamycin in mRNA expression of *MCT1, MCT4* and *LDH* genes and extracellular concentration of lactate of bladder cancer cells TCCSUP, which represents a grade IV. The effect of combined inhibition of mTOR and SIRT1 in TCCSUP cell line on the same parameters was also determined. The figure shows pooled data of independent experiments, indicating mRNA expression of *MCT1* (A), *MCT4* (B) and *LDH* (C) genes and lactate production (D) of TCCSUP cells exposed 24 hours to the single compounds of rapamycin, EX-527 and YK-3-237 (0.1 µM, 1 µM and 1 µM respectively) and to the combined treatment of rapamycin (0.1 µM) with EX-527 (1 µM). mRNA expression results are presented in arbitrary units. Results are presented as mean±SEM (n=6). **Indicates significantly different relatively to control group ($p<0.01$). a – indicates significant result relative to EX-527+Rapamycin group.

9.8 Acetate consumption is highly increased in HT-1376 bladder cancer cells after inhibition of Sirt1 and mTOR

Pyruvate is at a crossroad of several metabolic pathways, particularly lactate and alanine. Thus, we also determined alanine concentration in the extracellular media of the different experimental groups. In addition, we also detected the concentration of acetate in the extracellular media since it is necessary for fatty acids synthesis and as fuel for the TCA cycle (105, 178).

The alanine production by HT-1376 cells was only significantly decreased ($p<0.05$) after treatment with EX-527 alone (096±0.25 µmol/10^6cells) when comparing to the combined treatment of EX-527 with Rapamycin (1.77±0.24 µmol/10^6cells) (Figure 18, panel A). In the treatments of HT-1376 cells with YK-3-237 and rapamycin, alanine consumption was 1.88±0.63 µmol/10^6cells and 2.16±0.49 µmol/10^6cells, respectively, which was not significantly altered when compared with the control group, $p>0.05$ (1.20±0.32 µmol/10^6cells).

Concerning to acetate, our results show that its consumption was significantly increased in HT-1376 cells treated with the combination of EX-527 with rapamycin, $p<0.05$ (1.15±0.46 µmol/10^6cells) when compared to control group (0.69±0.15 µmol/10^6cells) (Figure 18, panel B). The treatments with YK-3-237 (1.38±0.52 µmol/10^6cells), EX-527 (1.03±0.26 µmol/10^6cells) and rapamycin (1.32±0.33 µmol/10^6cells) did not significantly change the acetate consumption by HT-1376 cells, $p>0.05$ (Figure 18, panel B).

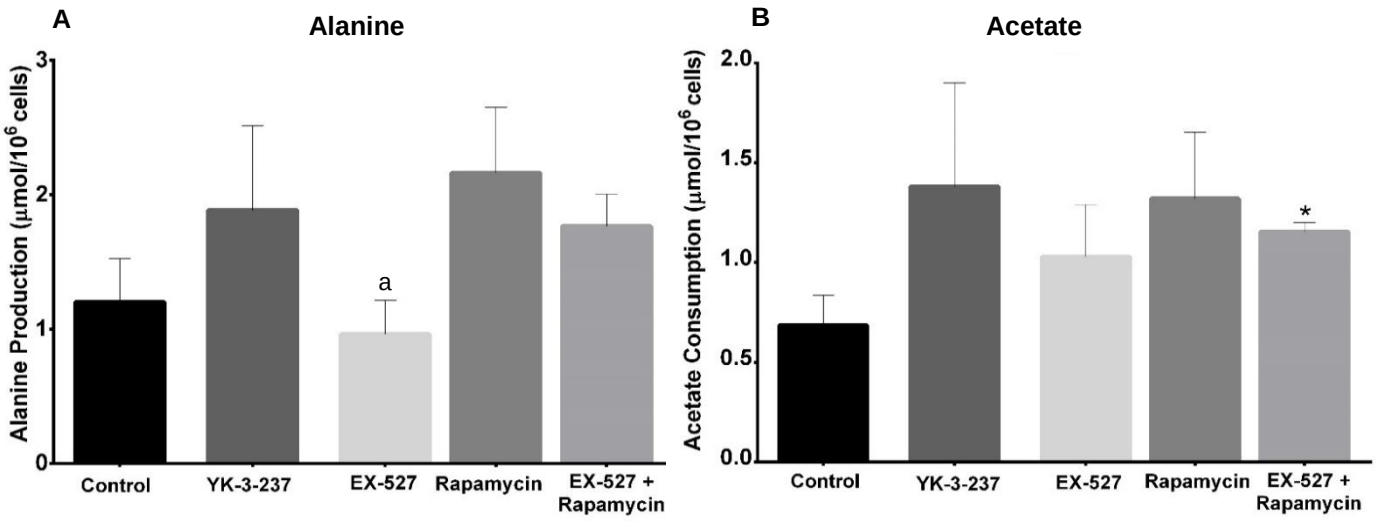

Figure 18: Effect of the inhibition of SIRT1 with EX-527 or activation with YK-3-237 as well as inhibition of mTOR pathway with Rapamycin in extracellular concentrations of alanine and acetate of bladder cancer cells HT-1376, which represents a grade III. The effect of combined inhibition of mTOR and SIRT1 in HT-1376 cell line on the same parameters was also determined. The figure shows pooled data of independent experiments, indicating extracellular concentrations of alanine (A) and acetate (B) of HT-1376 cells exposed 24 hours to the single compounds of rapamycin, EX-527 and YK-3-237 (0.1 µM, 1 µM and 1 µM respectively) and to the combined treatment of rapamycin (0.1 µM) with EX-527 (1 µM). Results are presented as mean ± SEM (n=6). *Indicates significantly different relatively to control group ($p<0.05$). a- indicates significantly different relatively to EX-527 + rapamycin experimental group.

Alanine production and acetate consumption were also analysed after TCCSUP cells were exposed to YK-3-237, EX-527, and rapamycin and also to Ex-527 plus rapamycin.

Alanine production was significantly reduced ($p<0.05$) when TCCSUP cells were exposed to the combined treatment of EX-527 plus rapamycin (-0.26±0.28 µmol/10^6cells), comparing not only to control group (0.72±0.19 µmol/10^6cells), but also to the individual exposition of rapamycin (0.95±0.45 µmol/10^6cells) and EX-527 (0.70±0.10 µmol/10^6cells) (Figure 19, panel A). These results suggest that after TCCSUP cells are exposed to EX-527 plus rapamycin, alanine is not produced but instead consumed. The other experimental groups (EX-527 and rapamycin alone) did not induce any significant change in alanine production, $p>0.05$ (Figure 19, panel A), relatively to the control group. In addition, no significant differences ($p>0.05$) in alanine production were observed when cells were treated with the SIRT1 activator, YK-3-237 (1.42±0.45 µmol/10^6cells) (Figure 19, panel A).

Regarding to acetate consumption (Figure 19, panel B), it was significantly reduced ($p<0.05$) in TCCSUP cells treated with the SIRT1 inhibitor, EX-527 (0.06±0.04 µmol/10^6cells) only when compared to the combined treatment of TCCSUP with EX-527 plus rapamycin (0.48±0.17 µmol/10^6cells). However, the exposure of TCCSUP cells to YK-3-237 (0.20±0.08 µmol/10^6cells) and rapamycin (0.11±0.06 µmol/10^6cells) did not induced any significant changes ($p>0.05$) in acetate consumption, when compared to experimental control group (0.06±0.12 µmol/10^6cells).

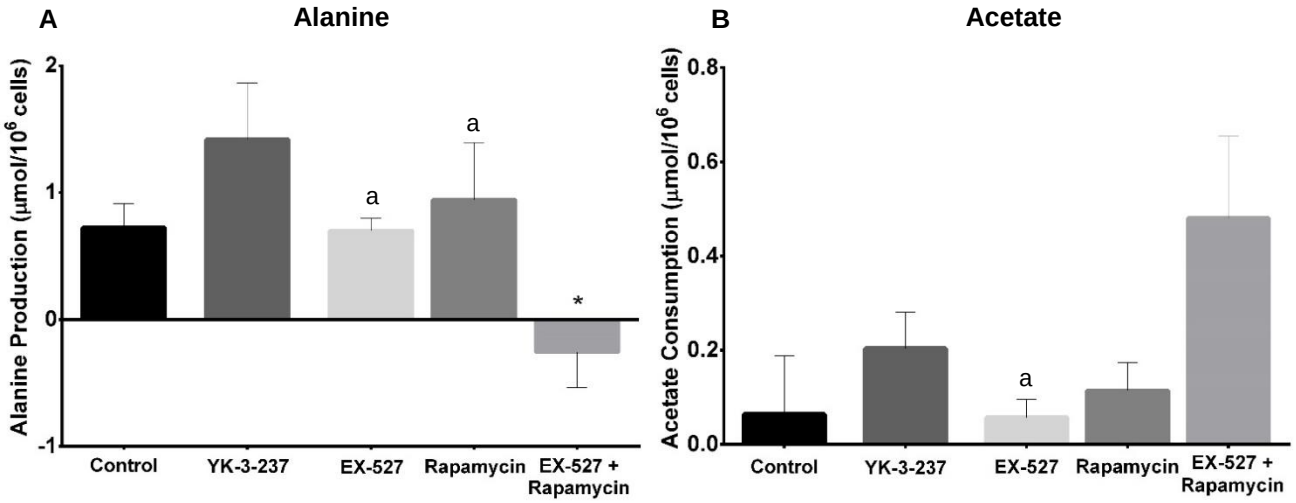

Figure 19: Effect of the inhibition of SIRT1 with EX-527 or activation with YK-3-237 as well as inhibition of mTOR pathway with Rapamycin in alanine production and acetate consumption of bladder cancer cells TCCSUP, which represents a grade IV. The effect of combined inhibition of mTOR and SIRT1 in TCCSUP cell line on the same parameters was also determined. The figure shows pooled data of independent experiments, indicating the production of alanine (A) and consumption of acetate (B) of TCCSUP cells exposed 24 hours to the single compounds of rapamycin, EX-527 and YK-3-237 (0.1 µM, 1 µM and 1 µM respectively) and to the combined treatment of rapamycin (0.1 µM) with EX-527 (1 µM). Results are presented as mean±SEM (n=6). *Indicates significantly different relatively to control group ($p<0.05$). a – indicates significant result relative to EX-527+Rapamycin group.

9.9 Inhibition of mTOR and SIRT1 alone or in combination decrease mitochondrial copy number of HT-1376 bladder cancer cells

Beyond the studies of the metabolic profile of HT-1376 and TCCSUP cells we also tested the hypothesis that inhibition or activation of SIRT1 by EX-527 or YK-3-237, respectively and the inhibition of mTOR by rapamycin could interfere with mitochondrial biogenesis, affecting mitochondrial DNA. Therefore, the analysis of mitochondrial copy number was performed for both bladder cancer cell lines after exposure to the individual treatments of rapamycin, EX-527 and YK-3-237 and to the combination of EX-527 plus rapamycin, by qPCR.

Regarding to HT-1376 cell line, which represent the lower bladder cancer stage studied, mitochondrial copy number was significantly lower ($p<0.01$), comparing to control group (911.0±120.2), when cells were exposed not only to rapamycin but also to the EX-527 alone (491.2±53.49 and 445.6 ± 63.16, respectively) (Figure 20, panel A). However, the combination of these compounds (EX-527 plus rapamycin) and the treatment with YK-3-237 (648.6±185.5 and 1074±225.1, respectively) did not significantly affect mitochondrial copy number, when compared to the control group, $p>0.05$.

Concerning to TCCSUP cell line, no significant differences ($p>0.05$) were observed after exposure to YK-3-237, EX-527, rapamycin and to the combined treatment with EX-527 plus rapamycin (416.5±37.97, 553.1±65.24, 599±80.39, 495.5±47.03, respectively), relatively to control group (508.4±58.68) (Figure 20, panel B).

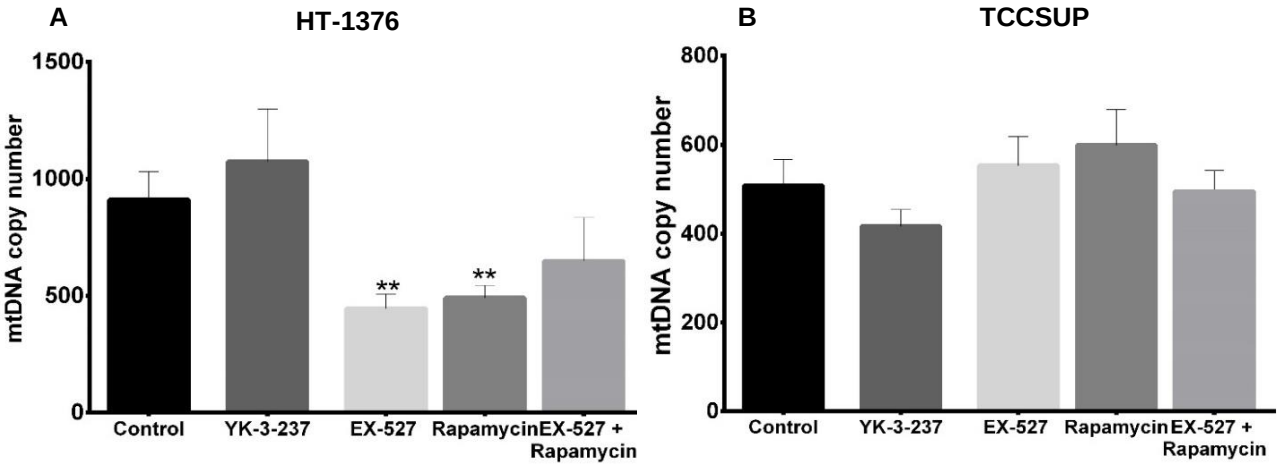

Figure 20: Effect of the inhibition of SIRT1 with EX-527 or activation with YK-3-237 as well as inhibition of mTOR pathway with Rapamycin in mitochondrial copy number of bladder cancer cells HT-1376, which represents a grade III and TCCSUP, which represents a grade IV. The effect of combined inhibition of mTOR and SIRT1 in HT-1376 and TCCSUP cell lines on the same parameter was also determined. The figure shows pooled data of independent experiments, indicating the mitochondrial copy number of HT-1376 (A) and TCCSUP (B) cells exposed 24 hours to the single compounds of rapamycin, EX-527 and YK-3-237 (0.1 µM, 1 µM and 1 µM respectively) and to the combined treatment of rapamycin (0.1 µM) with EX-527 (1 µM). mtDNA copy number results are presented in arbitrary units. Results are presented as mean±SEM (n=6). *Indicates significantly different relatively to control group ($p<0.05$). **Indicates significantly different relatively to control group ($p<0.01$).

9.10 mTOR inhibition decreases BAX/Bcl-2 ratio on bladder cancer cell lines from different stages

To analyse the effects of the inhibition or activation of SIRT1 by EX-527 or YK-3-237, respectively, as well as the inhibition of mTOR by rapamycin on cell death we analysed the mRNA expression of *BAX* and *BCL-2* to establish a *BAX/BCL-2* ratio that is well known as an indicator of apoptosis.

Regarding to HT-1376 cells, the *BAX/BCL-2* ratio was significantly ($p<0.05$) lower, comparing to control group (0.17±0.04), when cells were exposed to rapamycin (0.08±0.01) (Figure 21, panel A). However, concerning the other experimental groups, none promoted any significant differences ($p>0.05$) in *BAX/BCL-2* ratio, (0.17±0.08, 0.93±0.01, 0.12±0.04, for YK-3-237, EX-527 and EX-527 plus rapamycin treatments, respectively). Interestingly, TCCSUP cells no significant differences were observed after exposure to YK-3-237, EX-527, rapamycin and to the combined treatment of EX-527 plus rapamycin (0.18±0.06, 0.14±0.01, 0.05±0.01, 0.11±0.32, respectively), relative to the control group (0.38±0.20) (Figure 21, panel B).

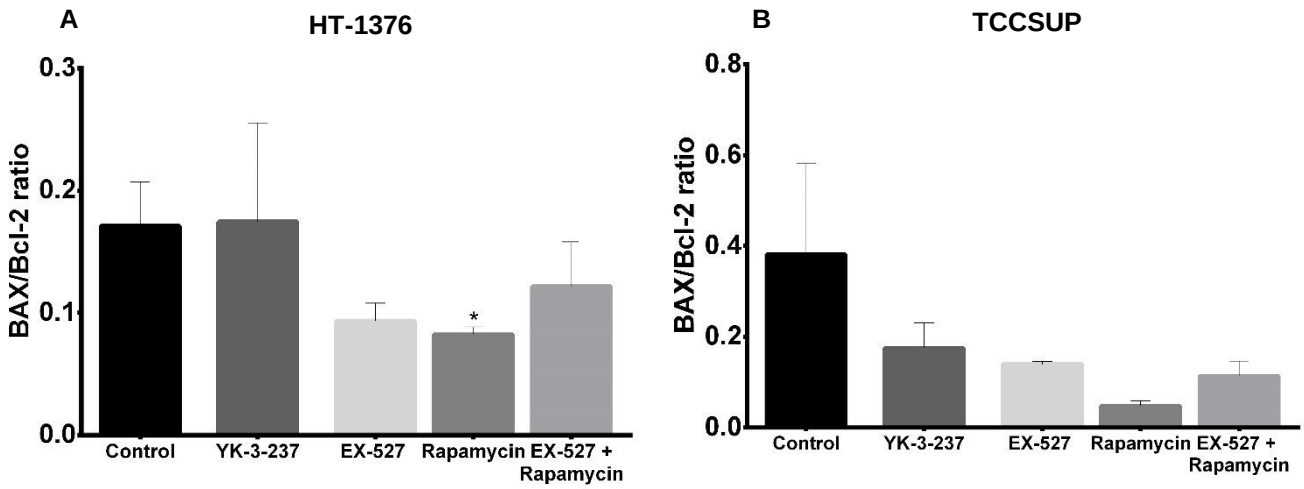

Figure 21: Effect of the inhibition of SIRT1 with EX-527 or activation with YK-3-237 as well as inhibition of mTOR pathway with Rapamycin in BAX/Bcl-2 ratio of bladder cancer cells HT-1376, which represents a grade III and TCCSUP, which represents a grade IV. The effects of combined inhibition of mTOR and SIRT1 in HT-1376 and TCCSUP cell lines on the same parameter was also determined. The figure shows pooled data of independent experiments, indicating the ratio between BAX and Bcl-2 mRNA expressions of HT-1376 (A) and TCCSUP (B) cells exposed 24 hours to the single compounds of rapamycin, EX-527 and YK-3-237 (0.1 µM, 1 µM and 1 µM respectively) and to the combined treatment of rapamycin (0.1 µM) with EX-527 (1 µM). mRNA expression results are presented in arbitrary units. Results are presented as mean±SEM (n=6). *Indicates significantly different relatively to control group ($p<0.05$).

9.11 TCCSUP cells respirometry

Respirometry was performed to analyse the consumption of oxygen by TCCSUP cells, representative of grade IV, under treatment conditions with 1 µM of YK-3-237, 1 µM of EX-527, 0.1 µM of rapamycin or 1 µM of EX-527 with 0.1 µM of rapamycin (combined treatment).

TCCSUP cells oxygen consumption was assessed in the presence of different mitochondrial modulators, enabling to obtain several respiratory parameters, such as basal respiration (initial respiration minus rotenone with antimycin A state), maximal respiration (FCCP state minus rotenone with antimycin A state), ATP turnover (initial respiration minus oligomycin state), proton leak (oligomycin state minus rotenone with antimycin A state), spare respiratory capacity (FCCP state minus initial respiration) and non-mitochondrial respiration (rotenone with antimycin A state).

Adherent cells, such TCCSUP and HT-1376 after being detached from plate shown high levels of oxidative stress (activating SOD and catalase), producing more oxygen than the one that is consumed, making difficult to reach a “real and physiological” initial respiration. Then, related parameters are affected by this experimental artifact. No statistically significant differences ($p>0.05$) were found for each respiratory parameter, among different experimental groups for TCCSUP cell line. However, the combination of 1 µM of EX-527 with 0.1 µM of rapamycin slightly increased the proton leak in these cells (Figure 22). The basal proton leak is cell-type specific and correlates with metabolic rate (179). Several mechanisms can be associated with proton leak increase like activation (or up-regulation) of the adenine nucleotide translocase (ANT) and uncoupling proteins (UCPs). Probably the synergistic behaviour of the two compounds can modulate any of those mechanisms. In counterpart, a low ATP turnover is associated with a low capacity for substrate oxidation (180).

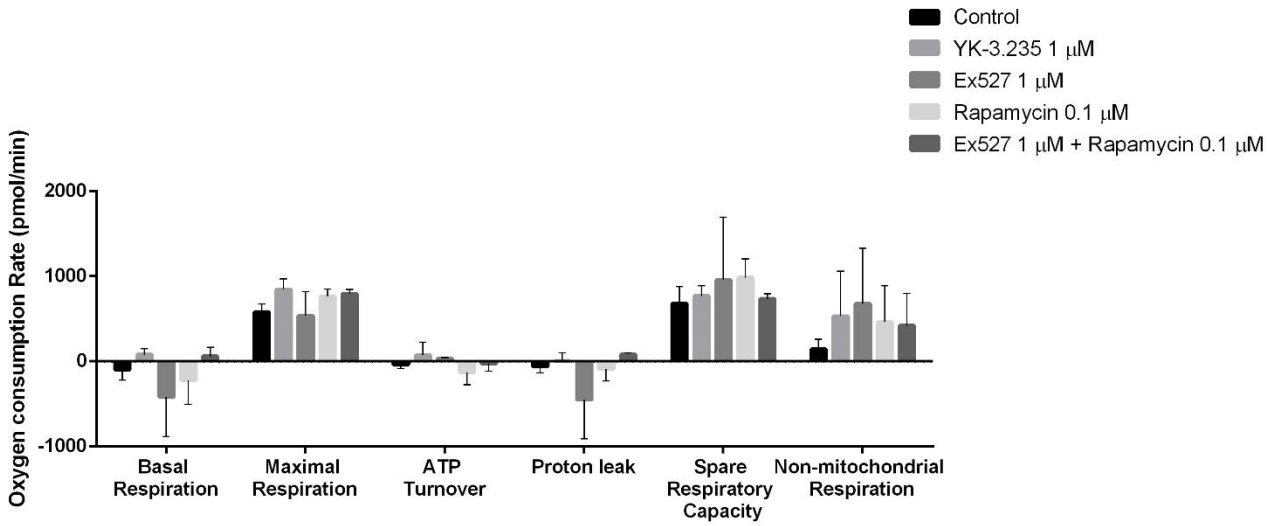

Figure 22: Effect of the inhibition of SIRT1 with EX-527 or activation with YK-3-237 as well as inhibition of mTOR pathway with rapamycin in oxygen consumption rate of bladder cancer cells TCCSUP, which represents a grade IV. The effect of combined inhibition of mTOR and SIRT1 in TCCSUP cell line on oxygen consumption rate was also determined. The figure shows pooled data of independent experiments, basal respiration, maximal respiration, ATP turnover, proton leak, spare respiration capacity and non-mitochondrial respiration of TCCSUP cells exposed 24 hours to the single compounds of rapamycin, EX-527 and YK-3-237 (0.1µM, 1µM and 1µM respectively) and to the combined treatment of rapamycin (0.1µM) with EX-527 (1µM). Results are presented as mean±SEM (n=3).

9.12 HT-1376 Migration

Cell migration assay was performed to study if the inhibition of SIRT1 by EX-527 or its activation by YK-3-237, as well as the inhibition of mTOR by rapamycin interferes in HT-1376 cells migration. Cell migration assay was assessed using Transwell-Clear Inserts and the quantitative results were obtained through optical density and the qualitative results through observation under a microscope. No statistically significant differences ($p>0.05$ were found among different experimental groups on HT-1376 cells migration (Figure 23). However, we were only able to perform this assay twice (n=2) and therefore, a higher sample number is definitely needed.

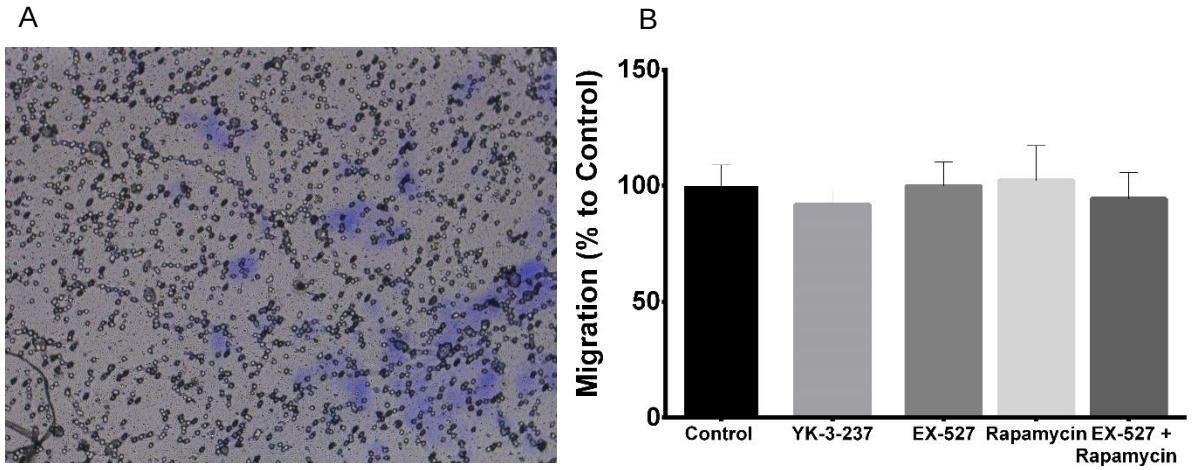

Figure 23: Effect of the inhibition of SIRT1 with EX-527 or activation with YK-3-237 as well as inhibition of mTOR pathway with rapamycin in migration of bladder cancer cells HT-1376, which represents a grade III. The effect of combined inhibition of mTOR and SIRT1 in HT-1376 cell line on cell migration was also determined. The figure shows a representative microphotography (100x magnification) of migrated cells (insert bottom observation), labelled with 0.2% crystal violet (A) and in (B) a quantitative approach for cell migration (O.D. measured at 570 nm) after 24 hours exposition to different pharmacological conditions (YK-3-237, EX-527 and rapamycin at 1 µM, 1 µM and 0.1 µM, respectively and to the combined treatment of rapamycin at 0.1 µM with EX-527 at 1 µM. Results are presented as mean±SEM (n=2).

9.13 Morphology analysis of HT-1376 and TCCSUP cells after treatments

The morphology analysis was performed to observe the effects of the inhibition of SIRT1 by EX-527 or its activation by YK-3-237, as well as the inhibition of mTOR by rapamycin interferes in both HT-1376 and TCCSUP cells. Representative microphotographies (200x magnification) of HT-1376 and TCCSUP cell lines, which represent a grade III and IV of bladder cancer cells, respectively, are presented.

Morphologically, HT-1376 cells present two major sub-populations, one with more licheniform aspect (a) and the other with stellar appearance (b), presenting dendrites (Figure 24, Panels A – I). The combined treatment with EX-527 and rapamycin induced some morphological changes, making cells susceptible (with increased licheniform cell granulation) and with increasing dendritic contact between stellate cells (Figure 24, Panels G and I).

The TCCSUP cells showed greater morphological homogeneity (Figure 24, Panels J – N). However, in none of the treatments significant morphological changes were observed.

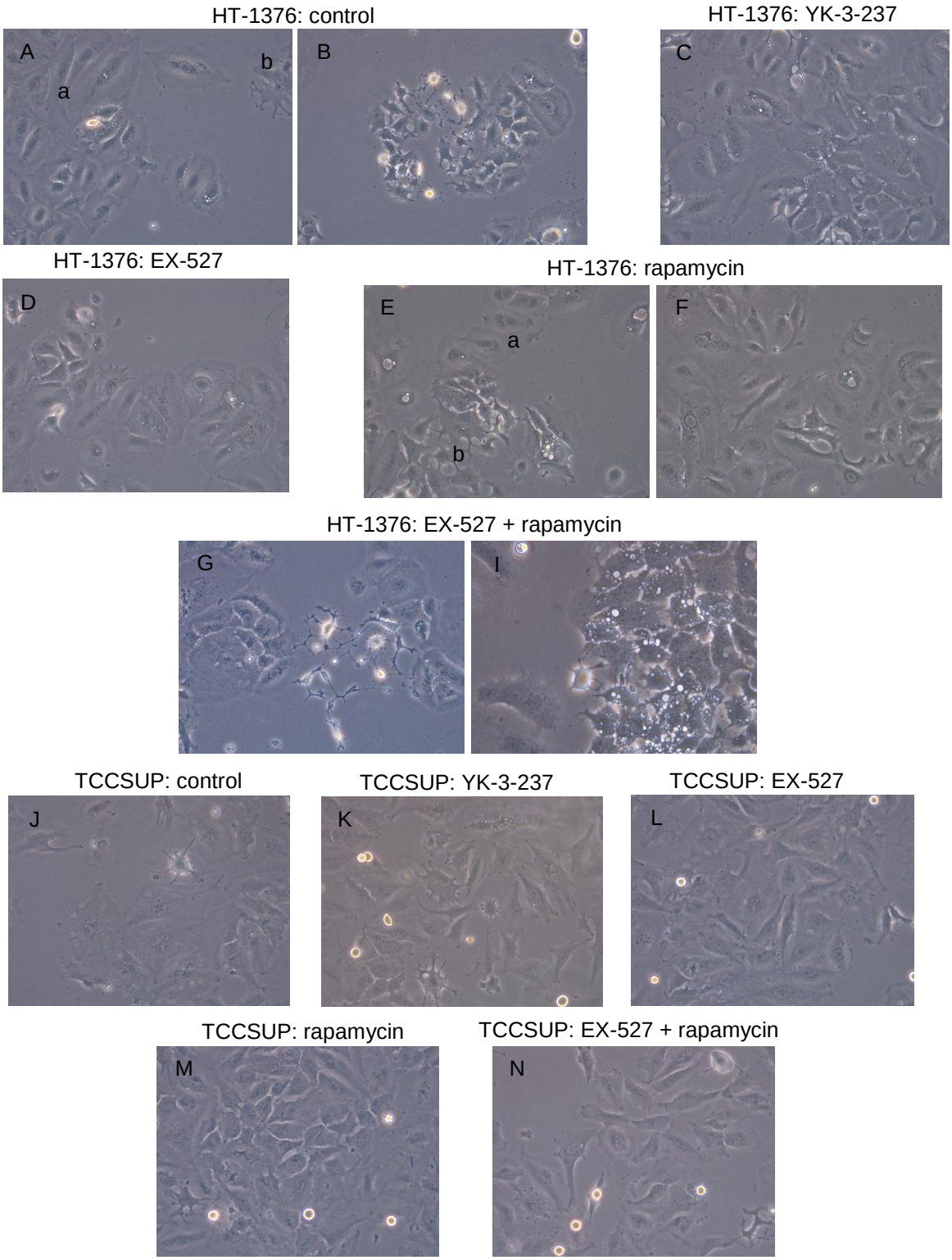

Figure 24: Effect of the inhibition of SIRT1 with EX-527 or activation with YK-3-237 as well as inhibition of mTOR pathway with rapamycin in cell morphology of bladder cancer cells HT-1376 and TCCSUP, which represent a grade III and grade IV, respectively. The effect of combined inhibition of mTOR and SIRT1 in HT-1376 and TCCSUP cell lines on cell morphology was also determined. The figure shows representative microphotographies (200x magnification for all panels, except panel I, which was observed with 400x magnification) of HT-1376 (Panels A - I) and TCCSUP (Panels J – N) cell lines, after 24 hours exposition to different pharmacological conditions (YK-3-237, EX-527 and rapamycin at 1 µM, 1 µM and 0.1 µM, respectively and to the combined treatment of rapamycin at 0.1 µM with EX-527 at 1 µM. a – indicates sub-population of HT-1376 with licheniform aspect. b - indicates sub-population of HT-1376 cells with stellar appearance.

10 DISCUSSION

Bladder cancer has a high incidence and recurrence rate (8, 14). In addition to this, many patients show a poor survival expectancy (8, 9) illustrating a high demand for a more accurate stage-specific classification of the tumour that will aid much for prognosis and better tailoring of the treatment based on characteristics such as recurrence and progression. An approach focused on that will possibly unveil biomarkers that can be valuable toward personalized medicine and treatment (181). The molecular classification and characterization of bladder cancer is pivotal as a tool to predict clinical outcomes, responses to chemotherapy and develop novel treatments. Here, we focused on the molecular study of the metabolic and bioenergetics profile of bladder cancer cells of two distinct stages: HT-1376 cells, which represent a stage III and TCCSUP cells that represent a highly invasive stage IV of the disease. Bladder tumours are characterized by a high heterogeneity with frequent alterations in multiple signalling pathways, including SIRT1 and mTOR. Thus, we aimed to characterize how activation and inhibition of SIRT1, as well as mTOR inhibition, would modulate the metabolic and bioenergetics profile of bladder cancer cells of different stages. In addition, we tested the hypothesis that both pathways may interact to control the metabolic and bioenergetics profile of bladder cancer cells according with the stage of the disease. As expected, our preliminary results showed that both cancer cell lines, representative of stage III and IV of bladder cancer, presented a distinct growth profile with the latter having a higher cell density for the same period of time. TCCSUP cells are derived from a grade IV transitional cell carcinoma and represent a highly proliferative and invasive stage and thus, these results were expected.

In recent years, the role of SIRT1 in carcinogenesis has been studied and generated some controversy since it appears to have a differential response according with the type and stage of the cancer (135). In addition, drugs that interfere with SIRT1 pathway show lack of selectively and even some toxicity (95, 135). Several studies have been performed to determine whether SIRT1 acts as a tumour promoter or suppressor (128-131, 133). Our results show that inhibition and activation of SIRT1 decreases HT-1376 cells viability after 24-hour treatment. However, in TCCSUP cells the effect was rather contrary with an increase of cell viability after SIRT1 inhibition or activation. These results further support the fact that SIRT1 acts in a different way concerning cells viability in bladder cancer. It appears that the progression of bladder cancer from stage III to stage IV may be associated with a role for SIRT1 pathway other molecular pathways than can be involved with this molecule. Carcinogenesis is also a metabolic process since cancer cells need to produce enough energy to survive and to divert enough metabolic components from energy production to supply cell growth, proliferation and migration (3, 21, 22, 182). Indeed, SIRT1 pathway has long been

associated with energy metabolism control in cells (104, 105). However, only medium or high concentration of SIRT1 inhibitor, in HT-1376 and TCCSUP cells respectively, induce alterations in mitochondrial membrane potential. These results also support that during bladder cancer progression sensitivity to SIRT1 inhibition is altered which may be of clinical significance. LDH release to the extracellular media was similar in both bladder cancer cells, being decreased after inhibition of SIRT1 illustrating that this pathway may be associated with an intact cell membrane and thus, tumorigenesis.

Glucose usage for maximum energy production in cancer cells is mainly achieved through a high glycolytic flux (21, 22). GLUT1 and GLUT3 are the main responsible for glucose shuttling across cell membrane. Both have high affinity for glucose and therefore, once expressed, play the essential role of ensuring efficient glucose uptake even when glucose becomes a limiting resource. High expression of GLUT1 and/or GLUT3 is associated with the poor prognosis of several types of human tumours, including bladder cancer (23, 182). Our results show that *GLUT3* expression is highly increased after SIRT1 activation in grade III bladder cancer cells. Direct molecular consequences of *GLUT3* overexpression could be increase in glucose consumption (182). In addition, it could stimulate also glutamine and/or pyruvate consumption. Glutamine has been shown to support the metabolism of cancer cells derived from several tissues (183-185). However, the consumption of glucose, pyruvate or glutamine was not affect. The same was noted for the grade IV bladder cancer cells illustrating that SIRT1 is not involved in the import of these metabolites. Nevertheless, after those metabolites enter the cells, the efficiency of their metabolization and the pathways they follow can be very different.

Although in healthy cells, pyruvate is preferentially used in TCA cycle, in tumour cells it is converted into lactate, which is then released (23, 186). The lactate transport out of the cell as well as its uptake is mediated by the action of MCTs, which support the high glycolytic rates in tumour cells (187-189). MCT1 is ubiquitously expressed in healthy and cancer cells and it facilitates the lactate uptake, which is then converted into pyruvate to fuel the TCA cycle (182, 190). MCT4 is the transporter with the lowest affinity to lactate, but it is well adapted to lactate secretion from tumour cells (191, 192) and thus plays a crucial role in cancer establishment, progression and even aggressiveness (193). Indeed, high expression of these lactate transporters, MCT1 and MCT4, is associated with the aggressiveness of some cancer cells (188, 190, 192-194). Our results show that *MCT1* expression is highly increased in HT-1376 cells after SIRT1 inhibition and activation. Interestingly *MCT4* expression was not affected by modulation of SIRT1 pathway suggesting that lactate import is sensitive to SIRT1 control and not lactate export, however the reason for this difference remains unclear. In cancer cells, pyruvate taken up from the extracellular media or catabolized from glucose is

mainly converted into lactate, under anaerobic conditions rather than being oxidized in the mitochondria, where it fuels the tricarboxylic acid (TCA) and the oxidative phosphorylation takes place, under aerobic conditions (182, 190, 195). In tumour cells, pyruvate is mainly converted into lactate, supporting the metabolic demands of highly invasive and proliferative bladder cancer cells (23, 189). In some cases, pyruvate is considered as the most important fuel to metabolic processes, rather than glucose, playing an important role in bladder cancer progression (23). The pyruvate interconversion into lactate is catalysed by LDH, which is an unfavourable prognostic marker for several human cancers (196, 197). Our data shows that LDH and lactate production are not altered by SIRT1 inhibition or activation in HT-1376 cells. The same was detected for TCCSUP cells except after SIRT1 inhibition combined with mTOR inhibition, which decreased lactate production thus illustrating again a differential effect of SIRT1 according to the bladder cancer stage. A reason for this fact might be that the lactate production is more marked in cells of a higher stage (23). In addition, inhibition of LDH has already been shown to inhibit SIRT1 and consecutively reduce cell survival (198-200). Although these studies only referred that LDH inhibition also inhibits SIRT1 and did not study the effects of SIRT1 inhibition on LDH, our results suggests that SIRT1 inhibition in a higher stage may be useful to avoid the excessive lactate production by these cells.

Concerning to pyruvate, it can also participate as a precursor for biosynthetic pathways. Besides been converted into lactate, pyruvate can also be converted into alanine. This alanine production is characteristic of several cancer cells, particularly during higher proliferative stages (23, 201). Our results show that alanine production is decreased when SIRT1 is inhibited in HT-1376 cells and TCCSUP cells thus illustrating that SIRT1 pathway is involved with pyruvate metabolization at the crossroad of several metabolic pathways, which can have implications in tumorigenesis.

However, with non-energy purposes, glucose and the other carbon sources can be metabolized to generate required pentoses for the synthesis of nucleic acids and nucleotides, through pentose phosphate cycle (PPP) and to promote reductive processes, such as biosynthesis of fatty acid (3, 202). Accordingly, glucose consumption by glycolysis instead of oxidative phosphorylation is due to the biosynthesis of necessary metabolic precursors to support cell proliferation and migration. Among those, we can highlight acetyl-CoA for fatty acids, lipids and cholesterol synthesis, glycolytic intermediates for non-essential amino acids and ribose group generation for nucleotides synthesis (3, 182, 202, 203). Glucose and glutamine contribute to acetyl-CoA synthesis and consequently to synthesis of fatty acids and cholesterol. However, acetate is also another source of acetyl-CoA for several types of cancer, which might incorporate this metabolite into fatty acids to sustain biomass production or into the TCA cycle (178, 202). Therefore, acetate is crucial to supply the cancer cell growth

demands. Our results show that acetate consumption is only decreased when TCCSUP were exposed to the inhibitor of SIRT1. Acetate is also a crossroad metabolite that can be used for biosynthesis and as fuel for mitochondrial functioning. Although cancer cells are known for their strongly marked metabolism that converts glucose into lactate, which is later excreted into cellular medium, reducing TCA activity and increasing glucose application for non-energy purposes, even under aerobic conditions for mitochondrial oxidative phosphorylation (3, 202, 203), mitochondrial function has been associated with cancer establishment, progression and aggressiveness (204, 205). Thus, mitochondria plays a highly relevant role in cell metabolism. However, the studies focused on mitochondrial dysfunction in bladder cancer are scarce, though it is described as a hallmark for cancer progression (204, 205). Indeed, mtDNA copy number presents a large diversity among cancer types (204). For instance, in bladder cancer patients, mtDNA copy number tested in urine significantly differed from its levels in blood illustrating the difficulty on assessing this parameter with sufficient robustness to have a definitive conclusion regarding its role on bladder cancer. Nevertheless, mtDNA levels in blood allowed to sensitively distinguish healthy from bladder cancer patients (206, 207). Some studies suggest that in bladder cancer cells, the mtDNA copy number is decreased when compared to normal tissue. However the authors showed that the expression of mitochondria-related genes and mitochondrial respiration were not down-regulated, suggesting that mitochondrial activity might not be compromised and correlated with mtDNA copy number (204, 208). Those studies proposed that other signalling mechanisms can be equilibrating the mtDNA depletion. Our results show that mtDNA copy number significantly decreased in grade III bladder cancer cells after SIRT1 inhibition. In addition, it was shown that SIRT1 plays a critical role in cell survival and death in prostate cancer, particularly due to mitochondria-mediated processes such as apoptosis (209). Nevertheless our results show that nor SIRT1 activation nor its inhibition alters Bax/BCL-2 ratio illustrating that in bladder cancer cells of stage III and IV this pathway appears to not be directed involved in apoptotic processes. Finally, respirometry of TCCSUP cells was determined. Our results show that some respirometry parameters such as basal respiration and proton leak are differentially modulated by SIRT1 activation or inhibition, which suggests that this pathway may be associated with the differential response of bladder cancer to therapies.

Stratification of bladder cancer has been taking in consideration signalling pathways. Among those, differential gene expression and protein activity associated with mTOR pathway has been used to stratify bladder cancer (210). In addition, alterations in mTOR pathway is frequently associated with invasive bladder cancer but there is a lack of functional studies to understand why targeted therapy on this pathway has had limited success (36, 211, 212). mTOR complex 2 (mTORC2) has been described as a major regulator of bladder cancer

invasion (213). Although mTOR-based therapies have been clinically used for some types of cancers, in bladder cancer only recently has undergone clinical evaluation but with limited success (47-49). Nevertheless, mTOR pathway has been suggested as a bladder cancer tumorigenesis predictor of disease progression and/or survival (24, 214). In fact, mTOR inhibitors have been already used for the treatment of metastatic renal carcinoma, breast cancer, among others (215). But the use of mTOR inhibitors is very complex and tricky since mTOR inhibition revealed heterogeneous responses indicating anti-tumour effects in some cases while in others induced intrinsic or acquired resistance to the drug (215). Concerning bladder cancer, mTOR pathway activation is increased in the tumour and its microenvironment in patients with adverse pathological findings at cystectomy (216) illustrating that this pathway may be involved in bladder cancer progression and aggressiveness. Thus, we analysed the metabolic and bioenergetics profile of stage III and IV bladder cancer cells after inhibition of mTOR pathway. As expected, cell density was decreased in both bladder cancer cells, HT-1376 and TCCSUP after mTOR inhibition, which was followed by an increase of LDH release to the extracellular media. Nevertheless, only the highest concentration of rapamycin, the mTOR inhibitor, decreased the membrane potential of the HT-1376 cells. These results suggest that mTOR inhibition has positive effects for cancer cells by decreasing the cells density and increasing apoptosis. Indeed, the *bax/bcl-2* ratio was decreased after mTOR inhibition. After mTOR inhibition *GLUT3* expression was increased and there was no difference in glucose, glutamine or pyruvate consumption. Interestingly, those mechanisms were not affected in TCCSUP cells illustrating that *GLUT3* might mediate the differential response of cells from different stages of bladder cancer to mTOR inhibition. *MCT1* and *MCT4* expression were also highly increased after mTOR inhibition in both, HT-1376 and TCCSUP cells though only the latter presented an increase production of lactate. This was expected since most aggressive tumour cells usually produce a higher amount of lactate, highlighting that the lactate production might be a hallmark of cancer development (217). Concerning alanine production, only TCCSUP showed a slight increase, which may be associated with a metabolic shift towards amino acid production instead of TCA enhancement. Interestingly, breast cancer cell growth inhibition was associated with mTOR-mediated mitochondrial biogenesis and function (218). Corroborating that mTOR interferes with mitochondrial biogenesis and function, as well as possible TCA cycle repression, mtDNA copy number was severely decreased in HT-1376 cells after inhibition of mTOR. In TCCSUP cells respirometry it was also possible to detect that mTOR inhibition decreases basal respiration, ATP turnover and proton leak thus suggesting a depression on mitochondrial respiration though further studies will be needed to consolidate these results.

Signalling pathways interact with each other to mediate effects in cancer cells. mTOR is known to have a collaborative role with SIRT1 to activate NF-kB in human fibrosarcoma cells (219). In addition, it was reported a negative regulation of mTOR signalling by SIRT1 activation in pleural mesothelioma (220). In hepatocellular carcinoma SIRT1 also exerted an anti-carcinogenic effect via mTOR pathway (221). These studies illustrate that SIRT1 and mTOR may interact in cancer cells. Nevertheless, the effects of the combined treatment of bladder cancer cells with mTOR and SIRT1 inhibition remained unknown. Our results showed that the combined treatment of TCCSUP cells with inhibition of both pathways resulted in a clear reduction of cell viability that was followed by decreased cell density thus illustrating the great potential of the inhibition of both pathways for cancer treatment and progression. Indeed, mitochondrial potential was severely depressed in HT-1376 and TCCSUP cells after inhibition of both pathways. This was followed by a decrease on LDH release to the extracellular media in both cancer cells of the different stages of bladder cancer. Interestingly, the metabolic profile of HT-1376 cells was not affected by the combined treatment with inhibitors of SIRT1 and mTOR. Nevertheless, one major difference was detected concerning TCCSUP cells: there was a significant reduction on lactate production after inhibition of SIRT1 and mTOR. As discussed above, tumour aggressiveness is associated with lactate production and thus, these results indirectly suggest that the combined treatment of TCCSUP cells with SIRT1 and mTOR inhibitors decreases the cells aggressiveness. Acetate consumption was increased in these cells further suggesting a metabolization though further studies are needed. Finally, TCCSUP cells start to consume alanine after the combined treatment with SIRT1 and mTOR inhibitors suggesting a TCA stimulation. This was further corroborated by a stimulation of basal respiration in this condition and increased proton leak, as noted in the respirometry studies. Taken together, these results suggest that although there is still a differential response of HT-1376 and TCCSUP cells to the combined treatment with SIRT1 and mTOR inhibitors, the cells from the highly proliferative and invasive stage are sensitive to this treatment. Thus, the joined treatment of higher bladder cancer stages with mTOR and SIRT1 inhibitors may have positive effects on bladder cancer treatment. Extensive analysis of molecular alterations in bladder cancer establishment, progression and aggressiveness may led to novel treatment approaches. Description of these molecular alterations in SIRT1 and mTOR pathways in bladder cancer contributes to our current knowledge and comprehension on the biology of the disease, which can lead to new molecular characterization and ultimately help to improve the patient care. In the context of personalized medicine, it is important to understand how these differences in signalling pathways may be essential for molecular classification and tumour suppression/response to therapy. This is a first assessment of the metabolic and bioenergetics response of bladder cancer cells from different stages to the joint treatment with mTOR and SIRT1 inhibitors, which showed promising results.

11 CONCLUSION AND FURTHER PERSPECTIVES

Bladder cancer high incidence, high recurrence rate and poor survival expectancy turns it into a major health problem. Several signalling pathways promote bladder cancer heterogeneity. A peculiar shift to aerobic glycolysis-dependent metabolism (the Warburg effect) is the hallmark of tumour cells, including bladder cancer cells (3). mTOR pathway is altered in most bladder cancer cases and SIRT1 has been demonstrated to have an important influence in tumour development. Thus, it urges to investigate these two pathways and their influence in carcinogenesis and therefore to find novel biomarkers for diagnosis and with potential therapeutic value. In order to clarify some of these mechanisms, we studied the effects of SIRT1 and mTOR modulation in cell proliferation and viability, in metabolic and bioenergetic profiles on HT-1376 and TCCSUP bladder cancer cells, from grade III and IV, respectively.

Our results suggest that the combined treatment with mTOR and SIRT1 inhibitors in higher bladder cancer stages may have positive effects on bladder cancer therapy highlighting that during progression tumours cells adapt to new environments as they grow and the molecular mechanisms by which that occurs is dependent of signalling pathways. Our results show promising results in the response of bladder cancer cells from different stages to the treatment with combined mTOR and SIRT1 inhibitors and thus, being the first analysis of metabolic and bioenergetic profiles. Further characterization of SIRT1 and mTOR pathways in bladder cancer enriches our knowledge on tumour development, which can lead to novel biomarkers discovery and certainly therapies improvement. These studies highlight the need to preselect patients based on metabolic cancer phenotype, since the cells' behaviour from different stages diverse not only in metabolic genes and in metabolites involved, but also in mitochondrial function. In the context of personalized medicine, these differences in signalling pathways are essential for a specific diagnosis and therapy of each particular tumour. It is important to highlight that bladder cancer has particular characteristics of plasticity and that *in vitro* studies might have different results from *in vivo* studies, therefore, further investigations are definitely needed.

To further investigations, it would be relevant to analyse the effects on the same parameters studies here but on normal bladder cells. It could also be interesting to compare the differences in an even lower stage of bladder cancer cell after exposure to the same experimental groups. Mitochondrial respirometry analyses for all bladder cells groups exposed to the different treatments would also be a relevant. In addition to studies on mitochondrial function, the determination of mtDNA protein expression and mtDNA integrity would be a significant accomplishment. For last, but not least, migration and invasion studies would also

be important to compare the aggressiveness of different bladder cells submitted to treatments. This is a first assessment to unveil the role of SIRT1 and mTOR in bladder cancer cells metabolic and bioenergetic profiles.

12 REFERENCES

1. Geavlete B, Stanescu F, Moldoveanu C, Jecu M, Adou L, Bulai C, et al. NBI cystoscopy and bipolar electrosurgery in NMIBC management - An overview of daily practice. Journal of medicine and life. 2013;6(2):140-5.
2. Lopez-Lazaro M. A new view of carcinogenesis and an alternative approach to cancer therapy. Molecular medicine (Cambridge, Mass). 2010;16(3-4):144-53.
3. Massari F, Ciccarese C, Santoni M, Iacovelli R, Mazzucchelli R, Piva F, et al. Metabolic phenotype of bladder cancer. Cancer treatment reviews. 2016;45:46-57.
4. Fowler CJ, Griffiths D, de Groat WC. The neural control of micturition. Nature reviews Neuroscience. 2008;9(6):453-66.
5. Bladder Anatomy [Internet]. Medscape. 2016. Available from: https://emedicine.medscape.com/article/1949017-overview.
6. Medscape. 2017. Available from: https://emedicine.medscape.com/article/438262-overview#a1.
7. About Bladder Cancer [Internet]. American Cancer Society. 2016.
8. Antoni S, Ferlay J, Soerjomataram I, Znaor A, Jemal A, Bray F. Bladder Cancer Incidence and Mortality: A Global Overview and Recent Trends. Eur Urol. 2017;71(1):96-108.
9. Cancer Today: International Agency for Research on Cancer. Available from: https://gco.iarc.fr/today.
10. Crawford JM. The origins of bladder cancer. Laboratory investigation; a journal of technical methods and pathology. 2008;88(7):686-93.
11. SEER Cancer Stat Facts: Bladder Cancer [Internet]. National Cancer Institute.
12. Cancer Mortality Database: World Health Organization; 2016. Available from: http://www-dep.iarc.fr/WHOdb.
13. Cumberbatch MG, Rota M, Catto JW, La Vecchia C. The Role of Tobacco Smoke in Bladder and Kidney Carcinogenesis: A Comparison of Exposures and Meta-analysis of Incidence and Mortality Risks. Eur Urol. 2016;70(3):458-66.
14. Wilcox AN, Silverman DT, Friesen MC, Locke SJ, Russ DE, Hyun N, et al. Smoking status, usual adult occupation, and risk of recurrent urothelial bladder carcinoma: data from The Cancer Genome Atlas (TCGA) Project. Cancer causes & control : CCC. 2016;27(12):1429-35.
15. Bladder Cancer [Internet]. Cancer Research UK. 2015.
16. Bladder Cancer [Internet]. National Cancer Institute.
17. Knowles MA, Hurst CD. Molecular biology of bladder cancer: new insights into pathogenesis and clinical diversity. Nature Reviews Cancer. 2014;15:25.
18. Babjuk M, Burger M, Zigeuner R, Shariat SF, van Rhijn BW, Comperat E, et al. EAU guidelines on non-muscle-invasive urothelial carcinoma of the bladder: update 2013. Eur Urol. 2013;64(4):639-53.
19. Sanguedolce F, Cormio A, Bufo P, Carrieri G, Cormio L. Molecular markers in bladder cancer: Novel research frontiers. Critical reviews in clinical laboratory sciences. 2015;52(5):242-55.
20. FDA Approves Immunotherapy Drugs for Patients with Bladder Cancer [Internet]. National Cancer Institute. 2017. Available from: https://www.cancer.gov/news-events/cancer-currents-blog/2017/approvals-fda-checkpoint-bladder.
21. Warburg O. On the origin of cancer cells. Science (New York, NY). 1956;123(3191):309-14.
22. Warburg O, Wind F, Negelein E. THE METABOLISM OF TUMORS IN THE BODY. The Journal of general physiology. 1927;8(6):519-30.

23. Conde VR, Oliveira PF, Nunes AR, Rocha CS, Ramalhosa E, Pereira JA, et al. The progression from a lower to a higher invasive stage of bladder cancer is associated with severe alterations in glucose and pyruvate metabolism. Experimental cell research. 2015;335(1):91-8.

24. Sun CH, Chang YH, Pan CC. Activation of the PI3K/Akt/mTOR pathway correlates with tumour progression and reduced survival in patients with urothelial carcinoma of the urinary bladder. Histopathology. 2011;58(7):1054-63.

25. Fahmy M, Mansure JJ, Brimo F, Yafi FA, Segal R, Althunayan A, et al. Relevance of the mammalian target of rapamycin pathway in the prognosis of patients with high-risk non-muscle invasive bladder cancer. Human pathology. 2013;44(9):1766-72.

26. Porta C, Paglino C, Mosca A. Targeting PI3K/Akt/mTOR Signaling in Cancer. Frontiers in oncology. 2014;4:64.

27. Matsushima M, Kikuchi E, Matsumoto K, Hattori S, Takeda T, Kosaka T, et al. Intravesical dual PI3K/mTOR complex 1/2 inhibitor NVP-BEZ235 therapy in an orthotopic bladder cancer model. International journal of oncology. 2015;47(1):377-83.

28. Kyou Kwon J, Kim SJ, Hoon Kim J, Mee Lee K, Ho Chang I. Dual inhibition by S6K1 and Elf4E is essential for controlling cellular growth and invasion in bladder cancer. Urologic oncology. 2014;32(1):51.e27-35.

29. Madka V, Mohammed A, Li Q, Zhang Y, Biddick L, Patlolla JM, et al. Targeting mTOR and p53 Signaling Inhibits Muscle Invasive Bladder Cancer In Vivo. Cancer prevention research (Philadelphia, Pa). 2016;9(1):53-62.

30. Costa C, Pereira S, Lima L, Peixoto A, Fernandes E, Neves D, et al. Abnormal Protein Glycosylation and Activated PI3K/Akt/mTOR Pathway: Role in Bladder Cancer Prognosis and Targeted Therapeutics. PloS one. 2015;10(11):e0141253.

31. Franke TF. PI3K/Akt: getting it right matters. Oncogene. 2008;27(50):6473-88.

32. Sathe A, Nawroth R. Targeting the PI3K/AKT/mTOR Pathway in Bladder Cancer. Methods in molecular biology (Clifton, NJ). 2018;1655:335-50.

33. Laplante M, Sabatini DM. mTOR signaling at a glance. Journal of cell science. 2009;122(Pt 20):3589-94.

34. Network TCGAR. Comprehensive molecular characterization of urothelial bladder carcinoma. Nature. 2014;507(7492):315-22.

35. Massari F, Ciccarese C, Santoni M, Brunelli M, Conti A, Modena A, et al. The route to personalized medicine in bladder cancer: where do we stand? Targeted oncology. 2015;10(3):325-36.

36. Platt FM, Hurst CD, Taylor CF, Gregory WM, Harnden P, Knowles MA. Spectrum of phosphatidylinositol 3-kinase pathway gene alterations in bladder cancer. Clinical cancer research : an official journal of the American Association for Cancer Research. 2009;15(19):6008-17.

37. Aveyard JS, Skilleter A, Habuchi T, Knowles MA. Somatic mutation of PTEN in bladder carcinoma. British journal of cancer. 1999;80(5-6):904-8.

38. Keniry M, Parsons R. The role of PTEN signaling perturbations in cancer and in targeted therapy. Oncogene. 2008;27(41):5477-85.

39. Puzio-Kuter AM, Castillo-Martin M, Kinkade CW, Wang X, Shen TH, Matos T, et al. Inactivation of p53 and Pten promotes invasive bladder cancer. Genes & development. 2009;23(6):675-80.

40. Vezina C, Kudelski A, Sehgal SN. Rapamycin (AY-22,989), a new antifungal antibiotic. I. Taxonomy of the producing streptomycete and isolation of the active principle. The Journal of antibiotics. 1975;28(10):721-6.

41. Sehgal SN, Baker H, Vezina C. Rapamycin (AY-22,989), a new antifungal antibiotic. II. Fermentation, isolation and characterization. The Journal of antibiotics. 1975;28(10):727-32.

42. Sehgal SN. Rapamune (Sirolimus, rapamycin): an overview and mechanism of action. Therapeutic drug monitoring. 1995;17(6):660-5.

43. Mukherjee T, Shah BV. Sirolimus: a new immunosuppressant. The Journal of the Association of Physicians of India. 2005;53:885-90.

44. Dai ZJ, Gao J, Ma XB, Kang HF, Wang BF, Lu WF, et al. Antitumor Effects of Rapamycin in Pancreatic Cancer Cells by Inducing Apoptosis and Autophagy. International Journal of Molecular Sciences. 2013;14(1):273-85.

45. Shen Y, Wang X, Xia W, Wang C, Cai M, Xie H, et al. Antiproliferative and Overadditive Effects of Rapamycin and FTY720 in Pancreatic Cancer Cells In Vitro. Transplantation proceedings.40(5):1727-33.

46. Sehgal SN. Sirolimus: its discovery, biological properties, and mechanism of action. Transplantation proceedings. 2003;35(3 Suppl):7s-14s.

47. National Center for Biotechnology Information. PubChem Compound Database. CID=6442177.

48. US Natl Inst Health; Daily Med. Drug Label Information for AFINITOR - everolimus [Internet]. 2017. Available from: https://dailymed.nlm.nih.gov/dailymed/drugInfo.cfm?setid=2150f73a-179b-4afc-b8ce-67c85cc72f04.

49. US Natl Inst Health; Daily Med. Drug Label Information for TORISEL - temsirolimus [Internet]. 2017. Available from: https://dailymed.nlm.nih.gov/dailymed/drugInfo.cfm?setid=95b7dc92-2180-42f1-8699-3c28f609e674.

50. Chiong E, Lee IL, Dadbin A, Sabichi AL, Harris L, Urbauer D, et al. Effects of mTOR inhibitor everolimus (RAD001) on bladder cancer cells. Clinical cancer research : an official journal of the American Association for Cancer Research. 2011;17(9):2863-73.

51. Vasconcelos-Nobrega C, Pinto-Leite R, Arantes-Rodrigues R, Ferreira R, Brochado P, Cardoso ML, et al. In vivo and in vitro effects of RAD001 on bladder cancer. Urologic oncology. 2013;31(7):1212-21.

52. Seront E, Rottey S, Sautois B, Kerger J, D'Hondt LA, Verschaeve V, et al. Phase II study of everolimus in patients with locally advanced or metastatic transitional cell carcinoma of the urothelial tract: clinical activity, molecular response, and biomarkers. Annals of oncology : official journal of the European Society for Medical Oncology. 2012;23(10):2663-70.

53. Yao JC, Shah MH, Ito T, Bohas CL, Wolin EM, Van Cutsem E, et al. Everolimus for advanced pancreatic neuroendocrine tumors. The New England journal of medicine. 2011;364(6):514-23.

54. Korfel A, Schlegel U, Herrlinger U, Dreyling M, Schmidt C, von Baumgarten L, et al. Phase II Trial of Temsirolimus for Relapsed/Refractory Primary CNS Lymphoma. Journal of clinical oncology : official journal of the American Society of Clinical Oncology. 2016;34(15):1757-63.

55. Levakov I, Vojinov S, Marusic G, Popov M, Levakov O, Popov M, et al. Safety profile of temsirolimus in patients with metastatic renal cell carcinoma. Journal of BUON : official journal of the Balkan Union of Oncology. 2016;21(6):1442-8.

56. Dong P, Hao F, Dai S, Tian L. Combination therapy Eve and Pac to induce apoptosis in cervical cancer cells by targeting PI3K/AKT/mTOR pathways. Journal of receptor and signal transduction research. 2018;38(1):83-8.

57. Baselga J, Campone M, Piccart M, Burris HA, 3rd, Rugo HS, Sahmoud T, et al. Everolimus in postmenopausal hormone-receptor-positive advanced breast cancer. The New England journal of medicine. 2012;366(6):520-9.

58. Lee SC, Kim KH, Kim OH, Lee SK, Hong HE, Choi BJ, et al. Everolimus Plus Ku0063794 Regimen Promotes Anticancer Effects against Hepatocellular Carcinoma Cells through the Paradoxical Inhibition of Autophagy. Cancer research and treatment : official journal of Korean Cancer Association. 2017.

59. Singla M, Bhattacharyya S. Autophagy as a potential therapeutic target during epithelial to mesenchymal transition in renal cell carcinoma: An in vitro study. Biomedicine & pharmacotherapy = Biomedecine & pharmacotherapie. 2017;94:332-40.

60. Lin JF, Lin YC, Yang SC, Tsai TF, Chen HE, Chou KY, et al. Autophagy inhibition enhances RAD001-induced cytotoxicity in human bladder cancer cells. Drug design, development and therapy. 2016;10:1501-13.

61. Pinto-Leite R, Arantes-Rodrigues R, Palmeira C, Gaivao I, Cardoso ML, Colaco A, et al. Everolimus enhances gemcitabine-induced cytotoxicity in bladder-cancer cell lines. Journal of toxicology and environmental health Part A. 2012;75(13-15):788-99.

62. Juengel E, Najafi R, Rutz J, Maxeiner S, Makarevic J, Roos F, et al. HDAC inhibition as a treatment concept to combat temsirolimus-resistant bladder cancer cells. Oncotarget. 2017;8(66):110016-28.

63. Pinto-Leite R, Arantes-Rodrigues R, Ferreira R, Palmeira C, Colaco A, Moreira da Silva V, et al. Temsirolimus improves cytotoxic efficacy of cisplatin and gemcitabine against urinary bladder cancer cell lines. Urologic oncology. 2014;32(1):41.e11-22.

64. Klar AJ, Fogel S, Macleod K. MAR1-a Regulator of the HMa and HMalpha Loci in SACCHAROMYCES CEREVISIAE. Genetics. 1979;93(1):37-50.

65. Frye RA. Phylogenetic classification of prokaryotic and eukaryotic Sir2-like proteins. Biochemical and biophysical research communications. 2000;273(2):793-8.

66. Schiedel M, Robaa D, Rumpf T, Sippl W, Jung M. The Current State of NAD+ -Dependent Histone Deacetylases (Sirtuins) as Novel Therapeutic Targets. Medicinal research reviews. 2017.

67. Imai S, Armstrong CM, Kaeberlein M, Guarente L. Transcriptional silencing and longevity protein Sir2 is an NAD-dependent histone deacetylase. Nature. 2000;403(6771):795-800.

68. Vaziri H, Dessain SK, Ng Eaton E, Imai SI, Frye RA, Pandita TK, et al. hSIR2(SIRT1) functions as an NAD-dependent p53 deacetylase. Cell. 2001;107(2):149-59.

69. Yeung F, Hoberg JE, Ramsey CS, Keller MD, Jones DR, Frye RA, et al. Modulation of NF-kappaB-dependent transcription and cell survival by the SIRT1 deacetylase. The EMBO journal. 2004;23(12):2369-80.

70. North BJ, Marshall BL, Borra MT, Denu JM, Verdin E. The human Sir2 ortholog, SIRT2, is an NAD+-dependent tubulin deacetylase. Molecular cell. 2003;11(2):437-44.

71. Tanno M, Sakamoto J, Miura T, Shimamoto K, Horio Y. Nucleocytoplasmic shuttling of the NAD+-dependent histone deacetylase SIRT1. The Journal of biological chemistry. 2007;282(9):6823-32.

72. North BJ, Verdin E. Interphase nucleo-cytoplasmic shuttling and localization of SIRT2 during mitosis. PloS one. 2007;2(8):e784.

73. Scher MB, Vaquero A, Reinberg D. SirT3 is a nuclear NAD+-dependent histone deacetylase that translocates to the mitochondria upon cellular stress. Genes & development. 2007;21(8):920-8.

74. Schwer B, North BJ, Frye RA, Ott M, Verdin E. The human silent information regulator (Sir)2 homologue hSIRT3 is a mitochondrial nicotinamide adenine dinucleotide-dependent deacetylase. The Journal of cell biology. 2002;158(4):647-57.

75. Michishita E, Park JY, Burneskis JM, Barrett JC, Horikawa I. Evolutionarily conserved and nonconserved cellular localizations and functions of human SIRT proteins. Molecular biology of the cell. 2005;16(10):4623-35.

76. Kiran S, Chatterjee N, Singh S, Kaul SC, Wadhwa R, Ramakrishna G. Intracellular distribution of human SIRT7 and mapping of the nuclear/nucleolar localization signal. The FEBS journal. 2013;280(14):3451-66.

77. Liszt G, Ford E, Kurtev M, Guarente L. Mouse Sir2 homolog SIRT6 is a nuclear ADP-ribosyltransferase. The Journal of biological chemistry. 2005;280(22):21313-20.

78. Radak Z, Koltai E, Taylor AW, Higuchi M, Kumagai S, Ohno H, et al. Redox-regulating sirtuins in aging, caloric restriction, and exercise. Free radical biology & medicine. 2013;58:87-97.

79. Kaeberlein M, McVey M, Guarente L. The SIR2/3/4 complex and SIR2 alone promote longevity in Saccharomyces cerevisiae by two different mechanisms. Genes & development. 1999;13(19):2570-80.

80. Zhao S, Xu W, Jiang W, Yu W, Lin Y, Zhang T, et al. Regulation of cellular metabolism by protein lysine acetylation. Science (New York, NY). 2010;327(5968):1000-4.

81. Kim HS, Patel K, Muldoon-Jacobs K, Bisht KS, Aykin-Burns N, Pennington JD, et al. SIRT3 is a mitochondria-localized tumor suppressor required for maintenance of mitochondrial integrity and metabolism during stress. Cancer cell. 2010;17(1):41-52.

82. Verdin E, Hirschey MD, Finley LW, Haigis MC. Sirtuin regulation of mitochondria: energy production, apoptosis, and signaling. Trends in biochemical sciences. 2010;35(12):669-75.

83. Allison SJ, Milner J. SIRT3 is pro-apoptotic and participates in distinct basal apoptotic pathways. Cell cycle (Georgetown, Tex). 2007;6(21):2669-77.

84. Firestein R, Blander G, Michan S, Oberdoerffer P, Ogino S, Campbell J, et al. The SIRT1 deacetylase suppresses intestinal tumorigenesis and colon cancer growth. PloS one. 2008;3(4):e2020.

85. Wong S, Weber JD. Deacetylation of the retinoblastoma tumour suppressor protein by SIRT1. The Biochemical journal. 2007;407(3):451-60.

86. Amat R, Planavila A, Chen SL, Iglesias R, Giralt M, Villarroya F. SIRT1 controls the transcription of the peroxisome proliferator-activated receptor-gamma Co-activator-1alpha (PGC-1alpha) gene in skeletal muscle through the PGC-1alpha autoregulatory loop and interaction with MyoD. The Journal of biological chemistry. 2009;284(33):21872-80.

87. Daitoku H, Hatta M, Matsuzaki H, Aratani S, Ohshima T, Miyagishi M, et al. Silent information regulator 2 potentiates Foxo1-mediated transcription through its deacetylase activity. Proceedings of the National Academy of Sciences of the United States of America. 2004;101(27):10042-7.

88. Liu TF, Vachharajani VT, Yoza BK, McCall CE. NAD+-dependent sirtuin 1 and 6 proteins coordinate a switch from glucose to fatty acid oxidation during the acute inflammatory response. The Journal of biological chemistry. 2012;287(31):25758-69.

89. Luo J, Nikolaev AY, Imai S, Chen D, Su F, Shiloh A, et al. Negative control of p53 by Sir2alpha promotes cell survival under stress. Cell. 2001;107(2):137-48.

90. Wang C, Chen L, Hou X, Li Z, Kabra N, Ma Y, et al. Interactions between E2F1 and SirT1 regulate apoptotic response to DNA damage. Nature cell biology. 2006;8(9):1025-31.

91. Jiang W, Wang S, Xiao M, Lin Y, Zhou L, Lei Q, et al. Acetylation regulates gluconeogenesis by promoting PEPCK1 degradation via recruiting the UBR5 ubiquitin ligase. Molecular cell. 2011;43(1):33-44.

92. Lalla R, Donmez G. The role of sirtuins in Alzheimer's disease. Frontiers in aging neuroscience. 2013;5:16.

93. Sebastian C, Satterstrom FK, Haigis MC, Mostoslavsky R. From sirtuin biology to human diseases: an update. The Journal of biological chemistry. 2012;287(51):42444-52.

94. Bosch-Persegué L, Vaquero A. The Dual Role of Sirtuins in Cancer. Genes & Cancer. 2011;2(6):648-62.

95. Chalkiadaki A, Guarente L. The multifaceted functions of sirtuins in cancer. Nature reviews Cancer. 2015;15(10):608-24.

96. Vaquero A, Scher M, Lee D, Erdjument-Bromage H, Tempst P, Reinberg D. Human SirT1 interacts with histone H1 and promotes formation of facultative heterochromatin. Molecular cell. 2004;16(1):93-105.

97. Kauppinen A, Suuronen T, Ojala J, Kaarniranta K, Salminen A. Antagonistic crosstalk between NF-kappaB and SIRT1 in the regulation of inflammation and metabolic disorders. Cellular signalling. 2013;25(10):1939-48.

98. Yang Y, Hou H, Haller EM, Nicosia SV, Bai W. Suppression of FOXO1 activity by FHL2 through SIRT1-mediated deacetylation. The EMBO journal. 2005;24(5):1021-32.

99. van der Horst A, Tertoolen LG, de Vries-Smits LM, Frye RA, Medema RH, Burgering BM. FOXO4 is acetylated upon peroxide stress and deacetylated by the longevity protein hSir2(SIRT1). The Journal of biological chemistry. 2004;279(28):28873-9.

100. Vaquero A, Scher M, Erdjument-Bromage H, Tempst P, Serrano L, Reinberg D. SIRT1 regulates the histone methyl-transferase SUV39H1 during heterochromatin formation. Nature. 2007;450(7168):440-4.

101. Wang RH, Sengupta K, Li C, Kim HS, Cao L, Xiao C, et al. Impaired DNA damage response, genome instability, and tumorigenesis in SIRT1 mutant mice. Cancer cell. 2008;14(4):312-23.

102. Yuan Z, Zhang X, Sengupta N, Lane WS, Seto E. SIRT1 regulates the function of the Nijmegen breakage syndrome protein. Molecular cell. 2007;27(1):149-62.

103. Jeong J, Juhn K, Lee H, Kim SH, Min BH, Lee KM, et al. SIRT1 promotes DNA repair activity and deacetylation of Ku70. Experimental & molecular medicine. 2007;39(1):8-13.

104. Li X, Zhang S, Blander G, Tse JG, Krieger M, Guarente L. SIRT1 deacetylates and positively regulates the nuclear receptor LXR. Molecular cell. 2007;28(1):91-106.

105. Hallows WC, Lee S, Denu JM. Sirtuins deacetylate and activate mammalian acetyl-CoA synthetases. Proceedings of the National Academy of Sciences of the United States of America. 2006;103(27):10230-5.

106. Qiao L, Shao J. SIRT1 regulates adiponectin gene expression through Foxo1-C/enhancer-binding protein alpha transcriptional complex. The Journal of biological chemistry. 2006;281(52):39915-24.

107. Zhang Y, Zhang M, Dong H, Yong S, Li X, Olashaw N, et al. Deacetylation of cortactin by SIRT1 promotes cell migration. Oncogene. 2009;28(3):445-60.

108. Wang RH, Lahusen TJ, Chen Q, Xu X, Jenkins LM, Leo E, et al. SIRT1 deacetylates TopBP1 and modulates intra-S-phase checkpoint and DNA replication origin firing. International journal of biological sciences. 2014;10(10):1193-202.

109. Asher G, Gatfield D, Stratmann M, Reinke H, Dibner C, Kreppel F, et al. SIRT1 regulates circadian clock gene expression through PER2 deacetylation. Cell. 2008;134(2):317-28.

110. Lou PH, Lucchinetti E, Scott KY, Huang Y, Gandhi M, Hersberger M, et al. Alterations in fatty acid metabolism and sirtuin signaling characterize early type-2 diabetic hearts of fructose-fed rats. Physiological reports. 2017;5(16).

111. Mortuza R, Feng B, Chakrabarti S. SIRT1 reduction causes renal and retinal injury in diabetes through endothelin 1 and transforming growth factor beta1. Journal of cellular and molecular medicine. 2015;19(8):1857-67.

112. Becatti M, Barygina V, Emmi G, Silvestri E, Taddei N, Lotti T, et al. SIRT1 activity is decreased in lesional psoriatic skin. Internal and emergency medicine. 2016;11(6):891-3.

113. Rasheed H, El-Komy M, Hegazy RA, Gawdat HI, AlOrbani AM, Shaker OG. Expression of sirtuins 1, 6, tumor necrosis factor, and interferon-gamma in psoriatic patients. International journal of immunopathology and pharmacology. 2016;29(4):764-8.

114. Krueger JG, Suarez-Farinas M, Cueto I, Khacherian A, Matheson R, Parish LC, et al. A Randomized, Placebo-Controlled Study of SRT2104, a SIRT1 Activator, in Patients with Moderate to Severe Psoriasis. PloS one. 2015;10(11):e0142081.

115. Khader A, Yang WL, Hansen LW, Rajayer SR, Prince JM, Nicastro JM, et al. SRT1720, a sirtuin 1 activator, attenuates organ injury and inflammation in sepsis. The Journal of surgical research. 2017;219:288-95.

116. Vachharajani VT, Liu T, Brown CM, Wang X, Buechler NL, Wells JD, et al. SIRT1 inhibition during the hypoinflammatory phenotype of sepsis enhances immunity and improves outcome. Journal of leukocyte biology. 2014;96(5):785-96.

117. Yanagisawa S, Papaioannou AI, Papaporfyriou A, Baker JR, Vuppusetty C, Loukides S, et al. Decreased Serum Sirtuin-1 in COPD. Chest. 2017;152(2):343-52.

118. Wang XL, Li T, Li JH, Miao SY, Xiao XZ. The Effects of Resveratrol on Inflammation and Oxidative Stress in a Rat Model of Chronic Obstructive Pulmonary Disease. Molecules (Basel, Switzerland). 2017;22(9).

119. Pallas M, Pizarro JG, Gutierrez-Cuesta J, Crespo-Biel N, Alvira D, Tajes M, et al. Modulation of SIRT1 expression in different neurodegenerative models and human pathologies. Neuroscience. 2008;154(4):1388-97.

120. Jiang M, Wang J, Fu J, Du L, Jeong H, West T, et al. Neuroprotective role of Sirt1 in mammalian models of Huntington's disease through activation of multiple Sirt1 targets. Nature medicine. 2011;18(1):153-8.

121. Jeong H, Cohen DE, Cui L, Supinski A, Savas JN, Mazzulli JR, et al. Sirt1 mediates neuroprotection from mutant huntingtin by activation of the TORC1 and CREB transcriptional pathway. Nature medicine. 2011;18(1):159-65.

122. Smith MR, Syed A, Lukacsovich T, Purcell J, Barbaro BA, Worthge SA, et al. A potent and selective Sirtuin 1 inhibitor alleviates pathology in multiple animal and cell models of Huntington's disease. Human molecular genetics. 2014;23(11):2995-3007.

123. Sussmuth SD, Haider S, Landwehrmeyer GB, Farmer R, Frost C, Tripepi G, et al. An exploratory double-blind, randomized clinical trial with selisistat, a SirT1 inhibitor, in patients with Huntington's disease. British journal of clinical pharmacology. 2015;79(3):465-76.

124. Westerberg G, Chiesa JA, Andersen CA, Diamanti D, Magnoni L, Pollio G, et al. Safety, pharmacokinetics, pharmacogenomics and QT concentration-effect modelling of the SirT1 inhibitor selisistat in healthy volunteers. British journal of clinical pharmacology. 2015;79(3):477-91.

125. Yuan H, Wang Z, Li L, Zhang H, Modi H, Horne D, et al. Activation of stress response gene SIRT1 by BCR-ABL promotes leukemogenesis. Blood. 2012;119(8):1904-14.

126. Brunet A, Sweeney LB, Sturgill JF, Chua KF, Greer PL, Lin Y, et al. Stress-dependent regulation of FOXO transcription factors by the SIRT1 deacetylase. Science (New York, NY). 2004;303(5666):2011-5.

127. Huffman DM, Grizzle WE, Bamman MM, Kim JS, Eltoum IA, Elgavish A, et al. SIRT1 is significantly elevated in mouse and human prostate cancer. Cancer research. 2007;67(14):6612-8.

128. Wang Z, Yuan H, Roth M, Stark JM, Bhatia R, Chen WY. SIRT1 deacetylase promotes acquisition of genetic mutations for drug resistance in CML cells. Oncogene. 2013;32(5):589-98.

129. Chung SY, Jung YY, Park IA, Kim H, Chung YR, Kim JY, et al. Oncogenic role of SIRT1 associated with tumor invasion, lymph node metastasis, and poor disease-free survival in triple negative breast cancer. Clinical & experimental metastasis. 2016;33(2):179-85.

130. Asaka R, Miyamoto T. Sirtuin 1 promotes the growth and cisplatin resistance of endometrial carcinoma cells: a novel therapeutic target. 2015;95(12):1363-73.

131. Wang RH, Zheng Y, Kim HS, Xu X, Cao L, Luhasen T, et al. Interplay among BRCA1, SIRT1, and Survivin during BRCA1-associated tumorigenesis. Molecular cell. 2008;32(1):11-20.

132. Herranz D, Munoz-Martin M, Canamero M, Mulero F, Martinez-Pastor B, Fernandez-Capetillo O, et al. Sirt1 improves healthy ageing and protects from metabolic syndrome-associated cancer. Nature communications. 2010;1:3.

133. Yuan J, Minter-Dykhouse K, Lou Z. A c-Myc-SIRT1 feedback loop regulates cell growth and transformation. The Journal of cell biology. 2009;185(2):203-11.

134. Bereshchenko OR, Gu W, Dalla-Favera R. Acetylation inactivates the transcriptional repressor BCL6. Nature genetics. 2002;32(4):606-13.

135. Fang Y, Nicholl MB. A dual role for sirtuin 1 in tumorigenesis. Current pharmaceutical design. 2014;20(15):2634-6.

136. Heltweg B, Gatbonton T, Schuler AD, Posakony J, Li H, Goehle S, et al. Antitumor activity of a small-molecule inhibitor of human silent information regulator 2 enzymes. Cancer research. 2006;66(8):4368-77.

137. Portmann S, Fahrner R, Lechleiter A, Keogh A, Overney S, Laemmle A, et al. Antitumor effect of SIRT1 inhibition in human HCC tumor models in vitro and in vivo. Molecular cancer therapeutics. 2013;12(4):499-508.

138. Yoon YK, Ali MA, Wei AC, Shirazi AN, Parang K, Choon TS. Benzimidazoles as new scaffold of sirtuin inhibitors: green synthesis, in vitro studies, molecular docking analysis and evaluation of their anti-cancer properties. European journal of medicinal chemistry. 2014;83:448-54.

139. Yoon YK, Ali MA, Wei AC, Choon TS, Osman H, Parang K, et al. Synthesis and evaluation of novel benzimidazole derivatives as sirtuin inhibitors with antitumor activities. Bioorganic & medicinal chemistry. 2014;22(2):703-10.

140. Li L, Wang L, Li L, Wang Z, Ho Y, McDonald T, et al. Activation of p53 by SIRT1 inhibition enhances elimination of CML leukemia stem cells in combination with imatinib. Cancer cell. 2012;21(2):266-81.

141. Jin Y, Cao Q, Chen C, Du X, Jin B, Pan J. Tenovin-6-mediated inhibition of SIRT1/2 induces apoptosis in acute lymphoblastic leukemia (ALL) cells and eliminates ALL stem/progenitor cells. BMC cancer. 2015;15:226.

142. Dai W, Zhou J, Jin B, Pan J. Class III-specific HDAC inhibitor Tenovin-6 induces apoptosis, suppresses migration and eliminates cancer stem cells in uveal melanoma. Scientific reports. 2016;6:22622.

143. Lain S, Hollick JJ, Campbell J, Staples OD, Higgins M, Aoubala M, et al. Discovery, in vivo activity, and mechanism of action of a small-molecule p53 activator. Cancer cell. 2008;13(5):454-63.

144. Li Z, Qin B, Qi X, Mao J, Wu D. Isoalantolactone induces apoptosis in human breast cancer cells via ROS-mediated mitochondrial pathway and downregulation of SIRT1. Archives of pharmacal research. 2016;39(10):1441-53.

145. Wu M, Zhang H, Hu J, Weng Z, Li C, Li H, et al. Isoalantolactone Inhibits UM-SCC-10A Cell Growth via Cell Cycle Arrest and Apoptosis Induction. PloS one. 2013;8(9):e76000.

146. Zhang Q, Zeng SX, Zhang Y, Zhang Y, Ding D, Ye Q, et al. A small molecule Inauhzin inhibits SIRT1 activity and suppresses tumour growth through activation of p53. EMBO molecular medicine. 2012;4(4):298-312.

147. Zhang Y, Zhang Q, Zeng SX, Zhang Y, Mayo LD, Lu H. Inauhzin and Nutlin3 synergistically activate p53 and suppress tumor growth. Cancer biology & therapy. 2012;13(10):915-24.

148. Napper AD, Hixon J, McDonagh T, Keavey K, Pons JF, Barker J, et al. Discovery of indoles as potent and selective inhibitors of the deacetylase SIRT1. Journal of medicinal chemistry. 2005;48(25):8045-54.

149. Oon CE, Strell C, Yeong KY, Ostman A, Prakash J. SIRT1 inhibition in pancreatic cancer models: contrasting effects in vitro and in vivo. European journal of pharmacology. 2015;757:59-67.

150. Ueno T, Endo S, Saito R, Hirose M, Hirai S, Suzuki H, et al. The sirtuin inhibitor tenovin-6 upregulates death receptor 5 and enhances cytotoxic effects of 5-fluorouracil and oxaliplatin in colon cancer cells. Oncology research. 2013;21(3):155-64.

151. Jin C, Zhang G, Zhang Y, Hua P, Song G, Sun M, et al. Isoalantolactone induces intrinsic apoptosis through p53 signaling pathway in human lung squamous carcinoma cells. PloS one. 2017;12(8):e0181731.

152. Howitz KT, Bitterman KJ, Cohen HY, Lamming DW, Lavu S, Wood JG, et al. Small molecule activators of sirtuins extend Saccharomyces cerevisiae lifespan. Nature. 2003;425(6954):191-6.

153. Jang M, Cai L, Udeani GO, Slowing KV, Thomas CF, Beecher CW, et al. Cancer chemopreventive activity of resveratrol, a natural product derived from grapes. Science (New York, NY). 1997;275(5297):218-20.

154. Baptista T, Graca I, Sousa EJ, Oliveira AI, Costa NR, Costa-Pinheiro P, et al. Regulation of histone H2A.Z expression is mediated by sirtuin 1 in prostate cancer. Oncotarget. 2013;4(10):1673-85.

155. Tessitore L, Davit A, Sarotto I, Caderni G. Resveratrol depresses the growth of colorectal aberrant crypt foci by affecting bax and p21(CIP) expression. Carcinogenesis. 2000;21(8):1619-22.

156. Chen Y, Tseng SH, Lai HS, Chen WJ. Resveratrol-induced cellular apoptosis and cell cycle arrest in neuroblastoma cells and antitumor effects on neuroblastoma in mice. Surgery. 2004;136(1):57-66.

157. Li ZG, Hong T, Shimada Y, Komoto I, Kawabe A, Ding Y, et al. Suppression of N-nitrosomethylbenzylamine (NMBA)-induced esophageal tumorigenesis in F344 rats by resveratrol. Carcinogenesis. 2002;23(9):1531-6.

158. Milne JC, Lambert PD, Schenk S, Carney DP, Smith JJ, Gagne DJ, et al. Small molecule activators of SIRT1 as therapeutics for the treatment of type 2 diabetes. Nature. 2007;450(7170):712-6.

159. Mitchell SJ, Martin-Montalvo A, Mercken EM, Palacios HH, Ward TM, Abulwerdi G, et al. The SIRT1 activator SRT1720 extends lifespan and improves health of mice fed a standard diet. Cell reports. 2014;6(5):836-43.

160. Minor RK, Baur JA, Gomes AP, Ward TM, Csiszar A, Mercken EM, et al. SRT1720 improves survival and healthspan of obese mice. Scientific reports. 2011;1:70.

161. Nguyen GT, Schaefer S, Gertz M, Weyand M, Steegborn C. Structures of human sirtuin 3 complexes with ADP-ribose and with carba-NAD+ and SRT1720: binding details and inhibition mechanism. Acta crystallographica Section D, Biological crystallography. 2013;69(Pt 8):1423-32.

162. Suzuki K, Hayashi R, Ichikawa T, Imanishi S, Yamada T, Inomata M, et al. SRT1720, a SIRT1 activator, promotes tumor cell migration, and lung metastasis of breast cancer in mice. Oncology reports. 2012;27(6):1726-32.

163. Kong Y, Wang K, Edler MC, Hamel E, Mooberry SL, Paige MA, et al. A boronic acid chalcone analog of combretastatin A-4 as a potent anti-proliferation agent. Bioorganic & medicinal chemistry. 2010;18(2):971.

164. Yi YW, Kang HJ, Kim HJ, Kong Y, Brown ML, Bae I. Targeting Mutant p53 by a SIRT1 Activator YK-3-237 Inhibits the Proliferation of Triple-Negative Breast Cancer Cells. Oncotarget. 2013;4(7):984-94.

165. Orellana EA, Kasinski AL. Sulforhodamine B (SRB) Assay in Cell Culture to Investigate Cell Proliferation. Bio-protocol. 2016;6(21):e1984.

166. Skehan P, Storeng R, Scudiero D, Monks A, McMahon J, Vistica D, et al. New colorimetric cytotoxicity assay for anticancer-drug screening. Journal of the National Cancer Institute. 1990;82(13):1107-12.

167. Mosmann T. Rapid colorimetric assay for cellular growth and survival: application to proliferation and cytotoxicity assays. Journal of immunological methods. 1983;65(1-2):55-63.

168. Terry L Riss RAM, Andrew L Niles, Sarah Duellman, Hélène A Benink, Tracy J Worzella, Lisa Minor. Cell Viability Assay. In: Sciences BMELCatNCfAT, editor. Assay Guidance Manual2016.

169. Burd JF, Usategui-Gomez M. A colorimetric assay for serum lactate dehydrogenase. Clinica chimica acta; international journal of clinical chemistry. 1973;46(3):223-7.

170. Pierce™ LDH Cytotoxicity Assay Kit [Internet]. VWR.

171. Pfaffl MW. A new mathematical model for relative quantification in real-time RT-PCR. Nucleic acids research. 2001;29(9):e45.

172. Rato L, Alves MG, Socorro S, Carvalho RA, Cavaco JE, Oliveira PF. Metabolic modulation induced by oestradiol and DHT in immature rat Sertoli cells cultured in vitro. Bioscience reports. 2012;32(1):61-9.

173. Mamchaoui K, Saumon G. A method for measuring the oxygen consumption of intact cell monolayers. American journal of physiology Lung cellular and molecular physiology. 2000;278(4):L858-63.

174. Djafarzadeh S, Jakob SM. High-resolution Respirometry to Assess Mitochondrial Function in Permeabilized and Intact Cells. Journal of visualized experiments : JoVE. 2017(120).

175. Silva AM, Oliveira PJ. Evaluation of Respiration with Clark Type Electrode in Isolated Mitochondria and Permeabilized Animal Cells. In: Palmeira CM, Moreno AJ, editors. Mitochondrial Bioenergetics: Methods and Protocols. Totowa, NJ: Humana Press; 2012. p. 7-24.

176. Gong J, Meng HB, Hua J, Song ZS, He ZG, Zhou B, et al. The SDF-1/CXCR4 axis regulates migration of transplanted bone marrow mesenchymal stem cells towards the pancreas in rats with acute pancreatitis. Molecular medicine reports. 2014;9(5):1575-82.

177. Hong Y, Liang H, Uzair Ur R, Wang Y, Zhang W, Zhou Y, et al. miR-96 promotes cell proliferation, migration and invasion by targeting PTPN9 in breast cancer. Scientific reports. 2016;6:37421.

178. Schug ZT, Peck B, Jones DT, Zhang Q, Grosskurth S, Alam IS, et al. Acetyl-CoA synthetase 2 promotes acetate utilization and maintains cancer cell growth under metabolic stress. Cancer cell. 2015;27(1):57-71.

179. Jastroch M, Divakaruni AS, Mookerjee S, Treberg JR, Brand MD. Mitochondrial proton and electron leaks. Essays in biochemistry. 2010;47:53-67.

180. Brand M D, Nicholls D G. Assessing mitochondrial dysfunction in cells. The Biochemical journal. 2011;435(Pt 2):297-312.

181. Kim J, Akbani R, Creighton CJ, Lerner SP, Weinstein JN, Getz G, et al. Invasive Bladder Cancer: Genomic Insights and Therapeutic Promise. Clinical cancer research : an official journal of the American Association for Cancer Research. 2015;21(20):4514-24.

182. Porporato PE, Dhup S, Dadhich RK, Copetti T, Sonveaux P. Anticancer targets in the glycolytic metabolism of tumors: a comprehensive review. Frontiers in pharmacology. 2011;2:49.

183. Davidson SM, Papagiannakopoulos T, Olenchock BA, Heyman JE, Keibler MA, Luengo A, et al. Environment Impacts the Metabolic Dependencies of Ras-Driven Non-Small Cell Lung Cancer. Cell metabolism. 2016;23(3):517-28.

184. Chiu M, Tardito S, Pillozzi S, Arcangeli A, Armento A, Uggeri J, et al. Glutamine depletion by crisantaspase hinders the growth of human hepatocellular carcinoma xenografts. British journal of cancer. 2014;111(6):1159-67.

185. Tardito S, Oudin A, Ahmed SU, Fack F, Keunen O, Zheng L, et al. Glutamine synthetase activity fuels nucleotide biosynthesis and supports growth of glutamine-restricted glioblastoma. Nature cell biology. 2015;17(12):1556-68.

186. Thangaraju M, Gopal E, Martin PM, Ananth S, Smith SB, Prasad PD, et al. SLC5A8 triggers tumor cell apoptosis through pyruvate-dependent inhibition of histone deacetylases. Cancer research. 2006;66(24):11560-4.

187. Doherty JR, Cleveland JL. Targeting lactate metabolism for cancer therapeutics. The Journal of clinical investigation. 2013;123(9):3685-92.

188. Feron O. Pyruvate into lactate and back: from the Warburg effect to symbiotic energy fuel exchange in cancer cells. Radiotherapy and oncology : journal of the European Society for Therapeutic Radiology and Oncology. 2009;92(3):329-33.

189. Gray LR, Tompkins SC, Taylor EB. Regulation of pyruvate metabolism and human disease. Cellular and molecular life sciences : CMLS. 2014;71(14):2577-604.

190. Sonveaux P, Vegran F, Schroeder T, Wergin MC, Verrax J, Rabbani ZN, et al. Targeting lactate-fueled respiration selectively kills hypoxic tumor cells in mice. The Journal of clinical investigation. 2008;118(12):3930-42.

191. Ullah MS, Davies AJ, Halestrap AP. The plasma membrane lactate transporter MCT4, but not MCT1, is up-regulated by hypoxia through a HIF-1alpha-dependent mechanism. The Journal of biological chemistry. 2006;281(14):9030-7.

192. Dimmer KS, Friedrich B, Lang F, Deitmer JW, Broer S. The low-affinity monocarboxylate transporter MCT4 is adapted to the export of lactate in highly glycolytic cells. The Biochemical journal. 2000;350 Pt 1:219-27.

193. Izumi H, Takahashi M, Uramoto H, Nakayama Y, Oyama T, Wang KY, et al. Monocarboxylate transporters 1 and 4 are involved in the invasion activity of human lung cancer cells. Cancer science. 2011;102(5):1007-13.

194. Rattigan YI, Patel BB, Ackerstaff E, Sukenick G, Koutcher JA, Glod JW, et al. Lactate is a mediator of metabolic cooperation between stromal carcinoma associated fibroblasts and glycolytic tumor cells in the tumor microenvironment. Experimental cell research. 2012;318(4):326-35.

195. Pavlides S, Vera I, Gandara R, Sneddon S, Pestell RG, Mercier I, et al. Warburg meets autophagy: cancer-associated fibroblasts accelerate tumor growth and metastasis via oxidative stress, mitophagy, and aerobic glycolysis. Antioxidants & redox signaling. 2012;16(11):1264-84.

196. Koukourakis MI, Giatromanolaki A, Simopoulos C, Polychronidis A, Sivridis E. Lactate dehydrogenase 5 (LDH5) relates to up-regulated hypoxia inducible factor pathway and metastasis in colorectal cancer. Clinical & experimental metastasis. 2005;22(1):25-30.

197. Koukourakis MI, Giatromanolaki A, Sivridis E, Bougioukas G, Didilis V, Gatter KC, et al. Lactate dehydrogenase-5 (LDH-5) overexpression in non-small-cell lung cancer tissues is linked to tumour hypoxia, angiogenic factor production and poor prognosis. British journal of cancer. 2003;89(5):877-85.

198. Vettraino M, Manerba M, Govoni M, Di Stefano G. Galloflavin suppresses lactate dehydrogenase activity and causes MYC downregulation in Burkitt lymphoma cells through NAD/NADH-dependent inhibition of sirtuin-1. Anti-cancer drugs. 2013;24(8):862-70.

199. Allison SJ, Knight JRP, Granchi C, Rani R, Minutolo F, Milner J, et al. Identification of LDH-A as a therapeutic target for cancer cell killing via (i) p53/NAD(H)-dependent and (ii) p53-independent pathways. Oncogenesis. 2014;3(5):e102-.

200. Knight J. Regulation of SIRT1 protein in cancer metabolism and ribosome biogenesis: University of York; 2011.

201. DeBerardinis RJ, Mancuso A, Daikhin E, Nissim I, Yudkoff M, Wehrli S, et al. Beyond aerobic glycolysis: transformed cells can engage in glutamine metabolism that exceeds the requirement for protein and nucleotide synthesis. Proceedings of the National Academy of Sciences of the United States of America. 2007;104(49):19345-50.

202. Vazquez A, Kamphorst JJ, Markert EK, Schug ZT, Tardito S, Gottlieb E. Cancer metabolism at a glance. 2016;129(18):3367-73.

203. Vander Heiden MG, Cantley LC, Thompson CB. Understanding the Warburg effect: the metabolic requirements of cell proliferation. Science (New York, NY). 2009;324(5930):1029-33.

204. Reznik E, Miller ML, Senbabaoglu Y. Mitochondrial DNA copy number variation across human cancers. 2016;5.

205. Shakhssalim N, Houshmand M, Kamalidehghan B, Faraji A, Sarhangnejad R, Dadgar S, et al. The mitochondrial C16069T polymorphism, not mitochondrial D310 (D-loop) mononucleotide sequence variations, is associated with bladder cancer. Cancer cell international. 2013;13(1):120.

206. Yoo JH, Suh B, Park TS, Shin MG, Choi YD, Lee CH, et al. Analysis of fluorescence in situ hybridization, mtDNA quantification, and mtDNA sequence for the detection of early bladder cancer. Cancer genetics and cytogenetics. 2010;198(2):107-17.

207. Ellinger J, Muller SC, Wernert N, von Ruecker A, Bastian PJ. Mitochondrial DNA in serum of patients with prostate cancer: a predictor of biochemical recurrence after prostatectomy. BJU international. 2008;102(5):628-32.

208. Cormio A, Sanguedolce F, Musicco C, Pesce V, Calo G, Bufo P, et al. Mitochondrial dysfunctions in bladder cancer: Exploring their role as disease markers and potential therapeutic targets. Critical reviews in oncology/hematology. 2017;117:67-72.

209. Zhou ZW, Li XX, He ZX, Pan ST, Yang Y, Zhang X, et al. Induction of apoptosis and autophagy via sirtuin1- and PI3K/Akt/mTOR-mediated pathways by plumbagin in human prostate cancer cells. Drug design, development and therapy. 2015;9:1511-54.

210. Hau AM, Nakasaki M, Nakashima K, Krish G, Hansel DE. Differential mTOR pathway profiles in bladder cancer cell line subtypes to predict sensitivity to mTOR inhibition. Urologic oncology. 2017;35(10):593-9.

211. Sjodahl G, Lauss M, Gudjonsson S, Liedberg F, Hallden C, Chebil G, et al. A systematic study of gene mutations in urothelial carcinoma; inactivating mutations in TSC2 and PIK3R1. PloS one. 2011;6(4):e18583.

212. Chen M, Cassidy A, Gu J, Delclos GL, Zhen F, Yang H, et al. Genetic variations in PI3K-AKT-mTOR pathway and bladder cancer risk. Carcinogenesis. 2009;30(12):2047-52.

213. Gupta S, Hau AM, Beach JR, Harwalker J, Mantuano E, Gonias SL, et al. Mammalian target of rapamycin complex 2 (mTORC2) is a critical determinant of bladder cancer invasion. PloS one. 2013;8(11):e81081.

214. Park SJ, Lee TJ, Chang IH. Role of the mTOR Pathway in the Progression and Recurrence of Bladder Cancer: An Immunohistochemical Tissue Microarray Study. Korean journal of urology. 2011;52(7):466-73.

215. Pinto-Leite R, Arantes-Rodrigues R, Sousa N, Oliveira PA, Santos L. mTOR inhibitors in urinary bladder cancer. Tumour biology : the journal of the International Society for Oncodevelopmental Biology and Medicine. 2016;37(9):11541-51.

216. Winters BR, Vakar-Lopez F, Brown L, Montgomery B, Seiler R, Black PC, et al. Mechanistic target of rapamycin (MTOR) protein expression in the tumor and its microenvironment correlates with more aggressive pathology at cystectomy. Urologic oncology. 2018.

217. Vaz CV, Alves MG, Marques R, Moreira PI, Oliveira PF, Maia CJ, et al. Androgen-responsive and nonresponsive prostate cancer cells present a distinct glycolytic metabolism profile. The international journal of biochemistry & cell biology. 2012;44(11):2077-84.

218. Zhang L, Han J. Branched-chain amino acid transaminase 1 (BCAT1) promotes the growth of breast cancer cells through improving mTOR-mediated mitochondrial biogenesis and function. Biochemical and biophysical research communications. 2017;486(2):224-31.

219. Liu P, Wilson MJ. miR-520c and miR-373 upregulate MMP9 expression by targeting mTOR and SIRT1, and activate the Ras/Raf/MEK/Erk signaling pathway and NF-kappaB factor in human fibrosarcoma cells. Journal of cellular physiology. 2012;227(2):867-76.

220. Pinton G, Manente AG, Murer B, De Marino E, Mutti L, Moro L. PARP1 inhibition affects pleural mesothelioma cell viability and uncouples AKT/mTOR axis via SIRT1. Journal of cellular and molecular medicine. 2013;17(2):233-41.

221. Zhang ZY, Hong D, Nam SH, Kim JM, Paik YH, Joh JW, et al. SIRT1 regulates oncogenesis via a mutant p53-dependent pathway in hepatocellular carcinoma. Journal of hepatology. 2015;62(1):121-30.

13 APPENDIX

13.1 RT4 cell culture

To perform this research project, it was intended to also use the RT4 cell line, which represents grade II of bladder cancer, besides HT-1376 and TCCSUP cell lines, which represents a grade III and IV of bladder cancer cells. However, it was not possible to work with viable RT4 cells, since cells did not developed although all the performed attempts, presented at table 7.

For cell culture application, a water bath was pre-warmed to 37 °C. Vials with frozen cells, which were stored at -80ºC, were thawed in the water bath with gentle agitation and resuspended in a pre-warmed medium.

Table 7: Attempts that were performed to culture RT4 bladder cancer cells. Alterations were made in different media, FBS concentration and culture site.

	Alterations
Medium	DMEM
	RPMI
FBS concentration	5 %
	10 %
	20 %
Culture site	T25 flask
	T75 flask
	6 well plate

13.2 tOXPHOS analysis through western blot assay

To accomplish the methods, it was intended to perform a tOXPHOS analysis through western blot assay, to study individual proteins expression from OXPHOS complex. However, this was not possible to achieve besides all the attempts performed since not all the OXPHOS complexes were detectable. Some examples are described at table 8 and the respective alterations that were made. Two representative results of all the attempts performed are presented in figure 25, panels B and C.

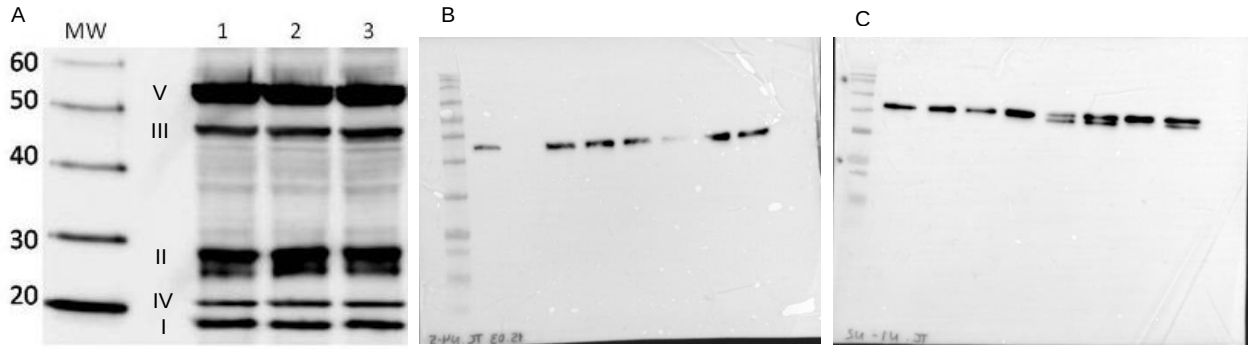

Figure 25: tOXPHOS detection through western blot assay. A – The five tOXPHOS complexes perfectly (complex I – 18kD, complex II – 29kD, complex III – 48kD, complex IV – 22kD and complex V – 54 kD), image from Abcam product data sheet – Total OXPHOS Human WB Antibody Cocktail – ab110411). B and C – Representative result from tOXPHOS detection after western blot assay in treated TCCSUP cells. Since not all the complexes are detectable, is not possible to identify them.

Table 8: Attempts that were performed for tOXPHOS analysis through western blot assay.

Samples denaturation	37ºC
	50ºC
Antibodies	Different concentrations
	New reagents
	Complex I incubation
Electrophoresis	New reagents
	Time and amperage
	Bio-Rad gels
Transference	Transblot turbo equipment (Bio-Rad, UK)
	Conventional (Mini Trans-Blot Cell – Bio-Rad, UK)
	New buffer
Detection method	Membrane division for different complexes' expositions